VINÍCIUS DA SILVA DUARTE

# USO DO BACTERIÓFAGO vB_EcoM-UFV13 COMO POTENCIAL AGENTE ANTIMASTÍTICO EM VACAS LEITEIRAS

Tese apresentada à Universidade Federal de Viçosa, como parte das exigências do Programa de Pós-Graduação em Microbiologia Agrícola, para obtenção do título de *Doctor Scientiae*.

VIÇOSA
MINAS GERAIS – BRASIL
2018

**Ficha catalográfica preparada pela Biblioteca Central da Universidade Federal de Viçosa - Câmpus Viçosa**

T
D812u
2018

Duarte, Vinicius da Silva, 1987-
Uso do bacteriófago vB_EcoM-UFV13 como potencial agente antimastítico em vacas leiteiras / Vinicius da Silva Duarte. – Viçosa, MG, 2018.
x, 126f. : il. (algumas color.) ; 29 cm.

Inclui anexos.
Orientador: Sérgio Oliveira de Paula.
Tese (doutorado) - Universidade Federal de Viçosa.
Inclui bibliografia.

1. Bacteriófagos. 2. Bacteriologia veterinária. 3. Mastite. I. Universidade Federal de Viçosa. Departamento de Microbiologia. Programa de Pós-Graduação em Microbiologia Agrícola. II. Título.

CDD 22. ed. 579.26

VINÍCIUS DA SILVA DUARTE

# USO DO BACTERIÓFAGO vB_EcoM-UFV13 COMO POTENCIAL AGENTE ANTIMASTÍTICO EM VACAS LEITEIRAS

Tese apresentada à Universidade Federal de Viçosa, como parte das exigências do Programa de Pós-Graduação em Microbiologia Agrícola, para obtenção do título de *Doctor Scientiae*.

APROVADA: 26 de Abril de 2018.

Cynthia Canedo da Silva
(Coorientador)

Michelle Dias de Oliveira

Ricardo Seiti Yamatogi

Roberto Sousa Dias
(Coorientador)

Sérgio Oliveira de Paula
(Orientador)

Dedico este trabalho aos meus pais Adalberto e Maria, minhas irmãs Larissa e Franciele, minha querida família e aos bons e velhos amigos.

*“É junto dos bão que a gente fica mió!”*
(Guimarães Rosa, Grande sertão:
Veredas)

## AGRADECIMENTOS

Agradeço a DEUS pelo dom da vida! Por colocar em minha trajetória pessoas sem as quais não teria chegado até aqui. Por me dar força para concluir mais uma sonhada etapa, o Doutorado.

*Agradeço* aos meus pais Adalberto e Maria, exemplos de vida, de dedicação, trabalho, superação e amor incondicional. Os maiores incentivadores da minha vida! Obrigado por existirem, amo vocês!!!

*Agradeço* às minhas irmãs Larissa e Franciele pelas palavras amorosas e incentivadoras. Vocês são um exemplo de dedicação e amizade. Eu amo vocês!!!

*Agradeço* à minha família, a base de tudo. Como a família é muito grande, seria leviano citar nomes, pois certamente me esqueceria de alguém. Contudo, em especial, gostaria de agradecer aos meus avós! Vô Zé Lopes e Vô Pedro, muita saudade e certeza de que vocês iluminam a minha trajetória. Vó Nega e Vó Pitita, mães duas vezes, que sempre em suas orações pediram que Deus guiasse a minha vida pelo melhor caminho.

*Agradeço* ao meu Orientador Sérgio Oliveira de Paula. Sinceramente não tenho palavras para agradecer o que você me proporcionou desde 2009 quando entrei no laboratório, uma mistura de crescimento pessoal e profissional. Todas as conversas que tivemos foram decisivas na minha vida! Obrigado por me aturar nas teimosias! Tenho certeza que a palavra orientador é mera formalidade, o sentimento que tenho é de um eterno amigo e irmão.

*Agradeço* ao Roberto Sousa Dias, o eterno MESTRE, no sentido literário da palavra mesmo. Brother, você sabe a admiração e respeito que tenho por ti. Muito obrigado pelos ensinamentos esses anos todos. Obrigado pela amizade sincera, por aguentar a minha teimosia. O ambiente de trabalho irreverente, a superaração nos momentos difíceis, só foi possível porque você estava lá! Este trabalho é tão seu quanto meu. Que esta parceria jamais acabe!

*Agradeço* aos amigos do Laboratório de Imunovirologia Molecular (LIVM), amizades de longos anos, por estarem sempre dispostos a sanar qualquer tipo de dúvida, pelo ambiente de trabalho ímpar, com certeza não encontrado em nenhum outro lugar.

*Agradeço* à Universidade de Padova, Itália. Aos ensinamentos e amigos adquiridos ao longo do Doutorado Sanduíche. Non ho parole per ringraziarvi. Grazie mille ragazzi!!! Vi penso ogni giorno!

*Agradeço* aos Pesquisadores Laura Treu e Stefano Campanaro, profissionais que são fonte de inspiração para qualquer pessoa que busca a excelência no que faz! Obrigado por acreditarem na minha capacidade! Obrigado pelas oportunidades! Adoro vocês!

*Agradeço* aos meus coorientadores, sempre dispostos a me atender e contribuir com sugestões de grande valia ao meu trabalho.

*Agradeço* às minhas ICs Marcella, Isabela e Gabriele. Não possuo palavras para descrever o quanto vocês me ajudaram ao longo desta trajetória. Adoro vocês! Sucesso sempre!

*Agradeço* aos meus amigos da Vet-08, Capivaras, [D.C] e a eterna República T.Q.P, minha segunda casa. Aos amigos de São Paulo, desde o tempo do Vaquinha, até as quintas no *Oliverrá*. Muitas amizades construídas, todas contribuíram para o meu crescimento pessoal e profissional e, de alguma forma, este trabalho é reflexo disso. Amo vocês!

*Agradeço* à Jessika pelo amor, paciência e palavras de incentivo durante esse período. Por sempre acreditar no meu potencial. Ao João e à Lucimar, pessoas diferenciadas! Amo vocês!

*Agradeço* à Universidade Federal de Viçosa e à cidade de Viçosa por me proporcionarem tamanho aprendizado desde a Graduação.

*Agradeço* ao Programa de Pós-Graduação em Microbiologia Agrícola, aos Professores, colegas, técnicos de laboratório e secretárias. Obrigado pela oportunidade!

*Agradeço* à banca examinadora pela disponibilidade e considerações.

*Agradeço* aos Núcleos de Biomoléculas e Microscopia da UFV. Obrigado pela atenção e disposição em me ajudar.

*Agradeço* à Fundação de Amparo à Pesquisa do Estado de Minas Gerais (FAPEMIG) pelo suporte financeiro.

*Agradeço* a todos que de alguma forma, direta ou indiretamente, contribuíram para a realização deste trabalho e a conclusão de mais uma etapa na minha vida.

# SUMÁRIO

## RESUMO

DUARTE, Vinícius da Silva, D.Sc., Universidade Federal de Viçosa, abril de 2018. **Uso do bacteriófago vB_EcoM-UFV13 como potencial agente antimastítico em vacas leiteiras.** Orientador: Sérgio Oliveira de Paula. Coorientadores: Hilário Cuquetto Mantovani, Cynthia Canedo da Silva, Denise Mara Soares Bazzolli e Roberto Sousa Dias.

A atividade leiteira no Brasil sofreu profundas transformações nos últimos anos no que diz respeito, principalmente, ao aumento da produtividade com um custo de produção cada vez menor. Para que tal resultado seja alcançado, o animal é invariavelmente desafiado a atender altos índices zootécnico. Dentro do manejo sanitário, a mastite bovina ainda é a principal causa de perdas econômicas para produtores de leite, estimado em $ 533 bilhões de dólares em todo o mundo. A *Escherichia coli* é responsável pela maioria dos casos de mastite ambiental (40%), enquanto que *Trueperella pyogenes* é um dos principais agentes causadores de mastite em novilhas no período seco. Embora a terapia com antimicrobianos convencionais seja a mais utilizada nos rebanhos, o uso de bacteriófagos como instrumento no controle de patógenos na Veterinária tem ganhado destaque. Neste trabalho, buscamos avaliar o uso do bacteriófago vB_EcoM-UFV13 (UFV13) contra estes dois importantes patógenos causadores de mastite bovina. Em um primeiro estudo, investigamos o uso do fago UFV13 na prevenção da formação do biofilme de *T. pyogenes*, um dos principais fatores de virulência apresentado por este micro-organismo. Empregando-se duas diferentes metodologias (cristal violeta e contagem de células sésseis), observou-se que somente a multiplicidade de infecção 10 apresentou redução, estatisticamente significativa, do biofilme formado. A análise das proteínas estruturais do vírus UFV13 revelou um repertório de proteínas com domínio hidrolase (*Virion-Associated Peptidoglycan Hydrolases* – VAPGHs) que potencialmente estão envolvidas no processo de adesão e desenvolvimento do biofilme. No segundo estudo, examinamos o fago UFV13 em termos genômico, a sua estabilidade em diferentes condições adversas, além da sua atividade contra *E. coli* em camundongos fêmeas lactantes. Estas análises revelaram que o vírus UFV13 é oriundo de uma recente infecção mista com *Shigella phage* Shfl2. Além disto, sua administração intramamária provocou uma redução de

10 vezes na carga bacteriana total, além de induzir a produção de citocinas pró-inflamatórias como IL-6 e TNF-α. Após esses estudos, a completa caracterização do fago UFV13 o torna um possível candidato para controle da mastite bovina no gado leiteiro.

## ABSTRACT

DUARTE, Vinícius da Silva, D.Sc., Universidade Federal de Viçosa, April, 2018. **Use of the bacteriophage vB_EcoM-UFV13 as potential antimastitic agent in dairy cattle.** Adviser: Sérgio Oliveira de Paula. Co-advisers: Hilário Cuquetto Mantovani, Cynthia Canedo da Silva, Denise Mara Soares Bazzolli and Roberto Sousa Dias.

The dairy activity in Brazil has undergone profound changes in recent years, mainly due to the high productivity with a low production cost. To this condition be achieved, animals are invariably challenged to meet high zootechnical rates. Within sanitary management, bovine mastitis is still the leading cause of economic loss for dairy farmers, estimated at $533 billion worldwide. *Escherichia coli* is responsible for most cases of environmental mastitis (40%), while *Trueperella pyogenes* is one of the main agents causing mastitis in heifers on the dry off period. Although conventional antimicrobial therapy is the most used in cattle, the use of bacteriophage as a tool to control pathogens in Veterinary has been investigated. In the first study, the use of the bacteriophage vB_EcoM-UFV13 (UFV13) in the prevention of the biofilm formation by *T. pyogenes*, one of its main virulence factors, was evaluated. Based upon two different approaches (crystal violet and sessile cell counting), it was observed that only the multiplicity of infection (MOI) 10 presented a statistically significant reduction. Analysis of the structural proteins revealed a repertoire of hydrolase viral proteins (Virion-Associated Peptidoglycan Hydrolases - VAPGHs) that are potentially involved. In the second study, the phage UFV13 was evaluated in genomic terms and its activity against an *E. coli* strain in mastitis mouse model. These analysis revealed that UFV13 virus originates from a recent mixed infection with Shigella phage Shfl2. In addition, its intramammary administration caused a 10-fold reduction in bacterial load. The production of proinflammatory cytokines such as IL-6 and TNF-α was also observed. After these studies, the complete characterization of the UFV13 phage makes it a possible candidate for control of bovine mastitis in dairy cattle.

# 1. Introdução Geral

## 1.1. Pecuária leiteira no Brasil

A atividade leiteira no Brasil sofreu profundas transformações nos últimos anos no que diz respeito, principalmente, ao aumento da produtividade com um custo de produção cada vez menor. Para que tal resultado seja alcançado, o animal é invariavelmente desafiado a atender altos índices zootécnicos (Lemos et al., 2003; Faria & Corsi, 1993).

De acordo com a Companhia Nacional de Abastecimento (FAGUNDES, 2017), o Brasil é o quinto maior produtor mundial de leite com projeção para ultrapassar a China nos próximos anos (Tabela 1). Deve-se dar destaque para a região Sul, atual líder nacional, que ultrapassou em produção a região Sudeste, todavia, o Estado de Minas Gerais ainda é o maior produtor brasileiro.

**Tabela 1. Produção mundial de leite de vaca (países selecionados) 2011 a 2016 em 1.000 toneladas.**

| País/Bloco | 2012 | 2013 | 2014 | 2015 | 2016[1] | 2017 |
|---|---|---|---|---|---|---|
| **UE (28)** | 139.000 | 140.100 | 146.500 | 150.200 | 152.000 | 152.500 |
| **EUA** | 91.010 | 91.277 | 93.485 | 94.620 | 96.343 | 98.339 |
| **Índia** | 55.500 | 57.500 | 60.500 | 64.000 | 68.000 | 72.000 |
| **China** | 32.600 | 34.300 | 37.250 | 37.550 | 35.700 | 35.000 |
| **Brasil** | 32.304 | 34.255 | 35.124 | 35.000 | 34.650 | 34.997 |

Fonte: Companhia Nacional de Abastecimento (CONAB), conjuntura mensal para o mês de Abril de 2017 (Adaptado).

Nesta atividade, os manejos nutricional, genético e sanitário, devem estar em consonância e qualquer alteração em um deles pode levar ao insucesso do produtor. Mesmo detentor do terceiro maior rebanho do mundo, atrás apenas da Índia e da União Europeia, o Brasil ainda possui animais com baixa produtividade (1.709 litros de leite por vaca/ano), abaixo da média mundial (2.200 litros/vaca/ano)(IBGE, 2017).

## 1.2. Mastite bovina

Dentro do manejo sanitário, a mastite bovina (conceituada abaixo) ainda é a principal causa de perdas econômicas para produtores de leite, estimado em $ 533 bilhões de dólares em todo o mundo (Thomas et al., 2015; Shaheen et al., 2016). Destes, 70% são perdas de leite no transcorrer da lactação (período em que o animal está produzindo e secretando leite), 14% dos custos é devido ao descarte prematuro dos animais, 8% com tratamento médico ou outros custos veterinários, 7% ocasionado pela baixa produção de leite e 1% com outros(Shaheen et al., 2016). Além das questões financeiras, é relevante destacar a significância do leite e derivados na saúde pública, visto que a matéria-prima de má qualidade é potencial veículo de patógenos.

Conceitualmente, a mastite bovina pode ser classificada em:

- Mastite clínica – presença de edema, hipertermia, fibrosamento da glândula mamária, dor à palpação e alterações visuais no leite como grumos, pus e sangue (Coser et al., 2012);
- Mastite subclínica – alterações na composição do leite, como aumento de Contagem de Células Somáticas (CCS) e variações nos teores de sólidos totais, acarretando menor tempo de prateleira (Coser et al., 2012);
- Mastite contagiosa – classificação devida à forma como ocorre a transmissão dos micro-organismos envolvidos, que se dá por meio de retireiros e ordenhadeiras, por exemplo (Coser et al., 2012);

Mastite ambiental – micro-organismos presentes nas fezes, solos, camas, por exemplo, oportunamente são capazes de provocar infecções que levam, na grande maioria das vezes, ao quadro de mastite clínica (Coser et al., 2012).Micro-organismos virais, fúngicos e bacterianos podem estar envolvidos no estabelecimento da doença, contudo deve-se acrescentar o papel do ambiente e as características inerentes ao animal como partes na etiologia da doença, o que a torna multifatorial (Coser et al., 2012; Shaheen et al., 2016).

Hoje, mais de 150 espécies de bactérias são isoladas de úberes com mastites, entretanto *Staphylococcus aureus* é o principal agente etiológico envolvido em casos de mastite contagiosa (40-70%), enquanto que

*Escherichia coli* é responsável pela maioria dos casos de mastite ambiental (40%) (Thomas et al., 2015; Shaheen et al., 2016). Já *Trueperella pyogenes*, antigo *Arcanobacterium pyogenes*, é um dos principais agentes causadores de mastite em novilhas no período seco, (Radostits *et al*., 2007; Ruegg, 2010; Domingues *et al*., 2008).

### 1.3. Tratamentos para mastite bovina

O tratamento para a mastite bovina ocorre, basicamente, em dois momentos dentro do ciclo de lactação do animal: produção de leite e período seco, definido aqui como o período em que o animal sai da linha da ordenha 60 dias antes do parto com o intuito de permitir a involução da glândula mamária. No primeiro momento, micro-organismos causadores da mastite clínica são os principais responsáveis pelos episódios de tratamentos com antibióticos que possuem curto tempo de ação local, visto que é necessário o retorno do animal à linha de ordenha para comercialização do leite produzido. Já a terapia vaca seca é realizada, principalmente, em um período de 30-60 dias pré-parto, caracterizada pela não produção de leite e involução da glândula mamária. Nessa terapia são utilizados antibióticos de longotempo de ação local e com espectro para bactérias causadoras de mastites subclínicas, pois casos clínicos são raros neste período (Crispie et al., 2004).

Embora a terapia com antimicrobianos convencionais seja a mais utilizada nos rebanhos (Thomas et al., 2015; Shaheen et al., 2016), sua eficácia depende de fatores como:

- Apresentação da doença (clínica ou subclínica);
- Extensão da lesão tecidual provocada na glândula mamária;
- Patógeno envolvido (infecção mista ou não);
- Resposta local ao medicamento;
- Padrão de sensibilidade ao antibiótico;
- Seleção de antimicrobianos com propriedades farmacológicas ideais;
- Adequações da dose e do intervalo de aplicação.

## 1.4. Bactérias causadoras da mastite bovina e a formação de biofilme

Dentre os fatores de virulência bacterianos capaz de levar ao uso refratário de antibióticos está a habilidade de formar biofilmes. Biofilmes são comunidades bacterianas densas e pluricelulares aderidas (forma séssil de vida) a uma superfície (biótica ou não). Os componentes mínimos de um biofilme são os micro-organismos, a matriz extracelular - Substância Polimérica Extracelular (SPE) e a superfície de crescimento (Donlan, 2002).

Este modo de crescimento abriga e protege os micro-organismos em ambientes hostis, como a presença de antimicrobianos, de bacteriófagos e de componentes do sistema imune. Esta forma de crescimento induz a expressão gênica diferenciada das células bacterianas que estão livres no ambiente, o que modifica o metabolismo e estabelece uma nova forma de desenvolvimento (Donlan, 2002).

A capacidade dos micro-organismos causadores da mastite bovina em formar biofilme é responsável pela baixa eficiência dos antibióticos e o aumento das recidivas da doença (infecção crônica no hospedeiro), mesmo em animais que apresentam baixa contagem de células somáticas (CCS), como macrófagos e queratinócitos, por exemplo, o que os torna reservatórios e disseminadores de patógenos causadores da doença (Gomes et al., 2016; Shaheen et al., 2016).

## 1.5. Bacteriófagos e a fagoterapia

Considerando-se as limitações expostas acima, além dos crescentes relatos de bactérias multi-drogras resistentes (BMDRs), diversos produtos foram desenvolvidos nos últimos anos com o intuito de diminuir ou abolir o uso de antibióticos como fitoterápicos, homeopáticos, bacteriocinas e coquetéis fágicos (Gill et al., 2006; Pieterse and Todorov, 2010; Aubry et al., 2013; Izabella et al., 2018).

Tendo em vista o uso de bacteriófagos como instrumento no controle de patógenos, é observado um difuso crescimento dos mesmos nos últimos anos, principalmente no que ser refere a avaliações *in vitro* e *in vivo* em vacas

de leite (Porter et al., 2016; Dias et al., 2013; Sulakvelidze, 2011; Gill et al., 2006; Merril et al., 2003).

Descobertos por Twort em 1915, os vírus procarióticos infectam membros dos domínios *Bacteria* (bacteriófagos ou fagos) e *Archaea* (archeovírus), possuem estrutura análoga a de outros vírus, consistindo em um ácido nucléico envolto por capsídeo de origem proteica, complexado ou não por um envelope lipoprotéico (Merril et al., 2003). Os procariotos são hospedeiros fundamentais, dotados de receptores específicos para que esses vírus possam adsorver e replicar seu material genético (Ackermann & Prangishvili, 2012).

Existem fagos de DNA ou RNA, com diferentes formas e tamanhos. Cerca de 96% dos bacteriófagos descritos são pertencentes à ordem *Caudovirales*, que engloba as famílias *Siphoviridae*, maior representante (11 subfamílias, 100 gêneros), *Myoviridae* (6 subfamílias, 41 gêneros), *Podoviridae* (3 subfamílias, 41 gêneros) e, mais recentemente, a família *Ackermannviridae* (2 subfamílias) (ICTV, 2011). Baseado na forma do capsídeo, as famílias *Myoviridae*, *Siphoviridae* e *Podoviridae* apresentam três morfotipos cada uma: A1, A2 e A3 para *Myoviridae*, B1, B2 e B3 para *Siphoviridae* e C1, C2 e C3 para *Podoviridae* (Adams et al., 2017). Os outros 4,0% constituem fagos poliédricos, filamentosos e pleomórficos (Ackermann & Prangishvili, 2012).

São descritos vírus que infectam membros de 16 gêneros do domínio *Archaea*, principalmente hipertermófilos e halófilos, e que infectam 179 gêneros bacterianos, sendo maioria membros dos filos *Firmicutes* e *γ-Proteobacteria* (Ackermann & Prangishvili, 2012)

Os fagos são uma alternativa natural ao uso de defensivos agrícolas e antibióticos, não tóxico, economicamente viável e que podem ser isolados de praticamente qualquer ambiente, como solo, água, leito oceânico, esgoto e trato gastrointestinal dos animais (Ashelford et al., 2000; Gorski et al., 2003). A atividade antibacteriana dos fagos possui vantagens sobre os antibióticos: alta especificidade (Sulakvelidze, 2011); replicação no local da infecção (Smith & Huggins, 1982); ausência de efeito colateral (Sulakvelidze, 2011); bactérias resistentes a determinados bacteriófagos permanecem suscetíveis a outros fagos e o isolamento de novos fagos contra tais bactérias é

relativamente rápido, podendo ser montado um coquetel de bacteriófagos contra vários isolados microbianos (Chopra et al., 1997).

A aplicação da fagoterapia, tornou-se disseminada por Felix d'Herelle no início do século XX no tratamento da febre tifóide em aves, disenteria por *Shigella* em coelhos e disenteria bacilar (shigelose) em humanos (Merril et al., 2003). Diversos trabalhos têm demonstrado a importância da terapia como alternativa ao uso de antibióticos em diversos gêneros bacterianos. Por exemplo Biswas e colaboradores recuperaram camundongos que foram inoculados com cepas de *Enterococcus faecium* resistentes à vancomicina com uma única injeção de bacteriófagos específicos contendo 3 x $10^8$ Unidades Formadoras de Placas (UFP) ,(Biswas, 2002). Outros exemplos de patógenos que podem ser controlados pela utilização de fagos são: *Pseudomonas aeruginosa* (Soothill, 1994), *Staphylococcus aureus* (Matsuzaki et al., 2003; Dias et al., 2013) e *Acinetobacter baumannii* (Soothill, 1992). Bacteriófagos também foram utilizados no tratamento de patógenos intracelulares (*Mycobacterium avium* ou *Mycobacterium tuberculosis*), doenças bacterianas em peixes e, até mesmo, em fitopatógenos do tomate (Merril et al., 2003). Recentemente, nos Estados Unidos, o FDA (*Food and Drug Administration*) consentiu o uso de fagos para o controle de *Listeria monocytogenes*, cuja contaminação ocorre durante a manipulação do alimento (Golkar et al., 2014).

Merril et al. (2003) relataram que o estudo apenas qualitativo sobre a eficácia da fagoterapia é um dos principais entraves ao uso comercial de fagos. A grande maioria dos países ocidentais requer certificação farmacêutica baseada em estudos de eficácia farmacocinética em animais e humanos para que sejam liberados comercialmente. Os princípios farmacocinéticos dos fagos podem diferir entre eles, o que requer análises virais individuais (Golkar et al., 2014).

Nas décadas de 20 e 30, a empresa Norte Americana Eli Lilly & Co. chegou a comercializar produtos em géis a base de fagos específicos para *Staphylococcus* spp. como "Staphylo jel", contudo a falta e a falha de estudos clínicos, preocupações teóricas e o ofuscamento com o uso dos antibióticos foram alguns dos motivos do abandono da fagoterapia nos Estados Unidos e na Europa Ocidental no século XX (Merril et al., 2003).

Dois países atualmente fazem uso da fagoterapia na Europa: Georgia e Polônia. Adicionalmente, o *Wound Care Center in Lubbock*, Texas, Estados Unidos, conduz fase de testes clínicos com fagos para *P. aeruginosa*, *S. aureus* e *E. coli* (http://www.phagetherapycenter.com). Contudo, apesar do pequeno número de países que fazem uso de bacteriófagos, diversas empresas já disponibilizam comercialmente a aplicação de fagos em diversas áreas (Tabela 2 – ANEXO 1).

## 2. Objetivo geral

Aqui, buscamos avaliar o efeito do vírus UFV13 na formação do biofilme produzido por *T. pyogenes* e a sua aplicação em modelo animal contra *E. coli* causadora de mastite clínica.

## 3. Objetivos específicos

- Avaliar o efeito do fago UFV13 em inibir a formação do biofilme por *T. pyogenes* usando-se as multiplicidades de infecção 0,1, 1 e 10;
- Predição de proteínas estruturais do vírus UFV13 com domínio hidrolase;
- Análise genômica do bacteriófago UFV13;
- Estabilidade do vírus UFV13 à condições adversas (e.g. pH, temperatura e detergentes);
- Resposta imune ao fago UFV13 utilizando-se camundongos fêmeas lactantes como modelo animal.

## 4. Referências


Ackermann, H. W. & Prangishvili, D. 2012. Prokaryote viruses studied by electron microscopy. Arch. Virol. 157:1843–1849. doi:10.1007/s00705-012-1383-y.

Adams, M.J., E.J. Lefkowitz, A.M.Q. King, B. Harrach, R.L. Harrison, N.J. Knowles, A.M. Kropinski, M. Krupovic, J.H. Kuhn, A.R. Mushegian, M. Nibert, S. Sabanadzovic, H. Sanfaçon, S.G. Siddell, P. Simmonds, A. Varsani, F.M. Zerbini, A.E. Gorbalenya, and A.J. Davison. 2017. Changes to taxonomy and the International Code of Virus Classification and Nomenclature ratified by the International Committee on Taxonomy of Viruses (2017).. Arch. Virol. 162:2505–2538. doi:10.1007/s00705-017-3358-5.

Ashelford, K.E., S.J. Norris, J.C. Fry, M.J. Bailey, and M.J. Day. 2000. Seasonal Population Dynamics and Interactions of Competing Bacteriophages and Their Host in the Rhizosphere. Appl. Environ. Microbiol. 66:4193–4199. doi:10.1128/AEM.66.10.4193-4199.2000.

Aubry, E., M.-N. Issautier, D. Champomier, and L. Terzan. 2013. Early udder inflammation in dairy cows treated by a homeopathic medicine (Dolisovet): a prospective observational pilot study. Homeopathy 102:139–44. doi:10.1016/j.homp.2013.02.003.

Biswas, B. 2002. Bacteriophage Therapy Rescues Mice Bacteremic from a Clinical Isolate of Vancomycin-Resistant *Enterococcus faecium*. Infect. Immun. 70:204–210. doi:10.1128/IAI.70.1.204-210.2002.

Chopra, I., J. Hodgson, B. Metcalf, and G. Poste. 1997. The search for antimicrobial agents effective against bacteria resistant to multiple

antibiotics. Antimicrob. Agents Chemother. 41:497–503.

Coser, S.M., M.A. Lopes, and G.M. Costa. 2012. Mastite bovina : Controle e Prevenção. Bol. Técnico UFL 1–30.

Crispie, F., J. Flynn, R.P. Ross, C. Hill, and W.J. Meaney. 2004. Dry cow therapy with a non-antibiotic intramammary teat seal - a review. Ir. Vet. J. 57:412. doi:10.1186/2046-0481-57-7-412.

Dias, R.S., M.R. Eller, V.S. Duarte, Â.L. Pereira, C.C. Silva, H.C. Mantovani, L.L. Oliveira, E. De, A.M. Silva, and S.O. De Paula. 2013. Use of phages against antibiotic-resistant *Staphylococcus aureus* isolated from bovine mastitis 1. J. Anim. Sci 91:3930–3939. doi:10.2527/jas2012-5884.

Donlan, R.M. 2002. Biofilms: Microbial Life on Surfaces. Emerg. Infect. Dis. J. 8:881. doi:10.3201/eid0809.020063.

FAGUNDES, M.H. 2017. Conjuntura Mensal Especial: Leite e derivados. CONAB – Cia. Nac. Abast. 1–7.

Gill, J.J., J.C. Pacan, M.E. Carson, K.E. Leslie, M.W. Griffiths, and P.M. Sabour. 2006. Efficacy and Pharmacokinetics of Bacteriophage Therapy in Treatment of Subclinical *Staphylococcus aureus* Mastitis in Lactating Dairy Cattle. Antimicrob. Agents Chemother. 50:2912–2918. doi:10.1128/AAC.01630-05.

Golkar, Z., O. Bagasra, and D. Gene Pace. 2014. Bacteriophage therapy: A potential solution for the antibiotic resistance crisis. J. Infect. Dev. Ctries. 8:129–136. doi:10.3855/jidc.3573.

Gomes, F., M.J. Saavedra, and M. Henriques. 2016. Bovine mastitis disease/pathogenicity: evidence of the potential role of microbial biofilms. Pathog. Dis. 74:ftw006. doi:10.1093/femspd/ftw006.

Gorski, A., K. Dabrowska, K. Switala-Jeleń, M. Nowaczyk, B. Weber-Dabrowska, J. Boratynski, J. Wietrzyk, and A. Opolski. 2003. New insights into the possible role of bacteriophages in host defense and disease.. Med. Immunol. 2:2. doi:10.1186/1476-9433-2-2.

IBGE. 2017. Produção Pecuária Municipal. Accessed. https://biblioteca.ibge.gov.br/visualizacao/periodicos/84/ppm_2016_v44_br.pdf.

ICTV. 2011. Virus Taxonomy: 2011 Release (Current). Accessed. http://www.ictvonline.org/virusTaxonomy.asp.

Izabella, I.C., E.G.A. Mariano, R.T. Careli, F. Morais-Costa, F.M. De Sant'Anna, M.S. Pinto, M.R. De Souza, and E.R. Duarte. 2018. Plants of the Cerrado with antimicrobial effects against *Staphylococcus* spp. and Escherichia coli from cattle. BMC Vet. Res. 14. doi:10.1186/s12917-018-1351-1.

Lemos, M.B., B. Galinari, E. Campos, E. Basi, and F. Santos. 2003. Tecnologia, especialização regional e produtividade: Um estudo da pecuária leiteira em minas Gerais. Rev. Econ. e Socilogia Rural 41:117–138.

Matsuzaki, S., M. Yasuda, H. Nishikawa, M. Kuroda, T. Ujihara, T. Shuin, Y. Shen, Z. Jin, S. Fujimoto, M.D. Nasimuzzaman, H. Wakiguchi, S. Sugihara, T. Sugiura, S. Koda, A. Muraoka, and S. Imai. 2003. Experimental protection of mice against lethal *Staphylococcus aureus* infection by novel bacteriophage phi MR11.. J. Infect. Dis. 187:613–24. doi:10.1086/374001.

Merril, C.R., D. Scholl, and S.L. Adhya. 2003. The prospect for bacteriophage

therapy in Western medicine.. Nat. Rev. Drug Discov. 2:489–97. doi:10.1038/nrd1111.

Pieterse, R., and S.D. Todorov. 2010. Bacteriocins: Exploring alternatives to antibiotics in mastitis treatment. Brazilian J. Microbiol. 41:542–562. doi:10.1590/S1517-83822010000300003.

Porter, J., J. Anderson, L. Carter, E. Donjacour, and M. Paros. 2016. *In vitro* evaluation of a novel bacteriophage cocktail as a preventative for bovine coliform mastitis. J. Dairy Sci. 99:2053–2062. doi:10.3168/jds.2015-9748.

Shaheen, M., H. Tantary, and S. Nabi. 2016. A Treatise on Bovine Mastitis: Disease and Disease Economics, Etiological Basis, Risk Factors, Impact on Human Health, Therapeutic Management, Prevention and Control Strategy. Adv. Dairy Res. 04:1–10. doi:10.4172/2329-888X.1000150.

Smith, H.W., and M.B. Huggins. 1982. Successful Treatment of Experimental *Escherichia coli* Infections in Mice Using Phage: its General Superiority over Antibiotics. Microbiology 128:307–318. doi:10.1099/00221287-128-2-307.

Soothill, J.S. 1992. Treatment of experimental infections of mice with bacteriophages. J. Med. Microbiol. 37:258–261. doi:10.1099/00222615-37-4-258.

Soothill, J.S. 1994. Bacteriophage prevents destruction of skin grafts by *Pseudomonas aeruginosa*. Burns 20:209–211. doi:10.1016/0305-4179(94)90184-8.

Sulakvelidze, A. 2011. The challenges of bacteriophage therapy. Ind. Pharm. 45:14–18. doi:10.1128/AAC.45.3.649.

Thomas, V., A. de Jong, H. Moyaert, S. Simjee, F. El Garch, I. Morrissey, H.

Marion, and M. Vallé. 2015. Antimicrobial susceptibility monitoring of mastitis pathogens isolated from acute cases of clinical mastitis in dairy cows across Europe: VetPath results. Int. J. Antimicrob. Agents 46:13–20. doi:10.1016/j.ijantimicag.2015.03.013.

# Manuscrito 1

A *T4virus* prevents biofilm formation by *Trueperella pyogenes*

Veterinary Microbiology – DOI 10.1016/j.vetmic.2018.03.025

A *T4virus* prevents biofilm formation by *Trueperella pyogenes*

Vinícius da Silva Duarte[a], Roberto Sousa Dias[a], Andrew M. Kropinski[b], André da Silva Xavier[c], Camila Geovana Ferro[d], Pedro M. P. Vidigal[e], Cynthia Canedo da Silva[a], Sérgio Oliveira de Paula[f]

[a] Department of Microbiology, Federal University of Viçosa, Av. Peter Henry Rolfs, s/n, Campus Universitário, 36570-900, Viçosa, Minas Gerais, Brazil

[b] Departments of Food Science, and Pathobiology, University of Guelph, Guelph, Ontario N1G 2W1 Canada

[c] Embrapa Maize and Sorghum, Rodovia MG 424, Sete Lagoas, Minas Gerais, Brazil

[d] Department of Plant Pathology, Federal University of Viçosa, Av. Peter Henry Rolfs, s/n, Campus Universitário, 36570-900, Viçosa, Minas Gerais, Brazil

[e] Núcleo de Análise de Biomoléculas (NuBioMol), Center of Biological Sciences, Federal University of Viçosa, Viçosa, Minas Gerais, Brazil

[f] Department of General Biology, Federal University of Viçosa, Av. Peter Henry Rolfs, s/n, Campus Universitário, 36570-900, Viçosa, Minas Gerais, Brazil

Vinícius da Silva Duarte – vinicius.duarte@ufv.br

Roberto Sousa Dias – rosousa318@yahoo.com.br

Andrew M. Kropinski – phage.canada@gmail.com

André da Silva Xavier – xavierandre23@hotmail.com

Camila Geovana Ferro – camila.gferro@hotmail.com

Pedro M. P. Vidigal – pedro.vidigal@ufv.br

Cynthia Canedo da Silva – ccanedo@ufv.br

Sérgio Oliveira de Paula – depaula@ufv.br

**Abstract**

*Trueperella pyogenes* is an opportunistic pathogen of many animal species. It causes economic losses worldwide, mainly through mastitis, metritis and endometritis in dairy cows. The ability of this bacterium to form biofilms is implicated in chronic infections through hampering immune system recognition and antibiotic penetration. Since it is difficult to eradicate *T. pyogenes* infections with antibiotics, phage therapy presents itself as a non-toxic, effective and economically viable alternative. The present study evaluated the use of the bacteriophage vB_EcoM-UFV13 (UFV13) in the prevention of *T. pyogenes* biofilm development. Based upon two different approaches (crystal violet and sessile cell counting) we observed that only a multiplicity of infection (MOI) of 10 showed a statistically significant reduction in biofilm formation. Although the exact mechanisms of biofilm disruption and cell-adhesion inhibition have not been determined, genome sequence analysis of the *Escherichia* phage UFV13 revealed a repertoire of virion-associated peptidoglycan hydrolases (VAPGHs). The present study presents new findings regarding the disruption of biofilm formation of a Gram-positive bacterium. Subsequent transcriptomic and proteomic research will help us to understand the exact interaction mechanisms between UFV13 and *T. pyogenes*.

**Keywords**: *Trueperella pyogenes*, mastitis, metritis, *T4virus*, biofilm, VAPGHs, virus, depolymerase.

## 1. Introduction

Bovine mastitis is of considerable economic importance worldwide, leading to financial losses of up to two billion dollars annually in the USA alone when all

etiological agents are considered (Federman et al., 2016; Jost and Billington, 2005; Donlan, 2002). While of polymicrobial origin, two bacteria, *Escherichia coli* and *Trueperella pyogenes* (formerly known as *Arcanobacterium pyogenes*) are of particular relevance. In uterine infections, *E. coli* prepares the uterine environment for the establishment of *T. pyogenes* (Wagener et al., 2014). The latter bacterium is a Gram-positive, rod-shaped, non-motile, non-spore-forming opportunistic pathogen with a broad range of virulence factors (Jost and Billington, 2005). It infects many animal species, however its ability to cause diseases such as mastitis and metritis in dairy cows is relevant to our research.

Little is known about the *in vivo* gene expression of the major virulence factor from *T. pyogenes*, pyolisin (PLO), but its expression is related to biofilm formation and it is positively regulated, in stationary phase, by response regulator PloR (Jost and Billington, 2005). Zhao et al. (2013) observed that 94.4% of *T. pyogenes* isolated from abscesses of the forest musk deer (*Moschus berezovskii*) were able to form biofilms. Olson et al. (2002) showed that *T. pyogenes*, isolated from bovine pneumonia, was highly resistant to a broad spectrum of antibiotics when the cells were in the sessile phase, whereas in the planktonic phase, *T. pyogenes* cells were susceptible to a large number of antibiotics. In addition, an increased number of multi-drug resistant strains have been observed (Golkar et al., 2014), which makes the development of new antimicrobials of great interest to veterinarians and dairy farmers.

Bacteriophages are non-toxic, effective and economically viable alternatives to antibiotics and have already been used therapeutically (Dias et al., 2013). Another alternative is the use of bacteriophage parts, like holins (which form pores in bacterial membranes), endolysins (at least four distinct enzyme types involved in phage peptidoglycan-degrading activity) and virion-associated peptidoglycan hydrolases

(VAPGHs). The high specificity of VAPGHs suggests their utility as enzybiotics leading to the lysis of Gram-positive cells (Abouhmad et al., 2016). Despite the increasing number of sequenced phage genomes in the NCBI Genome database, genomes of phages for *Trueperella* species are still unavailable.

Searching for alternative therapies to treat mastitis and control *T. pyogenes*, this study evaluated the use of the *Escherichia* phage vB_EcoM-UFV13 (UFV13) (Duarte et al., 2016), to disrupt *T. pyogenes* biofilms. We performed a biofilm assay at different multiplicities of infection (MOI) and analyzed UFV13 genome in terms of virion-associated peptidoglycan hydrolases (VAPGHs) seeking to understand the possible mechanisms involved in biofilm disruption.

## 2. Materials and methods

### *2.1* Bacteriophage vB_EcoM-UFV13

#### 2.1.1 Sample standardization and viral isolation

The bacteriophage UFV13 was isolated from samples collected from the Viçosa sewerage system, Minas Gerais, Brazil (Dias et al., 2013; Sambrook et al., 2001). Briefly, these samples were centrifuged at 12,000xg at 4 ºC for 15 min and the supernatant was firstly filtered in a 0.45 µm pore-size PES membrane followed by a second filtration through a 0.22 µm filter (Millipore, Billerica, MA, USA). 100 µL of the viral suspension was incubated (37 ºC, 30 min) with 900 µL of logarithmic phase (O.D ~ 0.7) *Escherichia coli* 30 culture to allow for phage adsorption. This *E. coli* strain was isolated from dairy cows with clinical mastitis and kindly provided by EMBRAPA Dairy Cattle (Juiz de Fora, Minas Gerais, Brazil). The mixture was then plated using the standard soft agar overlay technique and incubated overnight at 37 ºC. The lysis plates were harvested from plates, propagated and purified by a three-step

chromatography protocol (desalting – anion exchange – desalting columns) (Äkta chromatography system, GE Healthcare Life Sciences). The viral titre was determined using a well-established protocol (Sambrook et al., 2001). Stocks were added to the phage collection of the Laboratório de Imunovirologia Molecular (LIMV) at Universidade Federal de Viçosa (UFV).and kept at 4 ºC.

### 2.1.2 Morphology analysis

To analyze virus morphology, 10 µl of viral suspension was placed into a FormVar®-coated grid and incubated at room temperature for 5 min. Following this, excess liquid was removed using blotting with a filter paper aid. The phage particles were negatively contrasted with 2% of uranyl acetate for 20 sec. The grids were then visualized using a Zeiss EM 109 electron microscopy at 250,000x magnification. Electron microscopy was conducted at Núcleo de Microscopia e Microanálise (NMM) at UFV. Images were analyzed using ImageJ (Abràmoff et al., 2004; Schneider et al., 2012) to measure the length and diameter of viral capsid. vB_EcoM-UFV13 was classified according to criteria established by the International Committee on Taxonomy of Viruses (ICTV).

## *2.2* Biofilm assays

### 2.2.1 Strains and growth conditions

A biofilm formation assay was performed using *T. pyogenes* lineage 3934 that was kindly provided by the curator, Dr. Maria Aparecida Vasconcelos Paiva Brito, of the "Agribusiness Interest Microorganisms Collection of Embrapa Dairy Cattle" (Juiz de Fora, Brazil). It was grown on Brain Heart Infusion Agar (BHI) supplemented with 5% defibrinated sheep's blood and maintained at 37 ºC for 48 h in a 5% $CO_2$

atmosphere. Single colonies were cultivated on BHI broth and incubated at 37 ºC with vigorous shaking during the exponential growth phase ($OD_{600nm}$ 0.1 (~$10^6$ CFU/ml)).

The ability of *T. pyogenes* to form biofilms was assessed on 96-well microtiter plate following the method described by Weiss-Muszkat et al. (2010). Control wells contained 200 µL of *T. pyogenes* culture at a final concentration of $10^5$ CFU/ml and treated groups received the same bacterial concentration and distinct viral dilutions in order to get the multiplicity of infection (MOI) 10, 1 and 0.1.

The bacterial population density ($OD_{600nm}$) was measured using a Multiskan™ GO Spectrophotometer (Thermo Scientific, EUA) after incubation at 37 ºC, for 24 h. Culture medium was then discarded, and the wells washed twice with phosphate-buffered saline (PBS; NaCl 0.13 M, KCl 2mM, $Na_2HPO_4$ 9mM, $KH_2PO_4$ 1 mM, pH 7.2) to remove unattached cells. Adherent cells were stained with 0.1% (w/v) crystal violet (CV) for 30 min at room temperature. Afterward, wells were washed four times with PBS and air dried for one hour. The bound dye was dissolved in 250 µL ethanol-acetone (80:20 v/v) and after 30 min of room temperature incubation, 200 µL of sample was collected and transferred to a new plate for absorbance measurement ($Abs_{590nm}$).

### 2.2.2 Biofilm cell count

In order to establish if phage infection reduced the number of planktonic and sessile cells, viable cell counts were performed. For planktonic cell counting, a serial ten-fold dilution was performed in saline buffer and 100 µL aliquots were spread on BHI Agar supplemented with 5% defibrinated sheep's blood, maintained at 37 ºC for 48 h in a 5% $CO_2$ atmosphere.

Sessile cells were recovered and measured as described by Asséré et al. (2008), with some modifications. Briefly, pegs were broken and transferred to microcentrifuge tubes filled with saline buffer (0.9% w/v) and placed into a sonication bath at 47 kHz,

for 15 min. Detached cells were diluted, plated and incubated as described for planktonic bacteria.

### 2.2.3 Scanning electron microscopy

Scanning electron microscopy (SEM) was performed on MBEC (*Minimum Biofilm Eradication Concentration*) Assays™ pegs (Innovatech, Edmonton, AB, Canada), according to the company's instructions. Groups were arranged as described in the item 2.2.1, however only the MOI 10 was used as the treated group.

After incubation (37 ºC, 24 h), the recovered MBEC pegs were washed twice with 0.2 M PBS buffer pH 7.2; and fixed with 2.5% (v/v) glutaraldehyde at room temperature for 2 h. The pegs were dehydrated in an increasing ethanolic gradient (30% to 100% v/v), for 10 min at each step, with three repetitions at the highest concentration. Afterward, critical point drying was performed on a BAL-TEC model 030 Critical Point Dryer (BAL-TEC AG Föhrenweg, Balzers, Liechtenstein), metallized with gold and, finally, analyzed using Leo 1430 VP scanning electron microscope at Núcleo de Microscopia e Microanálise (NMM) with an accelerating voltage 20 kV.

### 2.2.4 Statistical analysis

All assays were performed in triplicate and statistical significance was evaluated by one-way ANOVA using GraphPad Prism program (GraphPad Software, La Jolla CA USA).

## *2.3* Genome analysis

### *2.3.1* Genome extraction

Viral suspension was concentrated by adding polyethylene glycol 8000 (PEG-8000) 10% (w/v) and kept at 4 ºC, for at least 12 h. After this time, the suspension was centrifuged 12,000xg (15 min, 4 ºC) and the pellet suspended in SM buffer (5.8 g/L NaCl, 2.0 g $MgSO_4.7H_2O$, 50 ml Tris-HCl 1M, 5 ml gelatin 2%, pH 7.5). An equal volume of chloroform was added and after a brief agitation, it was centrifuged (4,500xg, 15 min, 4 ºC) until phase separation. The aqueous phase was discarded, and the viral DNA was extracted using the proteinase K phenol/chloroform method, as described by Sambrook et al. (2001). The DNA concentration was estimated spectrophotometrically using a NanoDrop 2000c (Thermo Scientific, EUA).

The viral genome size was estimated by PFGE in a 1% (w/v) low-melting-point agarose gel in 0.5X TBE buffer (TBE 1X: Tris 0.89 M, borate 0.89 M and EDTA 0.02 M) for 14 hours at 6 V/cm and 14 ºC, with a switch time of 5 to 10 sec. The gel was stained for 20 min with ethidium bromide (0.5 μg/ml).

### *2.3.2* Genome sequence

The UFV13 genome was sequenced with paired-end reads using Illumina HiSeq 2500 by Macrogen (Seoul, Korea). The sequenced reads were analyzed using DNASTAR Lasergene Genomics Suite (Madison, WI, USA). *De novo* assembling was performed using SeqMan NGen12 software and gaps were closed with SeqMan Pro software. *Escherichia* phage UFV13 genome was opened to be collinear with *Yersinia phage* PST and the open reading frames (ORFs) were predicted and functionally annotated using MyRast software (Overbeek et al., 2014).

### *2.3.3* Bioinformatic analysis

To understand the mechanism involved in biofilm reduction, the phage genome was analyzed looking for enzymes that could act on exopolymers present in biofilm structure. Two different approaches were used in order to identify viral hydrolases: Viral proteins considered as hydrolases were identified with PHYpred (Ding et al., 2016) and forwarded to HyPe for identification and classification (Sharma et al., 2016).

Motifs conserved in the viral protein sequences were identified using the Pfam database (Finn et al., 2016), Phyre2 (Kelley et al., 2015), Swiss-model (Biasini et al., 2014) and Batch Web CD-Search Tool (Marchler-Bauer et al., 2013). The alignments were performed using ClustalW2 multiple alignment tool and edited on Sequence Manipulation Suite (Stothard, 2000).

## 3. Results

### 3.1 Isolation and morphological characterization

*Escherichia* phage UFV13 was isolated from samples collected from the Viçosa sewerage system (Minas Gerais, Brazil) following three single plaque platings to ensure that a single virus was isolated. After phage purification, stocks showed a titer of 1.0 x $10^8$ PFU/ml, and these were used for all subsequent assays.

Phage plaque formed in double-layer agar showed a 1 mm clear lytic zone with a surrounding halo (Supplementary Figure 1A), which is indicative of phage-derived enzymes able to destroy bacterial envelopes (Jurczak-Kurek et al., 2016). Virion morphological analysis revealed that this phage belongs to the *Caudovirales* order,

*Myoviridae* family, morphotype A1 (Supplementary Figure 1B) with a total length of 102 nm and an isometric capsid (72 nm in length and width).

### 3.2 Biofilm assays

Using the standard crystal violet (CV) assay, we were able to detect a statistically significant reduction in biofilm formation (Figure 1) but only at a MOI of 10, followed by a decrease in the final absorbance value after the incubation period (Supplementary Figure 2).

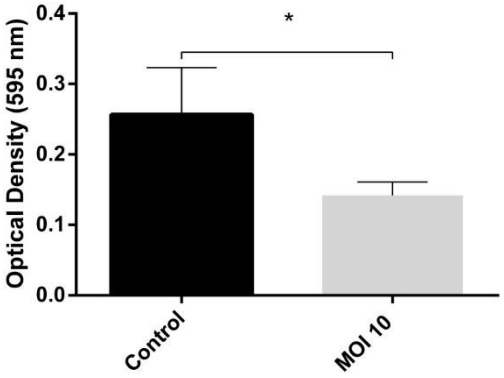


**Figure 1. Biofilm formation by *T. pyogenes* in the presence of the *Escherichia* phage UFV13 using CV assay as a method. Only MOI 10 is shown (* P ≤ 0.05).**

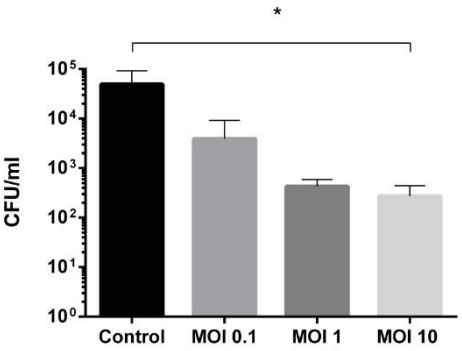


**Figure 2. *T. pyogenes* planktonic cell count. Statistically significant differences were not observed between control and treated groups (MOIs 0.1, 1 and 10).**

In order to quantify sessile and planktonic populations, culturable populations were recovered from MBEC pegs by ultrasound and plated, along with the floating cells. No statistically significant reduction was observed for planktonic cells in either MOIs (Figure 2), which indicates that the virus UFV13 is not able to infect or lyse *T. pyogenes*. In fact, there were no significant changes in viral titre after 24 h of incubation (Supplementary Figure 3). In relation to the biofilm cell count, only MOI 10 was statistically significant ($P \leq 0.05$) in reducing *T. pyogenes* cell-adhesion (Figure 3), which corroborates with the CV assay.

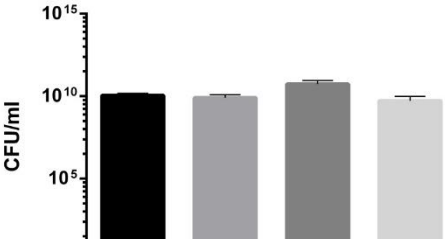


**Figure 3. *T. pyogenes* sessile cell count. A statistically significant difference was observed using only MOI 10 (* P ≤ 0.05).**

The scanning electron microscopy (SEM) approach was employed to confirm the previous results obtained by CV and sonication bath assays. SEM showed a decrease in cell adhesion using either the higher MOI, which we can see in Figure 4 where a diffuse biofilm formation is observed in the control group (Figure 4A), or it was possible to observe growth only at the air-liquid interface in the treated group (Figure 4B).

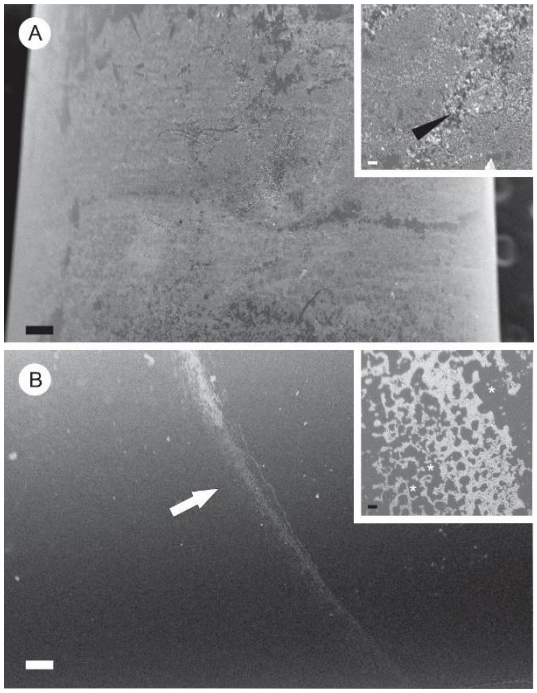


**Figure 4. Scanning electron microscopy (SEM) – A. Diffuse bacteria growth and biofilm formation by *T. pyogenes* (control). The major detail (arrowhead) shows extracellular matrix formation. B – Bacterial growth only at air-liquid interface when the phage UFV13 is added (arrow white). It is possible to observe in detail failures in the cellular layer as well as an absence of extracellular matrix (asterisks). Bars on figures A and B measure 200 µm and the detail bar value is 10 µm.**

### 3.3 Genome analysis

A genome size of nearly 170 kb (Supplementary Figure 4) was estimated by PFGE. DNA sequencing and assembly resulted in a single contig of 165,772 bp (570-fold coverage), with an average GC content of 34.8%. It displays high similarity to the genomes of *Shigella* phage Shfl2 and *Yersinia* phage PST (data not shown).

In order to investigate UFV13 genetic capability to produce putative VAPGHs, the genome was annotated revealing 269 ORFs, of which 48 were identified as virion proteins. Hydrolase domains were predicted in eight of these proteins (ORFs 31, 124, 153, 157, 160, 188, 245 and 246) using a compilation of two computational tools (PHYpred and HyPe). These proteins are homologs to protein Soc.1 from *Shigella* phage Shfl2 and some *Escherichia* phage T4 proteins: internal head protein 3 (IP3), baseplate lysozyme (gp5), baseplate wedge components (gp7, gp10 and gp25), hinge connector of tail fiber proximal connector (gp36) and tail fibers (gp37).

Based on their substrate specificity, five proteins (Soc.1, gp5, gp10, gp25 and gp37) were grouped as N-acetylmuramoyl-L-alanine amidases, one classified as peptidase (IP3), one as an enzyme that acts on the peptidoglycan chain (gp36) and one unclassified as amidase (gp7) (Table 1).

To identify conserved protein domains, three different servers (Pfam, Phyre2 and Swiss-model) were utilized (Table 2). An absence of domain information was verified for three viral proteins (Soc.1, IP3 and gp7) when Pfam

**Table 1. Eight vB_EcoM-UFV13 virion proteins with hydrolase domain were identified and categorized according theirs sites of action. Accession number, when available, is shown in parenthesis.**

| ORF | *E-value | **Amidase class | Feature |
|---|---|---|---|
| 31 | 0.99 | A | Cell wall hydrolase/autolysin |
| 124 | 0.99 | B | Peptidase (AIW13235.1) |
| 153 | 0.97 | A | Cell wall hydrolase CwlJ |
| 157 | 0.92 | E | LD-carboxypeptidase family protein |
| 160 | 0.83 | A | N-acetylmuramoyl-L-alanine amidase family |
| 188 | 0.64 | A | N-acetylmuramoyl-L-alanine amidase CwlD (AIY73246.1) |
| 245 | 0.92 | C | Membrane-bound lytic murein transglycosylase D (AGE87472.1) |
| 246 | 0.99 | A | N-acetyl-anhydromuranmyl-L-alanine amidase (AGE87562.1) |

* E-value was obtained from PHYpred;

** Classification according to HyPe software.

**Table 2. 8 of 48 gene-encoding virion structural proteins with hydrolase domain were aligned using three different databases. ORF31 displayed also a sugar-binding domain.**

| ORF | Pfam | | Phyre | | | Swiss-Model | | |
|---|---|---|---|---|---|---|---|---|
| | Template information | E-value | Template information | Confidence (%) | Identity (%) | Template information | GMQE (0 – 1) | Identity (%) |
| 31 | * | - | Soc.1 (ccl2 lectin) | 40.60 | 42.00 | Hematopoetic Cell Kinase, SH3 domain | 0.33 | 18.42 |
| 124 | * | - | Hydrolase (*Vibrio cholerae*) | 16.70 | 48.00 | Apaf-1 related killer DARK | 0.09 | 15.00 |
| 153 | Phage_lysozyme (PF00959.18) | 1.7e-27 | gp5 | 100.00 | 99.00 | Tail-associated lysozyme | 0.98 | 99.13 |
| 157 | * | - | baseplate wedge protein gp7 | 100.00 | 100.00 | Baseplate wedge protein gp7 | 0.99 | 98.52 |

Phyre confidence represents the probability (from 0 to 100) that the match between vB_EcoM-UFV13 protein and template is a true homology. GMQE is the Swiss-Model global quality estimation and has a range from 0 to 1. Asterisk means an absence of template information.

| | | | | | | | | |
|---|---|---|---|---|---|---|---|---|
| 160 | T4 gp9/10-like (PF07880.10) | 2.8e-10 | Baseplate structural protein gp10 | 100.00 | 100.00 | Baseplate wedge protein gp10 | 0.99 | 99.34 |
| 188 | Gene 25-like lysozyme (PF04965.13) | 1.7e-16 | gp25 (hydrolase tail lysozyme) | 100.00 | 98.00 | Baseplate wedge protein gp25 | 0.97 | 98.47 |
| 245 | T4 gp36 PF03903.12 | 1.8e-10 | Large tail fiber protein p34 | 30.30 | 31.00 | Hyaluronidase, phage associated | 0.05 | 25.58 |
| 246 | Peptidase_S74 (PF13884.5) | 2.0e-12 | gp37 (l-shaped tail fiber protein) | 99.20 | 21.00 | Endo-N-acetylneuraminidase | 0.03 | 19.00 |

311 was used. However, interestingly, results for Soc.1 were found when Phyre2 and
312 Swiss-model were adopted. Soc.1 shows an identity with a sugar-binding domain of
313 the CCL2 lectin and with the SH3 domain of hematopoetic cells. Interestingly, SH3
314 domain is also found as a component of the B30 lysin of the streptococcal phage B30,
315 as described by Schmelcher et al. (2015). Once a hydrolase domain was predicted in
316 Soc.1, we also investigated the canonical Soc of the *T4virus*, which is identical to a
317 hypothetical protein of the Gram-positive *Clostridioides difficile* and other T4 related
318 phages (Supplementary Figure 5).

319 Alignment was performed in order to verify the identity of two lysozyme-
320 associated proteins (gp5 and gp25) and the distal component of the long tail fiber
321 (gp37) with some related T4-like viruses. Figure 5 shows that the *Escherichia* phage
322 UFV13 possesses, in terms of length and identity, gp5 and gp25 with high similarity
323 to Shfl2, ime09, T4 and phiD1. Investigating only the endopeptidase S74, the figure 6
324 reveals that UFV13 shares the same amino acid sequence with *Shigella* virus Shfl2
325 and *Escherichia* phage Ime09. Nevertheless, nine conserved amino acids were
326 identified when *E. coli* K1 and *B. subtilis* phage GA-1 have been included.
327 Interestingly, eight amino acids were common between the viruses UFV13, Shfl2,
328 Ime09 and GA-1.
329
330
331
332
333
334
335

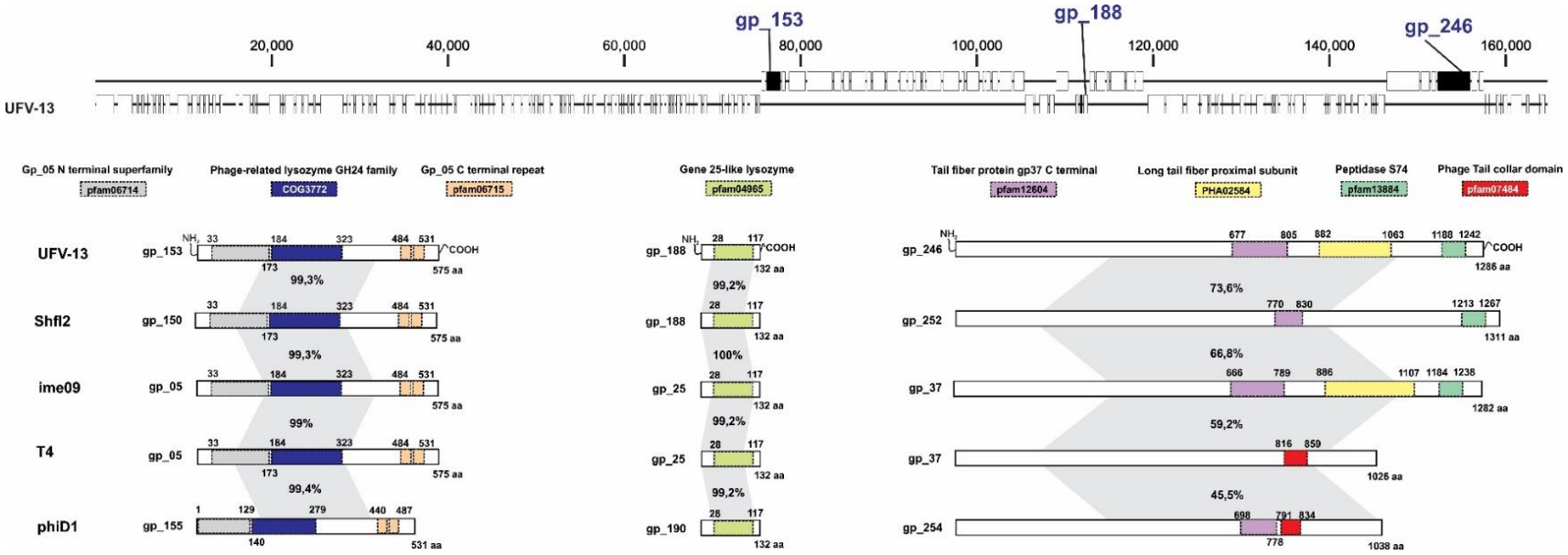


**Figure 5. Comparative analysis of three virion-associated peptidoglycan hydrolases (VAPGHs) identified (ORFs 153, 188 and 246) with other T4 viruses (Shfl2, ime09, T4 and phiD1). Different identities were seen only for the gp37 (ORF 246) associated with the serine endopeptidase S74.**

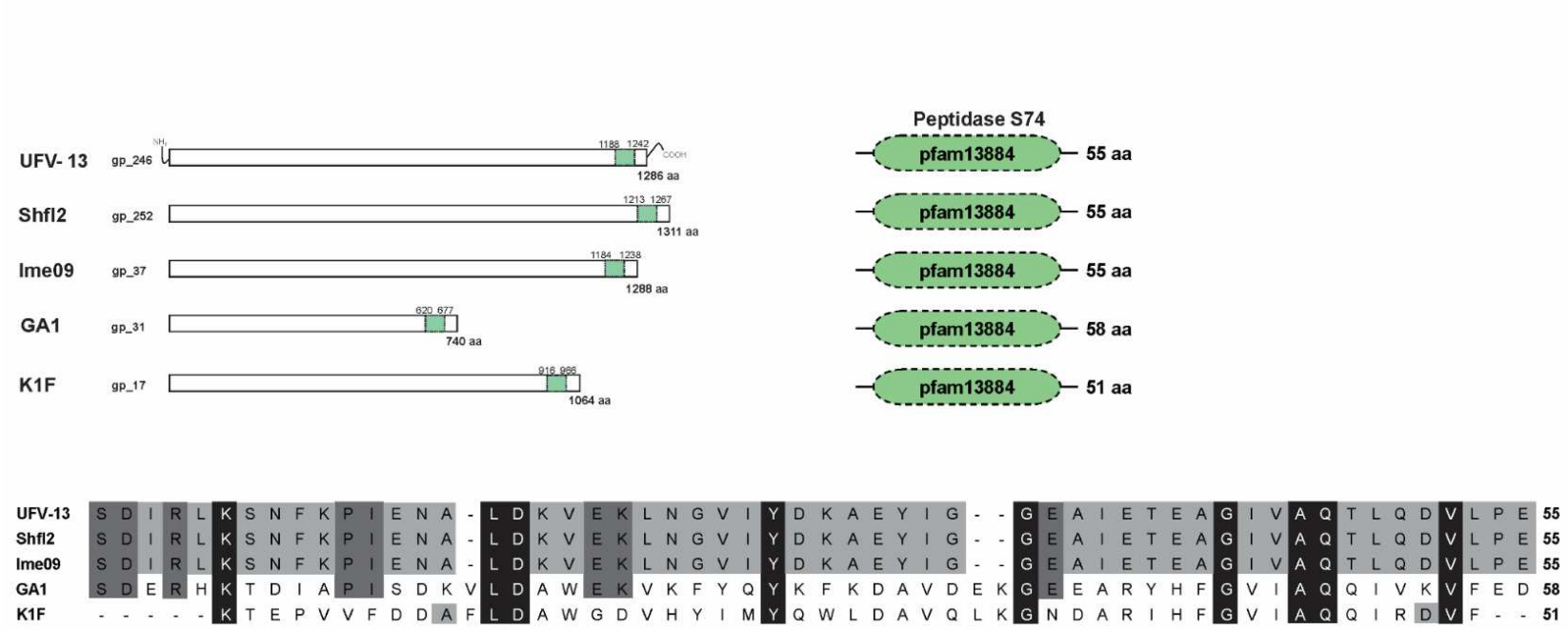


**Figure 6.** ***Escherichia*** **phage UFV13 peptidase S74 comparison analysis using Gram-negative (*Shigella* phage Shfl2, *Escherichia* phages Ime09 and K1F) and Gram-positive (*Bacillus subtilis* phage GA-1) viruses. Gray scale shows amino acid conservation among the viruses.**

## 4. Discussion

Urban sewage is a well-known environmental source of bacterial viruses, mainly due to high bacterial biodiversity, making it possible to discover new viruse types with interesting features. Phage plaque formed by *Escherichia* phage UFV13 in double-layer agar (Supplementary Figure 1A) shows viral enzymes that act on the bacterial cell envelope as described by Jurczak-Kurek et al. (2016) for the phage vB_Pae575P-4, able to lyse biofilm-forming *P. aeruginosa* strains. After propagation, the ion exchange chromatography method and viral titration successfully provided a homogeneous purified viral sample ($10^8$ PFU/ml). Capsid values found for the virus UFV13 allow its classification in the *Caudovirales* order, *Myoviridae* family (morphotype A1) (Ackermann, H. W. & Prangishvili, 2012) (Supplementary Figure 1B).

Considering the importance of *T. pyogenes* for dairy health, we evaluated the capability of the phage UFV13 to prevent biofilm formation by *T. pyogenes* employing three different approaches. The standard crystal violet assay was able to detect a statistically significant reduction in biofilm formation of *T. pyogenes* by the phage UFV13 only at the multiplicity of infection (MOI) 10 (Figure 1). Interestingly, the final optical density (after 24 h) was lower in the treated group MOI 10 ($P \leq 0.05$) even without a reduction in the planktonic cell count, as discussed below (Supplementary Figure 3). This was probably due to morphological changes, alterations in the cell size (Supplementary Figure 6) or compound production that potentially affected the final optical density.

Measuring culturable populations of sessile and planktonic cells, the phage UFV13 was shown as as capable of preventing biofilm formation without altering the

final planktonic cell count (Figure 2) keeping the same viral titration (Supplementary Figure 3) for both multiplicities of infection (MOIs), indicating that *T. pyogenes* is not susceptible to this virus. In relation to the biofilm cell count, only MOI 10 was statistically significant ($P \leq 0.05$) at reducing *T. pyogenes* cell-adhesion (Figure 3), which corroborates the CV assay. Qualitative observation of the biofilm formed by *T. pyogenes* in the absence (control) and presence (treatment) of the phage UFV13 was assessed using SEM. Diffuse cell colonization was observed (Figure 4A) in the control group with extracellular polymeric substance (EPS) production. Conversely, when MOI 10 was used (Figure 4B) growth was noted only at the air-liquid interface, failures in the cellular layer and absence of EPS production.

According to Bergey's Manual of Systematic Bacteriology, *Actinomyces* genus displays rhamnose such as whole-cell sugars (peptidoglycan type V) and the presence of FimA, the major fimbrial subunit. Both structures are *T4virus* receptors and could be involved in a primary recognition and attachment of the virus UFV13 (Rakhuba et al., 2010). Abedon (2011) describes how the phage's ability to adsorb the host cell is MOI and receptor dependent, which explains the results found for MOI 10 instead MOIs 1 and 0.1.

From the genome analysis, eight structural viral proteins and one lytic protein were highlighted and could be implicated in the biofilm disruption of *T. pyogenes* by vB_EcoM-UFV13, as Soc.1. The small outer capsid protein (Soc) is considered an auxiliary virus protein that acts as a clamp to stabilize the capsid at the end of the process of viral particle assembly and it is associated with the virus surviving in adverse conditions (Qin et al., 2010). Interestingly, Soc.1 and Soc.2, two related capsid genes found in bacterial viruses T2, T6 and *Shigella virus* Shfl2 were observed for UFV13. Although the role of Soc.1 and Soc.2 are not well-established, the presence of

these two proteins indicates a mixed infection with *Shigella virus* Shfl2 and the occurrence of a process analogous to intron homing, where *segF* is substituted for *soc.1* and *soc.2* during a recombinational event (Belle et al., 2002). Indeed, *segF* was not observed for the phage UFV13. In this study, Soc.1 analysis revealed the presence of two domains, one being considered a sugar-binding site homolog for the monomeric Ccl2 lectin which binds to 1,3-fucosylated N-glycan structures (Schubert et al., 2012) and a cell wall hydrolase one (Tables 1 and 2). Interestingly, Soc of UFV13 has shown high sequence similarity with one identified in *Clostrioides difficile*, a Gram-positive bacteria, (Supplementary Figure 5) and another *T4virus*, leading to possible acquisition due to an interaction between the *T4virus* and a precedent Gram-positive host across evolution.

In the UFV13 genome, lysozyme T4 (T4lyz) and gp5 encode a glycoside hydrolase with both classified as belonging to family 24 according to the Carbohydrate-Active Enzymes database (CAZy) (Lombard et al., 2014). As shown in the figure 5, *Escherichia* phage UFV13 displays T4lyz and gp25 with high identity when compared to related *T4virus* Shfl2, ime09, T4 and phiD1. The bactericidal property of the T4lyz against Gram-positive and negative bacteria was assessed by Abouhmad et al. (2016). Cell viability reductions of 97.5%, 99.96% and 95% were observed, respectively, for *Micrococcus luteus* (lysodeikticus), *Escherichia coli* and *Pseudomonas mendocina*.

In the present study, two proteins that are involved on the baseplate composition (gp25 and gp10) were classified as N-acetylmuramoyl-L-alanine amidases (LytA). The presence of this amidase class is not strictly related to bacterial processes such as cell wall biosynthesis and cellular division, but the presence of homologous *lytA*-like

genes was demonstrated in both temperate viruses *Streptococcus pneumonia* (φHER and φB6) and *Bacillus subtilis* 168 prophage SPβ (Romero et al., 2004).

Results revealed that UFV13 internal protein 3 (IP3) was classified as a murein endopeptidase (similarity with *Vibrio tubiashii* ATCC19109) and showed 48% identity with a hydrolase from *Vibrio cholerae*, while gp7 and gp36 were, respectively, classified as a LD-carboxypeptidase protein and a membrane-bound lytic murein transglycosylase D (homology with *Cronobacter sakazakii* SP291). Interestingly, ORF 245 also showed an identity (25.58%) with a hyaluronidase associated with bacterial virus, an enzyme especially found in prophages that have *Streptococcus pyogenes* and *Streptococcus equi* as their hosts (Latka et al., 2017).

Another interesting result is related to the UFV13 long tail fiber protein gp37. This protein is a distal half-fiber segment that together with gp34, gp35 and gp36, is involved in T4 long tail fiber composition, with its domain 11 (D11) being responsible for host recognition (Bartual et al., 2010). In this study, gp37 from the virus UFV13 showed the presence of Peptidase S74 domain, which was similar to other *T4viruses* (Figure 6). Peptidase S74 domain is found in an endosialidase protein of bacterial viruses able to infect the polysialic acid (polySia)-encapsulated *Escherichia coli* K1 and also identified in *Bacillus subtilis* phage GA-1 (Stummeyer et al., 2005). Indeed, results showed that nine amino acids are conserved when UFV13 Peptidase S74 is aligned with *E. coli* K1 and *B. subtilis* phage GA-1 sequences. According to Bartual et al. (2010), T4 tail fiber genes are under constant evolutionary pressure to acquire specific receptor-binding determinants that allow the infection of new hosts even if they are considered taxonomically distant, which is provided by a framework for mutations that confers this plasticity, however the presence of this conserved amino

449 acid in different phages with specific and distinct hosts shows the importance of this
450 residue for protein functionality.

451 Roach and Donovan (2015) showed that polysaccharide depolymerases like
452 endorhamnosidases, endolsialidases, alginate lysases and hyaluronidases are identified
453 only in viruses that belong to the order *Caudovirales* and have a role in disrupting
454 biofilms allowing the phage to bind itself tightly to the cell surface so that the injection
455 can occur.

456 Considering this possible interaction between UFV13 VAPGHs and *T. pyogenes*
457 cell-wall components, we hypothesize that biofilm disruption can be explained by
458 bacterial metabolism changes as described elsewhere, and/or direct enzyme action on
459 biofilm structure. Fallico et al. (2011) have shown in *Lactococcus lactis* subsp. lactis
460 IL1403 a general molecular cell wall response (membrane stress proteins, d-
461 alanylation of cell wall lipoteichoic acids and proton motive force maintenance) to
462 recover it from the lytic virus c2 infection. Fernández et al. (2017) also demonstrated
463 bacterial metabolism shifting when the chimeric protein CHAPSH3b was used
464 (hydrolase HydH5 associated with lysostaphin cell wall binding domain) in controlling
465 biofilm development of *S. aureus* by the downregulation of protein-encoding genes
466 for bacterial autolysins, mainly due to AtlA, a related biofilm protein.

467 Although the *Escherichia* phage UFV13 is not able to infect *T. pyogenes*, it can
468 act in biofilm disruption. Based on proteins identified in the UFV13 genome, we
469 believe that the uncommon number of VAPGHs found for this virus (eight virion
470 proteins and the lysozyme T4) interfere with biofilm formation by interacting with *T.*
471 *pyogenes* cell wall components and/or biofilm extracellular polymeric substances
472 (EPS).

473

## 5. Conclusion

This study showed that the virus UFV13 isolated using an *E. coli* strain, acts to prevent biofilm formation by *T. pyogenes*. These two pathogens are associated with mastitis and uterine diseases in dairy cows. Although the exact action mechanism has not been determined, UFV13 genome sequencing has revealed a broad range of virion-associated hydrolases. We hypothesized that heterologous phages with a large number of VAPGHs may possess activity by nonspecific hydrolase action against unrelated hosts when employed at high MOI. Hence, future transcriptomic and differential proteomic research will help to define the exact biofilm inhibition mechanism.

## Competing interests

The authors declare that they have no competing interests.

## Author's contributions

Conception of the work: Vinícius da Silva Duarte, Roberto Sousa Dias and Sérgio Oliveira de Paula; laboratory techniques: Vinícius da Silva Duarte and Roberto Sousa Dias; *In silico* analysis: Vinícius da Silva Duarte, Andrew M. Kropinski, André da Silva Xavier, Camila Geovana Ferro and Pedro M. P. Vidigal Laboratory funding: Cynthia Canedo da Silva. All authors read and approved the final manuscript.

## Acknowledgements

We are grateful to the Núcleo de Análise de Biomoléculas and Núcleo de Microscopia e Microanálise of the Universidade Federal de Viçosa for providing the facilities to conduct the experiments. We also acknowledge the financial support from the following Brazilian agencies: Fundação de Amparo à Pesquisa do Estado de Minas

Gerais (Fapemig), Coordenacão de Aperfeiçoamento de Pessoal de Nível Superior (CAPES), Conselho Nacional de Desenvolvimento Científico e Tecnológico (CNPq), Financiadora de Estudos e Projetos (Finep), Sistema Nacional de Laboratórios em Nanotecnologias (SisNANO)/Ministério da ciência, tecnologia e Informação (MCTI). We are also grateful to the Empresa Brasileira de Pesquisa Agropecuária (EMBRAPA), Gado de Leite Farm, Juiz de Fora, Minas Gerais, Brazil, that kindly provided us with *Escherichia coli* 30.

## 6. References

Abedon, S.T., 2011. Lysis from without. Bacteriophage 1, 46–49. doi:10.4161/bact.1.1.13980

Abouhmad, A., Mamo, G., Dishisha, T., Amin, M.A., Hatti-Kaul, R., 2016. T4 lysozyme fused with cellulose-binding module for antimicrobial cellulosic wound dressing materials. J. Appl. Microbiol. 121, 115–125. doi:10.1111/jam.13146

Abràmofff, M.D., Magalhães, P.J., Ram, S.J., 2005. Image processing with ImageJ Part II. Biophotonics Int. 11, 36–43. doi:10.1117/1.3589100

Ackermann, H. W. & Prangishvili, D., 2012. Prokaryote viruses studied by electron microscopy. Arch. Virol. 157, 1843–1849. doi:10.1007/s00705-012-1383-y

Asséré, A., Oulahal, N., Carpentier, B., 2008. Comparative evaluation of methods for counting surviving biofilm cells adhering to a polyvinyl chloride surface exposed to chlorine or drying. J. Appl. Microbiol. 104, 1692–1702. doi:10.1111/j.1365-2672.2007.03711.x

Bartual, S.G., Otero, J.M., Garcia-Doval, C., Llamas-Saiz, A.L., Kahn, R., Fox,

523 G.C., van Raaij, M.J., 2010. Structure of the bacteriophage T4 long tail fiber
524 receptor-binding tip. Proc. Natl. Acad. Sci. U. S. A. 107, 20287–92.
525 doi:10.1073/pnas.1011218107
526 Belle, A., Landthaler, M., Shub, D.A., 2002. Intronless homing: Site-specific
527 endonuclease SegF of bacteriophage T4 mediates localized marker exclusion
528 analogous to homing endonucleases of group I introns. Genes Dev. 16, 351–362.
529 doi:10.1101/gad.960302
530 Biasini, M., Bienert, S., Waterhouse, A., Arnold, K., Studer, G., Schmidt, T.,
531 Kiefer, F., Cassarino, T.G., Bertoni, M., Bordoli, L., Schwede, T., 2014. SWISS-
532 MODEL: Modelling protein tertiary and quaternary structure using evolutionary
533 information. Nucleic Acids Res. 42, 252–258. doi:10.1093/nar/gku340
534 Dias, R.S., Eller, M.R., Duarte, V.S., Pereira, Â.L., Silva, C.C., Mantovani, H.C.,
535 Oliveira, L.L., De, E., Silva, A.M., De Paula, S.O., 2013. Use of phages against
536 antibiotic-resistant *Staphylococcus aureus* isolated from bovine mastitis. J. Anim.
537 Sci 91, 3930–3939. doi:10.2527/jas2012-5884
538 Duarte, V.S., Dias, R.S., Kropinski, A.M., Vidigal, P.M.P., Sousa, F.O., Xavier,
539 A.S., Silva, C.C., de Paula, S.O., 2016. Complete genome sequence of vB_EcoM-
540 UFV13, a new bacteriophage able to disrupt *Trueperella pyogenes* biofilm.
541 Genome Announc. 4. doi:10.1128/genomeA.01292-16
542 Ding, H., Yang, W., Tang, H., Feng, P.-M., Huang, J., Chen, W., Lin, H., 2016.
543 PHYPred: a tool for identifying bacteriophage enzymes and hydrolases. Virol. Sin.
544 31, 350–352. doi:10.1007/s12250-016-3740-6
545 Donlan, R.M., 2002. Biofilms: Microbial Life on Surfaces. Emerg. Infect. Dis. J.
546 8, 881. doi:10.3201/eid0809.020063
547 Fallico, V., Ross, R.P., Fitzgerald, G.F., McAuliffe, O., 2011. Genetic response to

548 bacteriophage infection in Lactococcus lactis reveals a four-strand approach
549 involving induction of membrane stress proteins, D-alanylation of the cell wall,
550 maintenance of proton motive force, and energy conservation. J. Virol. 85, 12032–
551 42. doi:10.1128/JVI.00275-11
552 Federman, C., Joo, J., Almario, J.A., Salaheen, S., Biswas, D., 2016. Citrus-
553 derived oil inhibits *Staphylococcus aureus* growth and alters its interactions with
554 bovine mammary cells. J. Dairy Sci. 99, 3667–3674. doi:10.3168/jds.2015-10538
555 Fernández, L., González, S., Campelo, A.B., Martínez, B., Rodríguez, A., García,
556 P., 2017. Downregulation of Autolysin-Encoding Genes by Phage-Derived Lytic
557 Proteins Inhibits Biofilm Formation in *Staphylococcus aureus*. Antimicrob.
558 Agents Chemother. 61, e02724-16. doi:10.1128/AAC.02724-16
559 Finn, R.D., Coggill, P., Eberhardt, R.Y., Eddy, S.R., Mistry, J., Mitchell, A.L.,
560 Potter, S.C., Punta, M., Qureshi, M., Sangrador-Vegas, A., Salazar, G.A., Tate, J.,
561 Bateman, A., 2016. The Pfam protein families database: Towards a more
562 sustainable future. Nucleic Acids Res. 44, D279–D285. doi:10.1093/nar/gkv1344
563 Golkar, Z., Bagasra, O., Gene Pace, D., 2014. Bacteriophage therapy: A potential
564 solution for the antibiotic resistance crisis. J. Infect. Dev. Ctries. 8, 129–136.
565 doi:10.3855/jidc.3573
566 Jost, B.H., Billington, S.J., 2005. *Arcanobacterium pyogenes*: Molecular
567 pathogenesis of an animal opportunist. Antonie van Leeuwenhoek, Int. J. Gen.
568 Mol. Microbiol. 88, 87–102. doi:10.1007/s10482-005-2316-5
569 Jurczak-Kurek, A., Gąsior, T., Nejman-Faleńczyk, B., Bloch, S., Dydecka, A.,
570 Topka, G., Necel, A., Jakubowska-Deredas, M., Narajczyk, M., Richert, M.,
571 Mieszkowska, A., Wróbel, B., Węgrzyn, G., Węgrzyn, A., 2016. Biodiversity of
572 bacteriophages: morphological and biological properties of a large group of phages

573 isolated from urban sewage. Sci. Rep. 6, 34338. doi:10.1038/srep34338
574 Kelley, L.A., Mezulis, S., Yates, C.M., Wass, M.N., Sternberg, M.J.E., 2015. The
575 Phyre2 web portal for protein modeling, prediction and analysis. Nat. Protoc. 10,
576 845–858.
577 Latka, A., Maciejewska, B., Majkowska-Skrobek, G., Briers, Y., Drulis-Kawa, Z.,
578 2017. Bacteriophage-encoded virion-associated enzymes to overcome the
579 carbohydrate barriers during the infection process. Appl. Microbiol. Biotechnol.
580 101, 3103–3119. doi:10.1007/s00253-017-8224-6
581 Lombard, V., Golaconda Ramulu, H., Drula, E., Coutinho, P.M., Henrissat, B.,
582 2014. The carbohydrate-active enzymes database (CAZy) in 2013. Nucleic Acids
583 Res. 42. doi:10.1093/nar/gkt1178
584 Marchler-Bauer, A., Zheng, C., Chitsaz, F., Derbyshire, M.K., Geer, L.Y., Geer,
585 R.C., Gonzales, N.R., Gwadz, M., Hurwitz, D.I., Lanczycki, C.J., Lu, F., Lu, S.,
586 Marchler, G.H., Song, J.S., Thanki, N., Yamashita, R.A., Zhang, D., Bryant, S.H.,
587 2013. CDD: Conserved domains and protein three-dimensional structure. Nucleic
588 Acids Res. 41. doi:10.1093/nar/gks1243
589 Olson, M.E., Ceri, H., Morck, D.W., Buret, A.G., Read, R.R., 2002. Biofilm
590 bacteria: Formation and comparative susceptibility to antibiotics. Can. J. Vet. Res.
591 66, 86–92.
592 Overbeek, R., Olson, R., Pusch, G.D., Olsen, G.J., Davis, J.J., Disz, T., Edwards,
593 R.A., Gerdes, S., Parrello, B., Shukla, M., Vonstein, V., Wattam, A.R., Xia, F.,
594 Stevens, R., 2014. The SEED and the Rapid Annotation of microbial genomes
595 using Subsystems Technology (RAST). Nucleic Acids Res. 42.
596 doi:10.1093/nar/gkt1226
597 Qin, L., Fokine, A., O'Donnell, E., Rao, V.B., Rossmann, M.G., 2010. Structure

598 of the Small Outer Capsid Protein, Soc: A Clamp for Stabilizing Capsids of T4-
599 like Phages. J. Mol. Biol. 395, 728–741. doi:10.1016/j.jmb.2009.10.007
600 Rakhuba, D. V., Kolomiets, E.I., Szwajcer Dey, E., Novik, G.I., 2010.
601 Bacteriophage receptors, mechanisms of phage adsorption and penetration into
602 host cell. Polish J. Microbiol. 59, 145–155. doi:10.1016/j.micres.2015.01.008.1.94
603 Roach, D.R., Donovan, D.M., 2015. Antimicrobial bacteriophage-derived proteins
604 and therapeutic applications. Bacteriophage 5, e1062590.
605 doi:10.1080/21597081.2015.1062590

606 Romero, P., Lopez, R., Garcia, E., 2004. Characterization of LytA-Like N-
607 Acetylmuramoyl-L-Alanine Amidases from Two New *Streptococcus mitis*
608 Bacteriophages Provides Insights into the Properties of the Major Pneumococcal
609 Autolysin. J. Bacteriol. 186, 8229–8239. doi:10.1128/JB.186.24.8229-8239.2004

610 Sambrook, J., Fritsch, E.F., Maniatis, T., 2001. Molecular Cloning: A Laboratory
611 Manual., New York. doi:574.873224 1/198

612 Schmelcher, M., Powell, A.M., Camp, M.J., Pohl, C.S., Donovan, D.M., 2015.
613 Synergistic streptococcal phage λSA2 and B30 endolysins kill streptococci in cow
614 milk and in a mouse model of mastitis. Appl. Microbiol. Biotechnol. 99, 8475–
615 8486. doi:10.1007/s00253-015-6579-09

616 Schneider, C.A., Rasband, W.S., Eliceiri, K.W., 2012. NIH Image to ImageJ: 25
617 years of image analysis. Nat. Methods. doi:10.1038/nmeth.2089
618 Schubert, M., Bleuler-Martinez, S., Butschi, A., Wälti, M.A., Egloff, P., Stutz, K.,
619 Yan, S., Wilson, I.B.H., Hengartner, M.O., Aebi, M., Allain, F.H.T., Künzler, M.,
620 2012. Plasticity of the β-trefoil protein fold in the recognition and control of

621 invertebrate predators and parasites by a fungal defence system. PLoS Pathog. 8.
622 doi:10.1371/journal.ppat.1002706

623 Sharma, A.K., Kumar, S., K., H., Dhakan, D.B., Sharma, V.K., 2016. Prediction
624 of peptidoglycan hydrolases- a new class of antibacterial proteins. BMC Genomics
625 17, 411. doi:10.1186/s12864-016-2753-8

626 Stummeyer, K., Dickmanns, A., Mühlenhoff, M., Gerardy-Schahn, R., Ficner, R.,
627 2005. Crystal structure of the polysialic acid-degrading endosialidase of
628 bacteriophage K1F. Nat. Struct. Mol. Biol. 12, 90–6. doi:10.1038/nsmb874

629 Wagener, K., Grunert, T., Prunner, I., Ehling-Schulz, M., Drillich, M., 2014.
630 Dynamics of uterine infections with *Escherichia coli*, *Streptococcus uberis* and
631 *Trueperella pyogenes* in post-partum dairy cows and their association with clinical
632 endometritis. Vet. J. 202, 527–532. doi:10.1016/j.tvjl.2014.08.023

633 Weiss-Muszkat, M., Shakh, D., Zhou, Y., Pinto, R., Belausov, E., Chapman, M.R.,
634 Sela, S., 2010. Biofilm formation by and multicellular behavior of *Escherichia coli*
635 O55:H7, an atypical enteropathogenic strain. Appl. Environ. Microbiol. 76, 1545–
636 1554. doi:10.1128/AEM.01395-09

637 Zhao, K., Tian, Y., Yue, B., Wang, H., Zhang, X., 2013. Virulence determinants
638 and biofilm production among *Trueperella pyogenes* recovered from abscesses of
639 captive forest musk deer. Arch. Microbiol. 195, 203–209. doi:10.1007/s00203-
640 013-0869-7

641

642

643

644

645

646

# Manuscrito 2

Genomic analysis and immune response in a murine mastitis model of vB_EcoM-UFV13, a potential biocontrol agent for use in dairy cows.

Scientific Reports – DOI: 10.1038/s41598-018-24896-w

# Genomic analysis and immune response in a murine mastitis model of vB_EcoM-UFV13, a potential biocontrol agent for use in dairy cows.

Vinícius da Silva Duarte[a], Roberto Sousa Dias[a], Andrew M. Kropinski[b], Stefano Campanaro[c], Laura Treu[c, d], Carolina Siqueira[e], Marcella Silva Vieira[e], Isabela da Silva Paes[e], Gabriele Rocha Santana[e], Franciele Martins[e], Josicelli Souza Crispim[a], André da Silva Xavier[f], Camila Geovana Ferro[g], Pedro M. P. Vidigal[h], Cynthia Canêdo da Silva[a], Sérgio Oliveira de Paula[e]

[a] Department of Microbiology, Federal University of Viçosa, Av. Peter Henry Rolfs, s/n, Campus Universitário, 36570-900, Viçosa, Minas Gerais, Brazil

[b] Departments of Food Science, and Pathobiology, University of Guelph, Guelph, Ontario N1G 2W1 Canada

[c] Department of Biology, University of Padova, Padova, Italy

[d] Department of Environmental Engineering, Technical University of Denmark, Miljoevej, Building 115, DK-2800 Kgs. Lyngby, Denmark

[e] Department of General Biology, Federal University of Viçosa, Av. Peter Henry Rolfs, s/n, Campus Universitário, 36570-900, Viçosa, Minas Gerais, Brazil

[f] Embrapa Maize and Sorghum, Rodovia MG 424, Sete Lagoas, Minas Gerais, Brazil

[g] Department of Plant Pathology, Federal University of Viçosa, Av. Peter Henry Rolfs, s/n, Campus Universitário, 36570-900, Viçosa, Minas Gerais, Brazil

[h] Núcleo de Análise de Biomoléculas (NuBioMol), Center of Biological Sciences, Federal University of Viçosa, Viçosa, Minas Gerais, Brazil

**Abstract**

Bovine mastitis remains the main cause of economic losses for dairy farmers. Mammary pathogenic *Escherichia coli* (MPEC) is related to an acute mastitis and its treatment is still based on the use of antibiotics. In the era of antimicrobial resistance (AMR), bacterial viruses (bacteriophages) present as an efficient treatment or prophylactic option. However this makes it essential that its genetic structure, stability and interaction with the host immune system be thoroughly characterized. The present study analyzed a novel, broad host-range anti-mastitis agent, the *T4virus* vB_EcoM-UFV13 in genomic terms, and its activity against a MPEC strain in an experimental *E. coli*-induced mastitis mouse model. 4,975 Single Nucleotide Polymorphisms (SNPs) were assigned between vB_EcoM-UFV13 and *E. coli* phage T4 genomes with high impact on coding sequences (CDS) (37.60 %) for virion proteins. Phylogenetic trees and genome analysis supported a recent infection mix among vB_EcoM-UFV13 and Shigella phage Shfl2. After a viral stability evaluation (e.g pH and temperature), intramammary administration (MOI 10) resulted in a 10-fold reduction in bacterial load. Furthermore, pro-inflammatory cytokines, such as IL-6 and TNF, were observed after viral treatment. This work brings

the whole characterization and immune response to vB_EcoM-UFV13, a biocontrol candidate for bovine mastitis.

## 1. Introduction

Bovine mastitis remains the main cause of economic losses for dairy farmers, estimated at $ (US)533 billion worldwide, as well as public health concerns, since low quality milk can be considered a vehicle for pathogen transmission[1–3].

Mastitis treatment is typically based on the use of short and long-acting antibiotics, respectively, during the lactation and dry period[4]. In terms of the lactation period and specifically regarding clinical mastitis, *Escherichia coli*, *Streptococcus uberis*, *Streptococcus dysgalactiae* and *Staphylococcus aureus* are the main etiological agents involved that have been routinely isolated[5]. Among these pathogens, mammary pathogenic *Escherichia coli* (MPEC) is responsible for an acute mastitis characterized by inflammation, increased somatic cell count (SCC) and impaired milk quality even after the infection has been cured[6].

Using *E. coli* strains obtained from different types of mastitis (*e.g* per-acute and persistent) and the non-pathogenic strain K71, Blum *et al*. (2017) performed a mammary immune response comparison in experimentally infected cows and noticed differences regarding TNF-α, IL-6 and IL-17 secretion levels for each MPEC.

Within the current scenario of widespread antibiotic-resistant bacteria, bacterial viruses present as an efficient therapeutic or prophylactic tool in

order to control different pathogens in dairy cows at different lactation stages. This is supported by current *in vitro* and *in vivo* assays[7–13].

Considered a model system in molecular biology, coliphage T4 has been studied since the 1940s and possesses about 300 genes organized in a 168.9 kb linear dsDNA with an average GC content of 34.5%[14]. Lytic viruses related to T4 have awoken interest for their application in phage therapy due the absence of lysogenic modules, a broad-host-range (from *Proteobacteria* to *Cyanobacteria* phyla) and, recently, the identification of virion-associated peptidoglycan hydrolases (VAPGHs), which are considered potential enzybiotics[15–17].

Indeed, T4 was used by Bruttin (2005) in the first safety test of phage therapy in humans and in immunological assays in order to elucidate the interactions between viruses, its host and the immune system. Bocian et al. (2016) investigated how purified T4 phage and T4-generated *E.coli* lysate impact immune cells differentiation, highlighting that lysis of Gram-negative bacteria by phages might not trigger excessive monocyte induction.

Currently, several studies have been exploited the use of mouse models in the attempt to evaluate novels anti-mastitis drugs mainly against *E. coli* and *S. aureus*[20–26]. The use of animal models is time and cost effective approach, along with a previous step for pre-clinical and clinical assays[27]. However, the absence of intrinsic cow factors can be considered a bottleneck when data is analyzed[28]

The aims of the present study were to characterize the *Escherichia* phage UFV13, a *T4virus*, in genomic, protein and physiological terms and

evaluate the immune response in an experimental *E. coli*-induced mastitis mouse model with the aim to use it in clinical trials to control mastitis in dairy cows.

## 2. Materials and methods

### 2.1. vB_EcoM-UFV13 isolation and purification

vB_EcoM-UFV13 (UFV13) was obtained from the sewerage system of Viçosa, Minas Gerais state, Brazil and was propagated on *Escherichia coli* 30 following the well-established Sambrook & Russell (2001) protocol. This virus belongs to the bacterial virus collection of the Laboratório de Imunovirologia Molecular (LIMV) at Universidade Federal de Viçosa (UFV), Viçosa city, Brazil.

After virus propagation, viral particles were purified by a three-step protocol using ion exchange and desalting columns in a chromatography system (ÄKTAprime plus, GE Healthcare Life Sciences, Uppsala, Sweden). Briefly, an initial step using HiTrap Desalting prepacked column (GE Healthcare Life Sciences, Uppsala, Sweden) was conducted to remove any salts used at virus propagation stages and the first two peaks were collected and purified using an ion exchange chromatography column, with specific fractions (7 to 11) driven to the final step, a new desalting process. For the anion exchange column, start (20 mM Tris-HC, pH 8.0) and elution buffers (20 mM Tris-HC, 1 M NaCl, pH 8.0) were used, whereas in desalting steps a phosphate buffer (20 mM sodium phosphate, 0.15 M NaCl, pH 7.0) was prepared. Flow rate of 5 $mL.min^{-1}$ was adopted for both columns. Finally, viral titer was measured at 37ºC by double-agar

overlay method[30] using *E. coli* 30 as the plating host. Phage stocks were stored at 4 ºC for further analysis.

## 2.2. Bioinformatic analysis

Phage genome extraction, sequencing and annotation methodologies are described according to Duarte et al. (2016). Hypothetical proteins were manually checked for homologs using UNIPROT database. Protein isoelectric point and molecular weight were obtained using ExPASy[32]. Putative tRNAs and Rho-independent transcription terminators were, respectively, predicted using tRNAscan-SE[33] and ARNnold web tool[34]. The Database of Gene Regulation in Bacteriophages (phiSITE)[35] was used in order to check the three major classes of promoters (early, middle and late) as well as to confirm putative Rho-independent terminators. The CGView Server was used to generate a UFV13 genome graphical map[36].

Nucleotide differences between UFV13 and Enterobacteria phage T4 (accession number AF158101.6) genomes were performed by checking reading alignments. High-quality Illumina reads were filtered and adaptor sequences were removed using Trimmomatic software (ver 0.33)[37] (parameters: LEADING:10 TRAILING:10 SLIDINGWINDOW:4:15 MINLEN:65) and aligned to Enterobacteria phage T4 using Bowtie2 software (v2.2.4)[38]. SAMtools[39] was used to convert the output SAM format to BAM format and, subsequently, to sort the BAM file. The sorted BAM file was processed with mpileup tool (SAMtools package) in order to extract the variants. The Binary Call Format (BCF) created was converted to VCF

format using BCFtools[39]. VCF file and Enterobacteria phage T4 genes were used as input for SnpEff program[40]. Only variants with predicted "high" or "moderate" impact on the protein-coding gene were analyzed.

Whole-genomes that represent each genus from the subfamily *Tevenvirinae* (*T4virus*, *Cc31virus*, *S16virus*, *Js98virus* and *Sp18virus)* deposited on the International Committee on Taxonomy of Viruses (ICTV) were downloaded from NCBI (accession numbers are provided in Supplementary Table 4) and aligned with UFV13 genome using Progressive MAUVE[41]. Whole-genome single nucleotide polymorphisms (SNPs) were extracted as described in Treu et al. (2014) and a SNP-based phylogenetic tree was constructed using PHYLIP package[43] and visualized by dendroscope[44]. Furthermore, a whole-genome phylogenetic tree was formulated aligning previously cited genomes from the *Tevenvirinae* subfamily. Online tools ClustalW2[45] and MAFTTT version 7[46] were used for multiple alignment. A neighbor-joining tree was drafted with MEGA7[47] and visualized with FigTree (http://tree.bio.ed.ac.uk/software/figtree/).

*In silico* bacterial hosts of UFV13 were predicted using HostPhinder[48].

### 2.3. vB_EcoM-UFV13 structural protein analysis

With the aim of obtaining the UFV13 structural protein profile, proteomic analysis were conducted.

Viral propagation/purification (see item 2.1) were conducted and phage particles concentrated by adding NaCl 1M and polyethylene glycol 8000 (PEG8000) 10% (w/v). The mixture was kept overnight at 4ºC. After a centrifugation (10,000 x*g*, 15 min), viral pellet was resuspended in 1 mL

of SM buffer and one volume of chloroform followed by centrifugation at 4,000 *g* for 10 min. An equal volume of trichloroacetic acid (TCA) 10% (v/v) was added to the supernatant and incubated on ice for 30 min. The precipitated viral proteins were collected by centrifugation (11,000 x*g*, 20 min), washed three times with acetone (11,000 x*g*, 10 min) and resuspended in water. The *BCA Protein Assay Kit* (Boster Biological Technology, Wuhan, China) was used to estimate protein concentrations.

For protein profiling, the viral proteins were separated via sodium dodecyl sulfate-polyacrilamide electrophoresis (SDS-PAGE) on a15% gel[49]. Protein bands were highlighted by Coomassie Brilliant Blue R-250 dye and removed as described by Shevchenko et al. (2007). Mass spectrum (MS) was acquired by matrix-assisted laser desorption-ionization time of flight (MALDI/TOF-TOF) (Ultraflex III - BRUKER DALTONICS). Spectra intervals between 500 and 3,500 kDa were selected and forwarded for MS/MS analysis. Results were obtained by Mascot™ (Matriz Science) software using the NCBl nr protein database. Only proteins and peptides indicated as significant by Mascot were considered for further analysis.

**2.4. Physiological features**

Physiological features were assessed in triplicate following the protocols described by Jurczak-Kurek et al. (2016). In each of the following cases, following treatment the phage preparation was diluted and tittered as described above (2.1).

### 2.4.1. pH stability

Viral capability at different acidic and alkaline pH values was evaluated. One mL of purified viruses were transferred to 9 mL LB medium with pH 2, pH 4, pH 7 (control), pH 10 and pH 12 at a 1:9 ratio and incubated for 1 h at 37 ºC, being proceeded by a 10-fold serial dilution and plating as described in item 2.1. After overnight incubation at 37 ºC, virus stability was determined by the percentage of viruses able to produce lysis plate.

### 2.4.2. Thermal stability

Thermal stability studies on LB-diluted phage suspensions were made at -20 °C, 40 °C, 62 °C and 95 °C, respectively, for 12 h, 40 min, 40 min and 5 min. After these periods, a serial 10-fold dilution was conducted and a specific aliquot was plated and incubated overnight at 37 ºC. Viruses that did not undergo any thermal treatment were used as a control.

### 2.4.3. Viral ability to propagate in different temperatures

Viral replication at different temperatures (4ºC, 22ºC, 30ºC and 37ºC) was assessed by spot-assay after 24 hours of incubation using a 10-fold serially diluted viral stock in LB medium.

### 2.4.4. Osmotic shock effect

In order to verify the effect of the osmotic shock on virus particles, a stock aliquot was transferred to TM buffer (10 mM Tris–HCl, 10 mM MgSO4; pH 7.2) with sodium chloride 4.5 M, incubated at room temperature for 15 min and quickly diluted in TM buffer without sodium chloride. Bacterial viruses incubated in TM buffer without sodium chloride were used as a control.

### 2.4.5. Antiviral resistance

Antiviral activity of sodium dodecyl sulfate (SDS), sodium lauroyl sarcosinate (Sarkosyl) and cetyltrimethylammonium bromide (CTAB) on virus particles was determined incubating a standardized viral suspension with 0.09% SDS (20 min at 45 °C), 0.1% CTB (1 min at 22 °C) and 0.1% Sarkosyl (10 min at 22 °C). Controls were done considering the same conditions for each antiviral compound but they were substituted for TM buffer.

### 2.4.6. Organic solvent effect

To study the effect of four different organic solvents, a viral suspension was added to 63% ethanol, 90% acetone, 90% chloroform and 50% dimethyl sulfoxide (DMSO). Mixtures were incubated for 1 h at 22 °C (ethanol and acetone), 1.5 h at 4 °C (chloroform) and 10 min at 4 °C (DMSO). In the next step, 10-fold dilutions in TM buffer (10 mM Tris–HCl, 10 mM $MgSO_4$; pH 7.2) were prepared and used for plating. Phages incubated in TM buffer under conditions described above, were used as a control.

## 2.5. Animal model and immune response

### 2.5.1. *Escherichia coli* 30 strain

The mammary-pathogenic *E. coli* 30 was isolated from a dairy cow with acute mastitis and kindly provided by Brazilian Agricultural Research Corporation (Empresa Brasileira de Pesquisa Agropecuária – EMBRAPA) Dairy Cattle (Juiz de Fora, Minas Gerais, Brazil). *E. coli* 30 was evaluated for its ability to form biofilm as well as for motility capacity. Motility assays

were conducted according to Deziel et al. (2001). Briefly, an overnight *E. coli* 30 aliquot was washed, suspended in distilled and sterilized water, and inoculated in King B medium (peptone 20 g/L, $MgSO_4.7H_2O$ 1.5 g/L, $K_2HPO_4$ 1.5 g/L), supplemented with 1.5, 0.5 and 0.3 % of agar for twitching, swarming and swimming tests, respectively. Biofilm assay followed the common crystal violet (CV) staining method[53]. After incubation (37 °C for 48h), wells were washed 3 times with PBS buffer to remove not adherent cells. CV was added at a minimum volume capable overcome bacterial suspension volume, making possible quantify all bacterial biomass, and incubated for 30 minutes at room temperature. To biomass quantify, CV was removed, wells washed with PBS, added ethanol to solubilize biomass internal CV crystals, and optical density measured at 560 nm. All assays were performed in triplicate.

Antimicrobial susceptibility test of *E. coli* 30 was assessed by disc diffusion assay using polisensidiscs for 25 different antibiotics (DME, Araçatuba, São Paulo, Brazil) following the manufacture's recommendation. The results were interpreted according to the standards of the Clinical and Laboratory Standards Institute (CLSI)[54].

### 2.5.2. *E. coli*-induced mastitis in mouse

With the aim to evaluate UFV13 effectiveness and the immune response against *E. coli* 30 *in vivo*, an experimental *E. coli*-induced mastitis mouse model was used. The trial followed the methodology described by Chandler (1971), with some modifications, and was approved by the Ethics Committee (Comissão de ética no uso de animais/UFV) according to the protocol 64/2016. Lactating Balb/c female mice (5 to 15 days) was

intraperitoneally anesthetized with 10% Ketamine and 2% Xylazine, with subsequent surgical operation of the mammary gland by cutting the teat canal of the last two abdominal ceilings (R5 and L5 of each animal were used) (Supplementary Figure 4). *E. coli* 30 (100 UFC/ml), PBS and phage served as the control groups, while phage plus bacteria was considered the treatment group (MOI 10). Viral addition was done four hours after bacterial inoculation. Three animals were used to perform each experimental group.

In order to assess the lytic activity of the phage vB_EcoM-UFV13 in mammary glands, animals were euthanized 48 hours after the treatment by anesthetic overdose. Infected mammary glands were removed and transferred to 1.5 ml of (PBS), macerated and serially diluted (1:10) in PBS buffer. A microdrop assay[56] was performed to estimate *E. coli 30* colony-forming unit (CFU).

Cytokines IL-6, TNF-α, IL-2, IFN-γ, IL-4, IL-10 and IL-17A obtained from macerated mammary gland (L5 and R5 from each animal was pooled) were simultaneously quantified by the Cytometric Bead Array kit (CBA, BD Bioscience) in a BD FACSVerse Flow cytometry following manufacturer's recommendations.

**2.6. Histological analysis**

For histology, mice were euthanized 48 hours after phage treatment. The mammary glands were removed and fixed in Karnovsky fixative (paraformaldehyde 4% and glutaraldehyde 4%, pH 7.3). Further, the tissues were embedded in paraffin and a 5 µm section was obtained by

296 microtomy, stained with hematoxylin and eosin (H & E) and observed under
297 light microscopy. The images were acquired under an Olympus DP73
298 microscope.
299
300 **2.7. Statistical analysis**
301 Statistical analysis was performed with GraphPad Instat 3 software
302 (GraphPad, La Jolla, CA, USA) using the one-way analysis of variance
303 (ANOVA) at 95% accuracy level to evaluate the differences between
304 mammary gland cytokine production under different conditions. This assay
305 was set up in triplicate and, for each animal, the two abdominal ceilings
306 were pooled into one sample. Tukey's test was used as *post hoc* test.
307
308 **3. Results and discussion**
309 **3.1. vB_EcoM-UFV13 genome analysis**
310 Bacteriophage UFV13 was isolated from samples obtained in the
311 sewage system of Viçosa, Minas Gerais, Brazil, a well-known source of
312 novel viruses[51].
313 From the genome sequence (165,772 bp, GC content 34.8%), 269
314 ORFs were predicted and annotated. The size is similar to that of other
315 members of the T4virus genus[57]. In addition, a total of ten tRNA encoding
316 genes (Gln, Leu, Gly, Pro, Ser, Thr, Met, Tyr, Asn and Arg) were identified
317 and are organized in a gene cluster without introns or pseudogenes (Figure
318 1). 13 ORFs showed an identity below 70% with the reference phage T4,
319 while 24 ORFs were annotated as hypothetical protein coding sequences.
320 ORFs 50 and 232 are, respectively, coding sequences for T2 and T6

bacteriophage proteins. 13 ORFs encode for Shigella phage proteins (pSs-1, Shfl2, Shf125875, SH7, SHBML-50-1). Genes for IpII and IpX were not identified in the UFV13 phage genome. Gene and protein information such as genomic coordinates, protein weight, pI and putative function for each UFV13 ORF are reported in Supplementary Table 1.

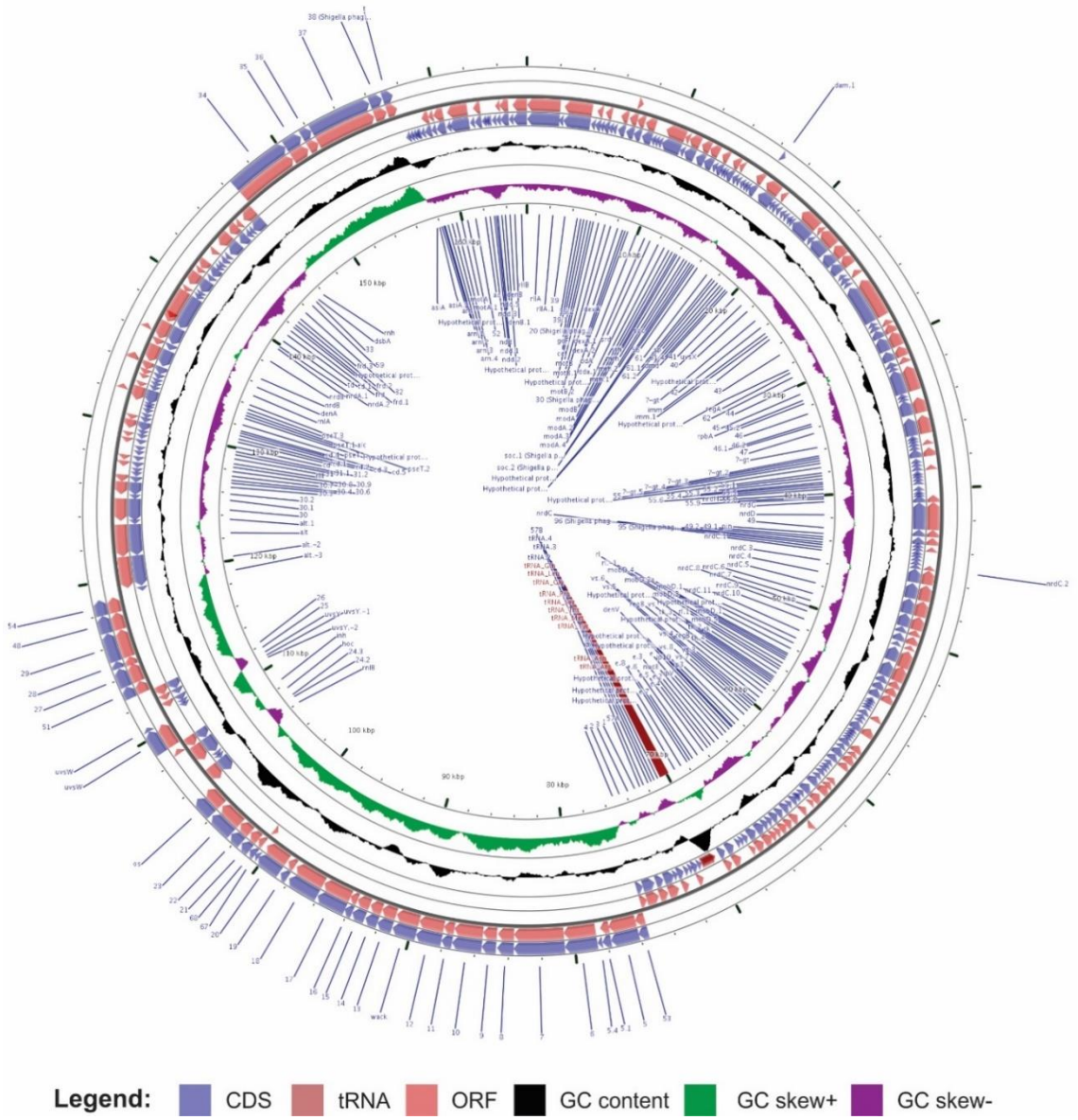


**Figure 1. Genome map of vB_EcoM-UFV13. The linear genome was circularized in order to improve its visualization. CDS, ORF, GC content, GC skew+ and GC skew- are reported in circles from outside inwards.**

Functional categorization of UFV13 genes (Supplementary table 2) revealed that nonessential and auxiliary genes mainly related to homing

endonucleases of introns such as *I-TevI*, *I-TevII* and *I-TevIII* are absent, as with some of their related introns like *mob* and *seg* genes (Table 1). Homing endonucleases of introns are considered systems associated with gene conversion events, transference of mobile elements and gene exclusion in mixed infections[14]. In fact, genome analysis suggests a recent mixed infection among UFV13 and Shigella phage Shfl2, once *segF* was substituted by *soc.1* and *soc.2* from Shigella phage Shfl2.

**Table 1. Genes not predicted in vB_EcoM-UFV13 based on the reference genome Enterobacteria phage T4 (accession number NC_000866). Function and relevance were integrally withdrawn from Miller et al. (2003).**

| Gene | Function | Relevance |
|---|---|---|
| ***mobA*** | Pseudogene of Mob site-specific DNA endonuclease | Nonessential |
| ***mobB*** | Putative site-specific intron-like DNA endonuclease | Nonessential |
| ***mobC*** | Putative intron-like DNA endonuclease | Auxiliary |
| ***mobD*** | Putative site-specific DNA endonuclease | Nonessential |
| ***mobE*** | Putative mobile endonuclease | Nonessential |
| ***segA*** | Site-specific intron-like DNA endonuclease | Nonessential |
| ***segB*** | Probable site-specific intron-like DNA endonuclease | Nonessential |
| ***segC*** | Site-specific intron-like DNA endonuclease | Nonessential |
| ***segD*** | Probable site-specific intron-like DNA endonuclease | Nonessential |
| ***segE*** | Probable site-specific intron-like DNA endonuclease | Nonessential |
| ***segF*** | Intron-like endonuclease. A probable fusion protein, generated from 56 and 69 by hopping of ribosomes across a pseudoknot, is larger | Nonessential |
| ***repEA*** | Protein auxiliary for initiation from *oriE* | Auxiliary |
| ***repEB*** | Protein required for initiation from *oriE* | Auxiliary |
| ***I-TevI*** | Intron-homing endonuclease | Nonessential |
| ***I-TevII*** | Endonuclease for nrdD-intron homing | Nonessential |
| ***I-TevIII*** | Defective intron homing endonuclease | Nonessential |
| ***rnaD*** | Stable RNA | Auxiliary |
| ***stp*** | Peptide modulating host restriction system | Auxiliary |
| ***nrdA*** | Ribonucleotide reductase α subunit | Auxiliary; *nrd*-defective hosts |

According to Belle et al. (2002), *segF* was absent in T2 phages, but the region is occupied by *soc.1* and *soc.2*.

Similarity analysis using the deposited genomes from Yersinia phage PST and Shigella phage Shfl2 showed that the bacteriophage UFV13 has 97% identity with both phages. However it has a larger percentage of aligned genome (96%) for the Shfl2, and 90% of genome aligned to phage PST (Supplementary figure 1). Comeau *et al*., (2014) characterized Yersinia phage PST genome, containing dsDNA with 167,785 bp, 35.3% GC content and 9 tRNAs, whose values are near to those found for the phage UFV13, with 34.8% GC content. Jun *et al*., (2016) identified 10 tRNAs for both pSs-1 and Shfl2 viruses infecting *Shigella* spp. as host. Despite little existing knowledge about tRNAs functioning in phage life cycles, high tRNAs numbers found in some bacteriophages could be proportional to phage genomes sizes and are related to a short latent period and high burst size value[60].

In the total, 35, 21 and 31, early, middle and late promoter regions respectively, were predicted, which corresponds to 73% of the promoters identified for the T4 genome (Supplementary table 3). As expected, no promoter regions for *mob* and *seg* genes were found, along with *I-TevII* and internal protein II (*ipII*).

Overall, termination of transcription in T4 bacteriophages occurs by an intrinsic termination signal, a stem-loop arrangement accompanied by a U-rich region, or a Rho-dependent termination mechanism[61]. For UFV13, 82 Rho-independent transcription terminators were predicted and compared against phiSITE database. 30 sequences displayed high identity with the reference phage, while five were not predicted but were found using the sequences available on the phiSITE. Terminators for the genes *45*, *5.4*/*6'*,

370 *34*/*35*, *35*, *37*, *nrdA*, *uvsY.-2* and *56*/*segF* were not found or even identified
371 using phiSITE (Table 2), while for the genes such as *regA*, *wac*, *24(b)* and
372 *30.9(b)* were, respectively, detected on the ORFs 52, 163, 178 and 208.
373 According to Miller *et al.* (2003), generally 34 terminators are found in the
374 T4 genome. The absence of terminators for the genes *nrdA* and *56/segF*
375 can be explained by their absence, since these genes were not annotated.
376 The significance of terminators within genes is unknown but have been
377 described for T4 phages[14].

378 A total of 5,071 filtered variants (4,975 SNPs, 86 insertions and 10
379 deletions) were identified (1 variant every 33 bases) between UFV13 and
380 T4. 83,656 effects were assigned and categorized (395 high (0.472%),
381 1,670 low (1.996%), 2,722 moderate (3.25%) and 78,869 modifier
382 (94.28%). The number of effects by functional class is: missense 2,879
383 (60.79%), nonsense 187 (3.95%) and silent 1,670 (35.26%). Considering
384 only genes with high or moderate variants, the mainly affected protein
385 category was that related to virion structural proteins, with gp7 being the
386 most affected (Figure 2).

387 **Table 2. Main features of the predicted Rho-independent transcription terminators. The asterisk means that absence of terminator**
388 **prediction by using Arnold or phiSITE programs.**

| Intergenic location | Genome position | Strand | Predicted Rho-independent transcription terminator site | Free energy (kcal/mol) |
|---|---|---|---|---|
| **39.1** | 4310..4341 | Minus | TTTAAATAAAAGGCCTTCGGGCCTTTAGCTTTATG | -10.60 |
| **soc** | 15135..15168 | Minus | AATTCAAGGACTCCTTCGGGAGTCCTTTTTCATT | -16.30 |
| **uvsX-40** | 21337..21371 | * | * | * |
| **Unknown gene** | 25445..25477 | Minus | TAAATCTAGGGACCTCCGGGTCCCTTTTTCACAC | -12.10 |
| **regA** | 28228..28259 | * | * | * |
| **α-gt** | 35109..35140 | Minus | ACAAAATAAAGGGCTTCGGCCCTTTAGCTTTATA | -10.60 |
| **α-gt.2** | 36378..36411 | Minus | TATGCGGATAGGAGCTTCGGCTCCTATATTGCTT | -14.20 |
| **55.3** | 38744..38775 | Minus | GTTTAGCTAAGGGCTTCGGCCCTTTTTGGATAAT | -10.60 |
| **nrdH** | 39707..39739 | Minus | GATTAAGACGGGCCCTCTGGGCCTTTCTTTCTCG | -8.80 |
| **Pin** | 43124..43166 | Minus | AAATACCCTTATCTATTTAAGGTAAGGGTTTATTA | -10.70 |
| **nrdC.11** | 51781..51818 | Minus | AATGATAGGGAGCCTTCGGGCTCCCTTTTTTATT | -18.40 |
| **rI.-1** | 55358..55389 | Minus | TAACATTAGTCTCCTTCGGGAGACTTTTTTCATT | -13.50 |
| **Vs** | 58098..58128 | Minus | TATATCAAGGGCGATATTGTCGCCCTTTTTCTTTA | -11.40 |
| **e.6** | 66465..66498 | Minus | ATAATGATAAGGGGCTTCGGCCCCTATTACTTGG | -13.90 |
| **RNA C** | 69462..69503 | Minus | GCTTAGCCCCAGCCGAAAGGTTGGGGCTTTTTA | -17.40 |
| **8** | 84691..84728 | Plus | TAAATTAAGGGAGCCCATGGGCTCCCTTTTTCTT | -16.50 |
| **wac** | 91126..91161 | * | * | * |
| **19** | 98662..98695 | Minus | AAGCAGGATGGGGATTTCTCCCCATTCaTTTTAT | -14.50 |
| **23** | 151432..151461 | Plus | AATTGAGGGAGCCTTCGGGTTCCCTTTTTCTTTA | -16.70 |
| **24(a)** | 105412..105447 | Plus | AAAACAAAGGGACCTTTCGGTCCCTTTTTATTTA | -12.30 |
| **24(b)** | 105467..105499 | * | * | * |
| **hoc** | 106999..107032 | Minus | TAATCATAAGGGGCTTCGGCCCCTTTCTTCATTT | -14.50 |
| **54** | 118931..118972 | Plus | CTAACAATGGGGACCGAAAGGTCCCCATATTTTT | -19.90 |
| **alt.1** | 123501..123532 | Minus | GATTACTAAAGGCCTTCGGGCCTTTAaTTTTATAA | -14.80 |
| **30.9(a)** | 128117..128154 | Minus | AAGTTGAGGACTCCTTCGGGAGTCCTTTTTTATT | -16.30 |
| **30.9(b)** | 128162..128198 | * | * | * |
| **nrdB** | 135904..135939 | Minus | TTAAGGAGTGGGCCGCAAGGCCCATTTTATTATG | -15.30 |
| **32** | 143116..143152 | Minus | ATTAATTGGGGACCTCTAGGGTCCCCTTTTTTAT | -14.90 |
| **T** | 157574..157618 | Plus | CAAACCCTCGTTGAATTCGTCGATGAGGGTTTTC | -11.10 |

| | | | | |
|---|---|---|---|---|
| **motA.1** | 160357..160396 | Minus | ATTTTAGGGAGAGCTTCGGCTCTCCCTTTTTTAT | -19.60 |
| **Ac** | 161968..162004 | Minus | TGCCCTTGCTACTTTATTGGTAGCAcTATATTATG | -8.60 |
| **denB.1** | 164573..164601 | Minus | CAAATAAATAAGGGCTTCGGCCCTTTTGTTTTAA | -10.60 |
| **5.4** | 78461..78499 | Minus | GTCACTCCGCCATGTGTTTCATATGGCTTTTTAA | -10.20 |
| **Stp** | 162165..162200 | Plus | TTCCTCACTGGCGTCCGAAGACGCCTTTAATTTT | -10.30 |
| **rIIB** | 164798..164834 | Plus | TCCTTAGTTAAGGGCCGAAGCCCTTATTTAAATT | -10.00 |

389

390 This protein is considered the second largest protein in the baseplate
391 and is one of the seven components associated with wedge assembly and
392 stability[62]. The large number of SNPs found in virion proteins reflects the
393 diversification of phage UFV13 from the classical T4 and can be associated
394 with the high capability to infect different bacterial genus such as
395 *Escherichia*, *Morganella* and *Shigella*, an uncommon phage feature (data
396 not shown).

397 In order to evaluate the phylogenetic relationship between UFV13 and
398 genera belonging to the subfamily *Tevenvirinae* (*T4virus*, *Cc31virus*,
399 *S16virus*, *Js98virus* and *Sp18virus*), a whole-genome tree was
400 constructed. The phylogenetic tree divided phages into four clusters with
401 vB_EcoM-UFV13 possessing the closest relationship with Shigella Shfl2
402 and Yersinia phage PST (Figure 3), a result also supported by the SNP-
403 based phylogenetic tree (Supplementary figure 2).

| Proteins (Functional categorization) | Number of protein-encoding genes | (%) |
|---|---|---|
| Virion proteins | 135 | 37.60 |
| DNA replication, recombination, repair, packaging and processing | 83 | 23.12 |
| Nucleotide metabolism | 32 | 8.91 |
| Transcription | 32 | 8.91 |
| Host or phage interactions | 25 | 6.96 |
| Without classification | 13 | 3.62 |
| Translation | 11 | 3.06 |
| Homing endonucleases and homologs | 9 | 2.51 |
| Host alteration/shutoff | 7 | 1.95 |
| Lysis | 5 | 1.39 |
| Predicted integral membrane or periplasmic proteins | 5 | 1.39 |
| Chaperonins/assembly catalysts | 2 | 0.56 |
| Total | 359 | 100.0 |

**Figure 2. Variants calling between vB_EcoM-UFV13 and Enterobacteria phage T4 were predicted using SnpEff. Only variants with predicted "high" or "moderate" impact on the protein-coding gene were analyzed and functionally categorized.**

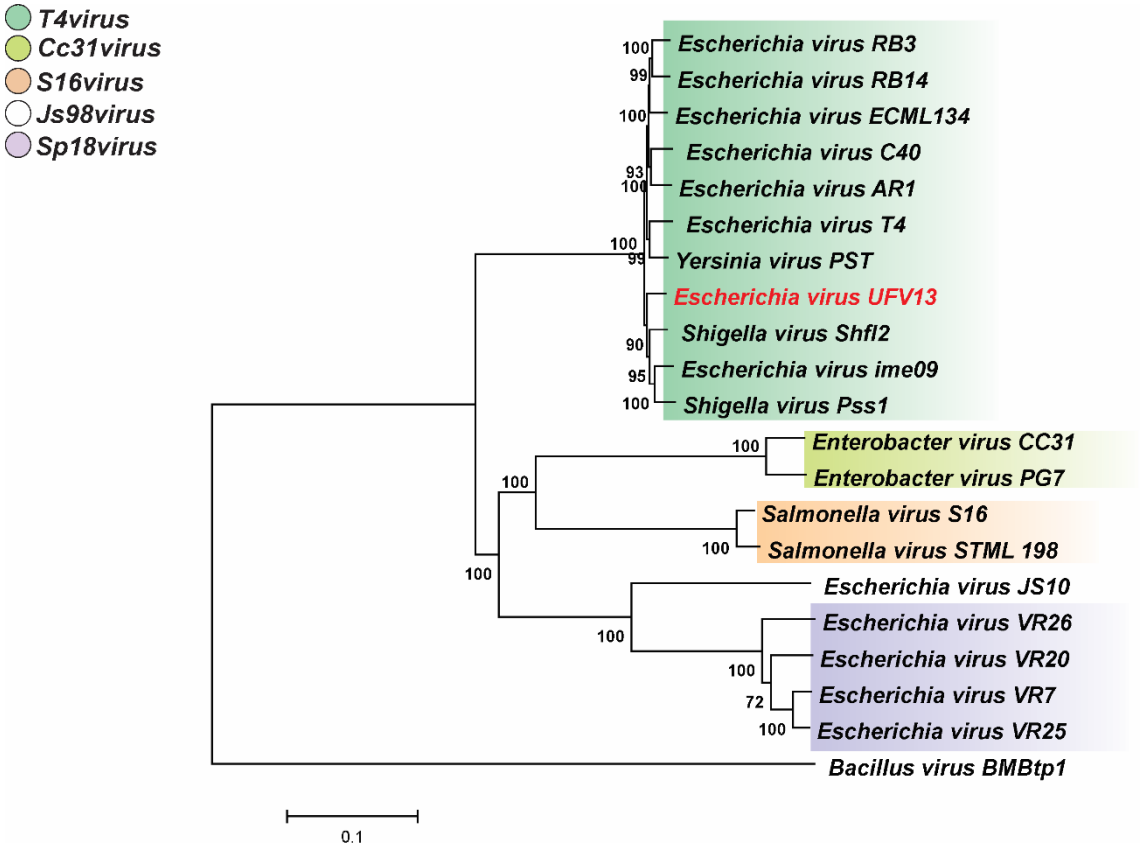


**Figure 3. Phylogenetic relationship between phage UFV13 and genera belonging to the subfamily *Tevenvirinae* (*T4virus*, *Cc31virus*, *S16virus*, *Js98virus* and *Sp18virus*). vB_EcoM-UFV13 is most closely related to *Shigella* phage Shfl2 and *Yersinia* phage PST, and is clearly a member of the *T4virus* genus.**

With the aim to establish the host range of phage UFV13 host range, *in silico* Host Phinder test was conducted. Four bacterial genera were predicted to be infected by UFV13: *Escherichia* (E-value: $5.9e^{-1}$), *Yersinia* (E-value: $5.8e^{-1}$), *Shigella* (E-value: $6.3e^{-1}$) and *Salmonella* (E-value: $1.1e^{-2}$).

### 3.2. Viral protein analysis

SDS PAGE analysis revealed the presence of eight proteins (Supplementary figure 3). Among these, four proteins were chosen and analyzed by MALDI/TOF-TOF, with the following being identified: UFV13_gp243 long tail fiber proximal subunit (139.95 kDa), *E. coli*

chaperonin GroL (57.36 kDa), Escherichia phage *vB_EcoM_112* major capsid protein (56.09 KDa) and *E. coli* outer membrane protein C (36.77 kDa). These proteins are deposited at UNIPROT under accession numbers A0A160CBJ3, A0A017I9Q1, A0A160CBB0 and A0A148HSV3, correspondingly. The presence of a common viral receptor (OmpC) and the chaperonin GroL highlights the need for viral purification enhancement. Viral isoelectric points are usually below six and some of them are able to bind to anion and cation exchange matrixes. However, host cell DNA is efficiently removed by cation exchanger columns, while host cell proteins are effectively eliminated by anion exchange[63].

### 3.3. Physiological features

Viral ability to survive in a wide range of adverse conditions is a desired characteristic for therapeutic as well as a biological control agents[64]. Thus, phage stability was evaluated in different physical and chemical conditions.

UFV13 was relatively stable within a pH range of 7.0 – 12.0. An approximate 1 log-fold reduction on viral titer was observed after incubation at pH 4.0 (18% of survivability) (Figure 4A). Interestingly, phage UFV13 was inactivated after 1 h of incubation at pH 2.0, but not at pH 12 (68% viral viability), which is indicative of considerable virion stability at basic pH values.

UFV13 was able to lyse *E. coli* at 30 ºC and 22 ºC with a plating efficiency of 69 and 56%, respectively (Figure 4B). No lysis plates were observed after storage at 4 ºC, which may be indicative of DNA injection without host lysis.

Viral thermal inactivation occurred in the extreme tested temperatures 95 and -20 °C (0 and 24% survival, respectively), while viral titer dropped to 50% when UFV13 was incubated for 40 min at 62 °C (Figure 4C). No significant reduction of phage titer was observed after thermal treatment at 40 °C.

It was found that osmotic pressure change, detergent and organic solvents determined a significant titer drop of UFV13. A survivability of 12% was observed when UFV13 underwent a rapid dilution from high-concentration NaCl buffer to low-concentration ones (Figure 4D). The anionic detergent Sarkosyl reduced the number of viable viral particles by 74%, while CTAB and SDS resulted in a complete inactivation of this virus (Figure 5). Anti-phage activity was also evidenced after exposure to ethanol, chloroform, acetone and DMSO.

Physiological features evaluated in this study are in accordance with Jurczak-Kurek et al. (2016). In a broad physiological study using 83 bacteriohages isolated from urban sewage, the same source of UFV13, it was verified that the vast majority of phages were sensitive to a temperature of 62ºC (survival below 70%), were able to survive in basic

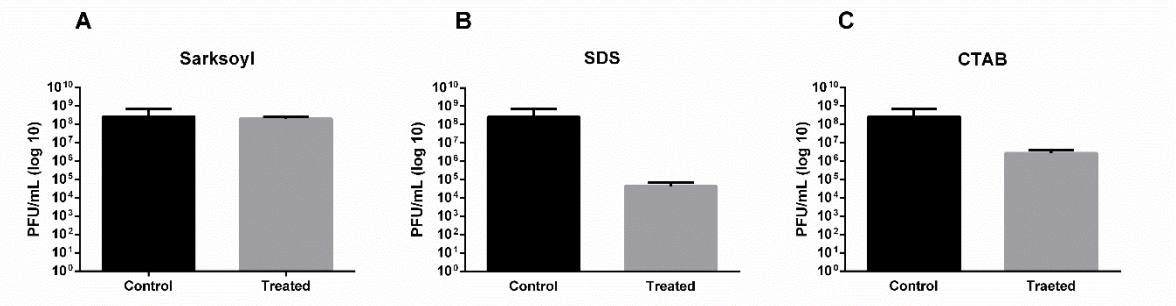


**Figure 4. Viral stability under anionic and cationic detergents showed that vB_EcoM-UFV13 was sensible in all conditions.**

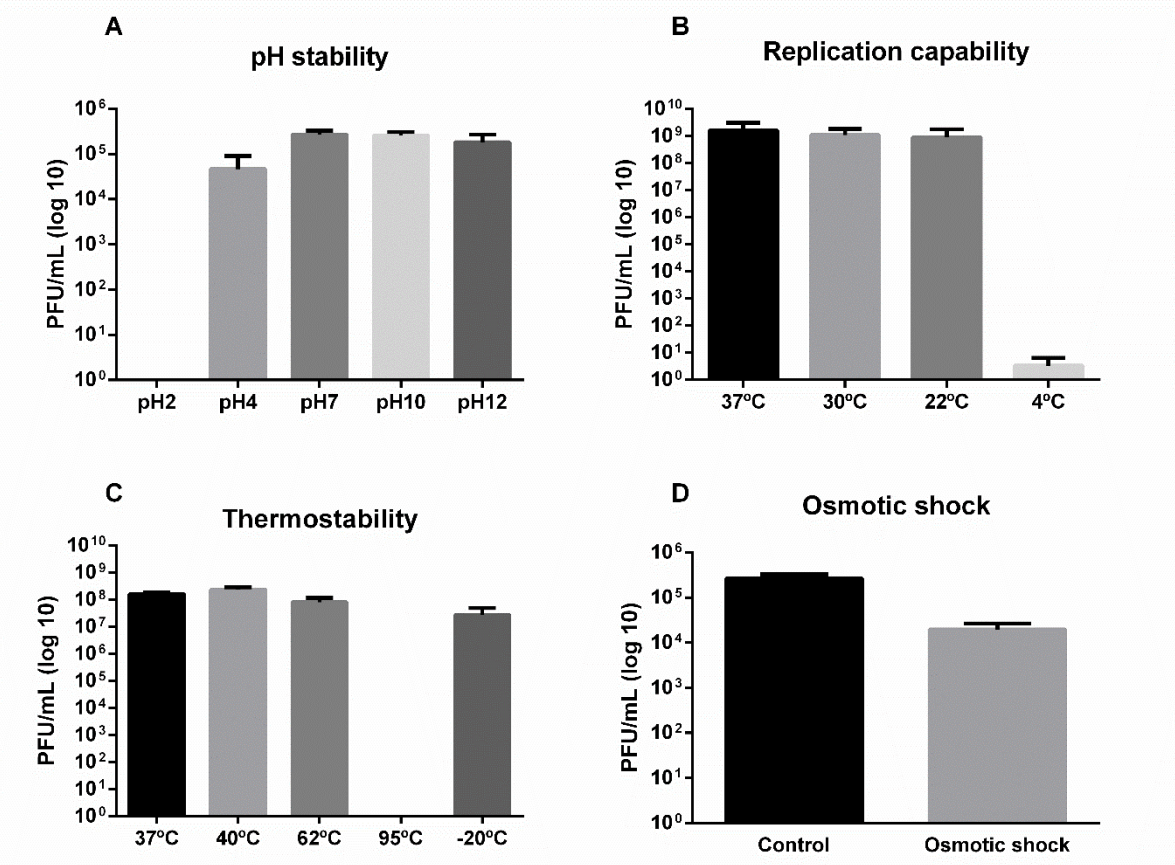


**Figure 5. The stability of vB_EcoM-UFV13 under different conditions was evaluated. A – reductions of 100, 82, 4 and 32% of viable particles were observed after incubations, respectively, at pHs 2, 4, 10 and 12.; B – vB_EcoM-UFV13 was able to replicate at 30 and 22 ºC with an efficiency of plating of 69 and 56%, corresponding; C – vB_EcoM-UFV13 was inactivated at 95 ºC for 5 min; D – Osmotic shock changing reduced in 84% viral viability.**

pHs (ranging from 10 to 12), were susceptible to detergents and organic solvents, except chloroform, and were also resistant to osmotic shock.

Viral stability assays have also been shown that UFV13 can survive in raw milk and it has potential capability to survive in mastitic milk. In general, mastitis can dampen the quality of raw milk composition, which includes increased levels of $Na^+/Cl^-$ and pH[65]. Evaluating a bacteriophage cocktail composed of two T4 phages in raw milk against *E. coli*, Porter et al. (2016) observed a 3.3- to 5.6-log reduction of bacterial growth over a 12-h

physiologic temperature. As discussed below (item 3.4), this study showed UFV13 activity against *E. coli* in lactating female mice.

### 3.4. *E. coli*-induced mastitis mouse model

*E. coli* 30, an isolate obtained from a dairy cow with acute mastitis, displays resistance to 14 of 25 evaluated antibiotics (Supplementary Table 5). This bacterium is resistant to at least three different antimicrobial drug classes, which allows its classification as a multi-drug resistant strain[66] Moreover, of the four types of virulence factors analyzed (biofilm forming capability and motility types: swarming, swimming and twitching) the *E. coli* 30 was positive for biofilm formation, swarming, and swimming, being negative only for the twitching (Supplementary Table 6). Studies correlated this virulence factors to an increase in pathogenicity and immune response evasion[67,68].

Nowadays, several studies have been used mouse mastitis models with the aim to evaluate potential anti-mastitis agents for use in dairy cows[20–25,69–71] although the authors are aware that cow factors are relevant in the mastitis establishment[28].

In order to evaluate UFV13's *in vivo* activity against an MPEC strain and immune response to this treatment, an *E. coli*-induced mastitis model was employed. A 10-fold reduction of bacterial load was observed after viral inoculation using MOI 10 (Supplementary Figure 5).

Seven different cytokines (IL-6, TNF-α, IL-2, IFN-γ, IL-4, IL-10 and IL-17A) were measured, however only IL-10, TNF-α and IL-6 were identified as statistically significant ($p < 0.05$) (Figure 6).

Studying whether T4 bacteriophage and T4-generated *E. coli* lysate influence cultures of peripheral blood mononuclear cells (PBMCs) activated or not by lipopolysaccharide (LPS), Bocian et al. (2016) observed that both preparations considerably increased the percentage of CD14+CD16−CD40+ and CD14+CD16−CD80+ monocytes in LPS-unactivated PBMCs cultures, as well as the concentration of IL-6 and IL-12. Notwithstanding, this result suggests that T4 bacteriophages may act both as a pro-inflammatory inducer, and also as CD40 activator, for this

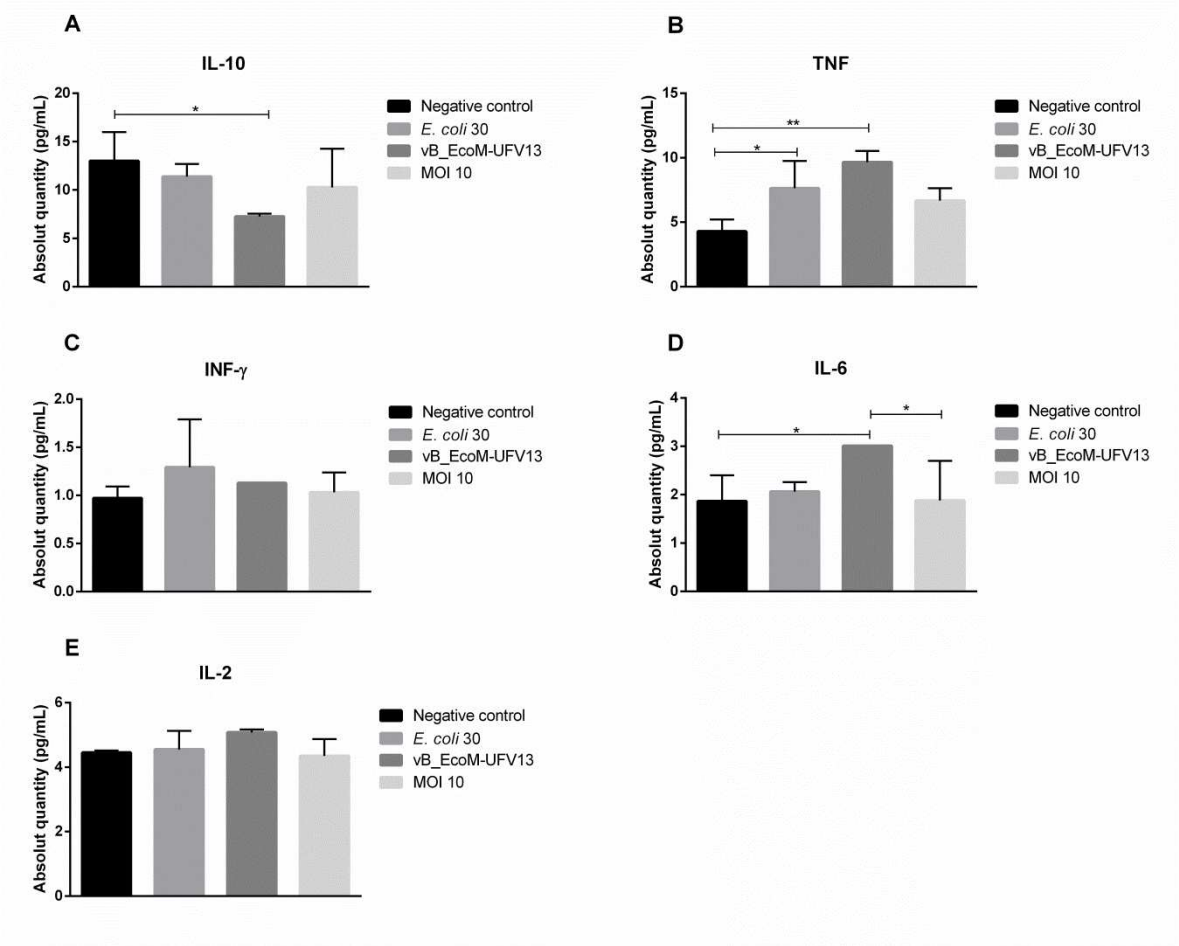


**Figure 6. Five different cytokines (IL-6, TNF-α, IL-2, IFN-γ and IL-10) were locally measured. Only IL-10, TNF-α and IL-6 were statistically significant (*$p < 0.05$; **$p < 0.01$) and is indicative of a pro-inflammatory pattern after phage treatment. IL-17A and IL-4 levels were not detected by the Cytometric Bead Array kit.**

503 reason the increased expression of IL-6, IL-10, and TNF-α as a
504 consequence of the presence of contaminating LPS left after the
505 purification step rather than a property of the virion.

506 In an *In vivo* assessment of cytokine patterns followed by a single-dose
507 T4 bacteriophage application in an *E. coli* induced mastitis mouse model,
508 our work indicates that IL-10 levels decreased locally in phage therapeutic
509 group when compared to the negative control (PBS buffer) (Figure 6A). IL-
510 10 has been extensively studied due its immunosuppressive features
511 associated with the downregulation of pro-inflammatory cytokines, such as
512 TNF-α and IFN-γ, and the resolution of the inflammatory process[72,73].
513 Evaluation of cytokine expression in the mammary gland in a mouse model
514 of *Streptococcus agalactiae* mastitis performed by Trigo et al. (2009)
515 revealed that the maximum concentration of IL-10 occurred after 72 hours
516 and was correlated with a decreased level of TNF-α. This finding is in
517 accordance with our results. Reduced IL-10 levels (Figure 6A) and
518 increased TNF- α (Figure 6B) and IL-6 (Figure 6D) is indicative of an
519 ongoing inflammatory process. In fact, when only *E. coli* 30 was inoculated,
520 an increased abundance of TNF-α was also observed when compared with
521 the negative control. Although phage and *E. coli* 30 were individually able
522 to induce an inflammatory response, phage treatment ($10^3$ PFU) did not
523 provoke an additive effect on the production of any pro-inflammatory

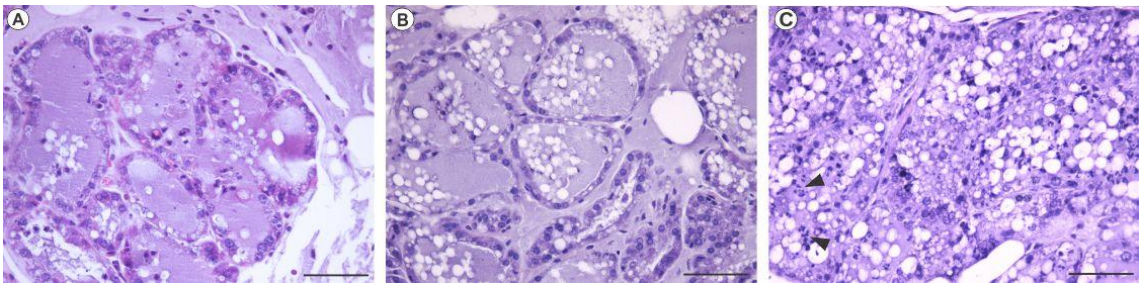


**Figure 7. Histological analysis of mammary gland after PBS (A), *E. coli* 30 (B) and treatment with vB_EcoM-UFV13 (C). In C, neutrophil infiltration (indicated by arrow head) was detected 48 hours after phage treatment using MOI 10. Bars: 100 micrometers.**

524 cytokine. Indeed, the IL-6 level diminished (Figure 6D) after phage
525 treatment. Different to what was found by Trigo et al. (2009), IFN-γ levels
526 were detected in all groups, however no statistical difference was observed
527 between the groups, which was also applicable to IL-2 (Figures 6C and 6E,
528 respectively).

529 The absence of detectable IL-4 and IL-17A cytokines, respectively
530 present in Th2 and Th17 inflammatory responses, indicates that the use of
531 T4 phage in mammary glands infected with *E. coli* induces Th1 T-cell
532 responses. Th1 pattern is involved in a cellular immune response that
533 protects against intracellular infections by viruses and microorganisms that
534 grow in macrophages [74].

535 Histological analysis of the mammary gland in the control group (Figure
536 7A) shows intact tissue morphology described by well delimited cells and
537 acini, as well as the presence of fatty cells and a milky secretion, even
538 when *E. coli* 30 (~100 cells) were inoculated (Figure 7B). Inoculation of the
539 phage UFV13 (MOI 10) in the treated group led to an inflammatory reaction
540 characterized by tissue damage, neutrophil infiltrates and
541 mischaracterization of the acini border, although low levels of pro-

542 inflammatory cytokines have been found as discussed previously (Figure
543 7C).
544
545 **4. Conclusion**
546 Viral genomic analysis is a crucial step in bacteriophage screening for
547 their use as an antibacterial agent. The UFV13 virus has no lysogenic
548 modules or genes conferring antibiotic resistance. Viral stability analysis in
549 the presence of detergents and organic solvents and incubation at different
550 pHs and temperatures, have shown that the UFV13 virus presents high
551 survivability at basic pHs and is relatively resistant under incubation at 62
552 °C for 40 min. vB_EcoM-UFV13 used in an animal model for mastitis
553 reduced the total bacterial load by 90%, as well as inducing pro-
554 inflammatory cytokines such as IL-6 and TNF-α, which makes it a potential
555 biological agent capable of controlling acute infections caused by *E. coli*
556 dairy cows.
557
558 **Acknowledgements**
559 We are grateful to the Núcleo de Análise de Biomoléculas and Núcleo
560 de Microscopia e Microanálise of the Universidade Federal de Viçosa for
561 providing the facilities to conduct the experiments. We also acknowledge
562 the financial support of the following Brazilian agencies: Fundação de
563 Amparo à Pesquisa do Estado de Minas Gerais (Fapemig), Coordenacão
564 de Aperfeiçoamento de Pessoal de Nível Superior (CAPES), Conselho
565 Nacional de Desenvolvimento Científico e Tecnológico (CNPq),
566 Financiadora de Estudos e Projetos (Finep), Sistema Nacional de

Laboratórios em Nanotecnologias (SisNANO)/Ministério da ciência, tecnologia e Informação (MCTI). We are also grateful to Empresa Brasileira de Pesquisa Agropecuária (EMBRAPA), Gado de Leite Farm, Juiz de Fora, Minas Gerais, Brazil, that kindly provided us with *Escherichia coli* 30.

## 5. References

1. Shaheen, M., Tantary, H. & Nabi, S. A Treatise on Bovine Mastitis: Disease and Disease Economics, Etiological Basis, Risk Factors, Impact on Human Health, Therapeutic Management, Prevention and Control Strategy. *Adv. Dairy Res.* **4,** 1–10 (2016).
2. Thomas, V. *et al.* Antimicrobial susceptibility monitoring of mastitis pathogens isolated from acute cases of clinical mastitis in dairy cows across Europe: VetPath results. *Int. J. Antimicrob. Agents* **46,** 13–20 (2015).
3. Zeinhom, M. M. A. & Abdel-Latef, G. K. Public health risk of some milk borne pathogens. *Beni-Suef Univ. J. Basic Appl. Sci.* **3,** 209–215 (2014).
4. Crispie, F., Flynn, J., Ross, R. P., Hill, C. & Meaney, W. J. Dry cow therapy with a non-antibiotic intramammary teat seal - a review. *Ir. Vet. J.* **57,** 412 (2004).
5. Down, P. M., Green, M. J. & Hudson, C. D. Rate of transmission: A major determinant of the cost of clinical mastitis. *J. Dairy Sci.* **96,** 6301–6314 (2013).
6. Blum, S. E., Heller, E. D., Jacoby, S., Krifucks, O. & Leitner, G. Comparison of the immune responses associated with experimental

592 bovine mastitis caused by different strains of *Escherichia coli*. 190–
593 197 (2017). doi:10.1017/S0022029917000206
594 7. Schmelcher, M., Powell, A. M., Camp, M. J., Pohl, C. S. & Donovan,
595 D. M. Synergistic streptococcal phage λSA2 and B30 endolysins kill
596 streptococci in cow milk and in a mouse model of mastitis. *Appl.*
597 *Microbiol. Biotechnol.* **99,** 8475–8486 (2015).
598 8. Bryan, D., El-Shibiny, A., Hobbs, Z., Porter, J. & Kutter, E. M.
599 Bacteriophage T4 infection of stationary phase *E. coli*: Life after log
600 from a phage perspective. *Front. Microbiol.* **7,** (2016).
601 9. Porter, J., Anderson, J., Carter, L., Donjacour, E. & Paros, M. *In vitro*
602 evaluation of a novel bacteriophage cocktail as a preventative for
603 bovine coliform mastitis. *J. Dairy Sci.* **99,** 2053–2062 (2016).
604 10. Dias, R. S. *et al.* Use of phages against antibiotic-resistant
605 *Staphylococcus aureus* isolated from bovine mastitis 1. *J. Anim. Sci*
606 **91,** 3930–3939 (2013).
607 11. Sulakvelidze, A. The challenges of bacteriophage therapy. *Ind.*
608 *Pharm.* **45,** 14–18 (2011).
609 12. Gill, J. J. *et al.* Efficacy and Pharmacokinetics of Bacteriophage
610 Therapy in Treatment of Subclinical *Staphylococcus aureus* Mastitis
611 in Lactating Dairy Cattle. *Antimicrob. Agents Chemother.* **50,** 2912–
612 2918 (2006).
613 13. Merril, C. R., Scholl, D. & Adhya, S. L. The prospect for
614 bacteriophage therapy in Western medicine. *Nat. Rev. Drug Discov.*
615 **2,** 489–97 (2003).
616 14. Miller, E. S. *et al.* Bacteriophage T4 Genome Bacteriophage T4

617 Genome †. *Microbiol. Mol. Biol. Rev.* **67,** 86–156 (2003).
618 15. Chibani-Chennoufi, S., Dillmann, M. L., Marvin-Guy, L., Rami-
619 Shojaei, S. & Brüssow, H. *Lactobacillus plantarum* bacteriophage
620 LP65: A new member of the SPO1-like genus of the family
621 myoviridae. *J. Bacteriol.* **186,** 7069–7083 (2004).
622 16. Abouhmad, A., Mamo, G., Dishisha, T., Amin, M. A. & Hatti-Kaul, R.
623 T4 lysozyme fused with cellulose-binding module for antimicrobial
624 cellulosic wound dressing materials. *J. Appl. Microbiol.* **121,** 115–125
625 (2016).
626 17. Rodríguez-Rubio, L., Martínez, B., Donovan, D. M., Rodríguez, A. &
627 García, P. Bacteriophage virion-associated peptidoglycan
628 hydrolases: potential new enzybiotics. *Crit. Rev. Microbiol.* **39,** 427–
629 434 (2013).
630 18. Bruttin, A., Brüssow, H. & Bru, H. Human Volunteers Receiving
631 *Escherichia coli* Phage T4 Orally : a Safety Test of Phage Therapy
632 These include : Human Volunteers Receiving Escherichia coli Phage
633 T4 Orally : a Safety Test of Phage Therapy. *Antimicrob. Agents*
634 *Chemother.* **49,** 2874–2878 (2005).
635 19. Bocian, K. *et al.* LPS-activated monocytes are unresponsive to T4
636 phage and T4-generated *Escherichia coli* lysate. *Front. Microbiol.* **7,**
637 (2016).
638 20. Olson, M. A., Siebach, T. W., Griffitts, J. S., Wilson, E. & Erickson,
639 D. L. Genome-wide identification of fitness factors in
640 mastitisassociated Escherichia coli. *Appl. Environ. Microbiol.* **84,**
641 (2018).

21. Wang, J. *et al.* Oligopeptide Targeting Sortase A as Potential Anti-infective Therapy for *Staphylococcus aureus*. *Front. Microbiol.* **9,** 1–10 (2018).
22. Iwano, H. *et al.* Bacteriophage ΦSA012 Has a Broad Host Range against *Staphylococcus aureus* and Effective Lytic Capacity in a Mouse Mastitis Model. *Biology (Basel).* **7,** 8 (2018).
23. Hu, G. *et al.* Cynatratoside-C from Cynanchum atratum displays anti-inflammatory effect via suppressing TLR4 mediated NF-κB and MAPK signaling pathways in LPS-induced mastitis in mice. *Chem. Biol. Interact.* **279,** 187–195 (2018).
24. Roussel, P. *et al. Escherichia coli* mastitis strains: In vitro phenotypes and severity of infection in vivo. *PLoS One* **12,** 1–20 (2017).
25. Johnzon, C. F. *et al.* Mastitis pathogens with high virulence in a mouse model produce a distinct cytokine profile in vivo. *Front. Immunol.* **7,** 1–11 (2016).
26. Yu, Y. *et al.* Efficacy of cefquinome against *Escherichia coli* environmental mastitis assessed by pharmacokinetic and pharmacodynamic integration in lactating mouse model. *Front. Microbiol.* **8,** 1–9 (2017).
27. Ingman, W. V., Glynn, D. J. & Hutchinson, M. R. Mouse models of mastitis – how physiological are they? *Int. Breastfeed. J.* **10,** 12 (2015).
28. Burvenich, C., Van Merris, V., Mehrzad, J., Diez-Fraile, A. & Duchateau, L. Severity of *E. coli* mastitis is mainly determined by cow factors. *Veterinary Research* **34,** 521–564 (2003).

29. Sambrook, J. & Russell, D. W. Molecular Cloning - Sambrook & Russel - Vol. 1, 2, 3. *Cold Springs Harb. Lab. Press* 3th Editio**,** (2001).

30. Adams, M. Bacteriophages. *Bacteriophages* 620 (1959).

31. Duarte, V. S. *et al.* Complete genome sequence of vB_EcoM-UFV13, a new bacteriophage able to disrupt *Trueperella pyogenes* biofilm. *Genome Announc.* **4,** (2016).

32. Gasteiger, E. *et al.* ExPASy: The proteomics server for in-depth protein knowledge and analysis. *Nucleic Acids Res.* **31,** 3784–3788 (2003).

33. Lowe, T. M. & Eddy, S. R. TRNAscan-SE: A program for improved detection of transfer RNA genes in genomic sequence. *Nucleic Acids Res.* **25,** 955–964 (1996).

34. Naville, M., Ghuillot-Gaudeffroy, A., Marchais, A. & Gautheret, D. ARNold: a web tool for the prediction of Rho-independent transcription terminators. *RNA Biology* **8,** 11–13 (2011).

35. Klucar, L., Stano, M. & Hajduk, M. phiSITE: database of gene regulation in bacteriophages. *Nucleic Acids Res.* **38,** D366–D370 (2010).

36. Grant, J. R. & Stothard, P. The CGView Server: a comparative genomics tool for circular genomes. *Nucleic Acids Res.* **36,** (2008).

37. Bolger, A. M., Lohse, M. & Usadel, B. Trimmomatic: A flexible trimmer for Illumina sequence data. *Bioinformatics* **30,** 2114–2120 (2014).

38. Langmead, B. & Salzberg, S. L. Fast gapped-read alignment with

692 Bowtie 2. *Nat. Methods* **9,** 357–359 (2012).
693 39. Li, H. *et al.* The Sequence Alignment/Map format and SAMtools.
694 *Bioinformatics* **25,** 2078–2079 (2009).
695 40. Cingolani, P. *et al.* A program for annotating and predicting the
696 effects of single nucleotide polymorphisms, SnpEff: SNPs in the
697 genome of *Drosophila melanogaster* strain w1118; iso-2; iso-3. *Fly*
698 *(Austin).* **6,** 80–92 (2012).
699 41. Darling, A. C. E., Mau, B., Blattner, F. R. & Perna, N. T. Mauve:
700 Multiple alignment of conserved genomic sequence with
701 rearrangements. *Genome Res.* **14,** 1394–1403 (2004).
702 42. Treu, L. *et al.* The impact of genomic variability on gene expression
703 in environmental *Saccharomyces cerevisiae* strains. *Environ.*
704 *Microbiol.* **16,** 1378–1397 (2014).
705 43. Tuimala, J. A primer to phylogenetic analysis using the PHYLIP
706 package. Espoo Finland Center for Scientific Computing *Ltd* **6,**
707 (2006).
708 44. Huson, D. H. *et al.* Dendroscope: An interactive viewer for large
709 phylogenetic trees. *BMC Bioinformatics* **8,** 460 (2007).
710 45. Larkin, M. A. *et al.* Clustal W and Clustal X version 2.0. *Bioinformatics*
711 **23,** 2947–2948 (2007).
712 46. Katoh, K. & Standley, D. M. MAFFT Multiple Sequence Alignment
713 Software Version 7: Improvements in Performance and Usability.
714 *Mol. Biol. Evol.* **30,** 772–780 (2013).
715 47. Kumar, S., Stecher, G. & Tamura, K. MEGA7: Molecular
716 Evolutionary Genetics Analysis version 7.0 for bigger datasets. *Mol.*

*Biol. Evol.* msw054 (2016). doi:10.1093/molbev/msw054

48. Villarroel, J. *et al.* HostPhinder: A phage host prediction tool. *Viruses* **8,** (2016).

49. Green, M. R. & Sambrook, J. Molecular Cloning: A Laboratory Manual (Fourth Edition). *Cold Spring Harbor Laboratory Press; 4th edition (June 15, 2012)* 2028 (2012). Available at: http://www.amazon.com/Molecular-Cloning-Laboratory-Edition-Three/dp/1936113422.

50. Shevchenko, A., Tomas, H., Havli\[sbreve], J., Olsen, J. V & Mann, M. In-gel digestion for mass spectrometric characterization of proteins and proteomes. *Nat. Protoc.* **1,** 2856–2860 (2007).

51. Jurczak-Kurek, A. *et al.* Biodiversity of bacteriophages: morphological and biological properties of a large group of phages isolated from urban sewage. *Sci. Rep.* **6,** 34338 (2016).

52. Déziel, E., Comeau, Y. & Villemur, R. Initiation of biofilm formation by *Pseudomonas aeruginosa* 57RP correlates with emergence of hyperpiliated and highly adherent phenotypic variants deficient in swimming, swarming, and twitching motilities. *J. Bacteriol.* **183,** 1195–1204 (2001).

53. Belgini, D. R. B. *et al.* Culturable bacterial diversity from a feed water of a reverse osmosis system, evaluation of biofilm formation and biocontrol using phages. *World J. Microbiol. Biotechnol.* **30,** 2689–2700 (2014).

54. CLSI. Performance Standards for Antimicrobial Susceptibility Testing; Twenty-Seventh Edition. Clinical and Laboratory Standards

Institute (2017).

55. Chandler, R. L. Studies on experimental mouse mastitis relative to the assessment of pharmaceutical substances. *J. Comp. Pathol.* **81,** 507–514 (1971).

56. Naghili, H. *et al.* Validation of drop plate technique for bacterial enumeration by parametric and nonparametric tests. *Vet. Res. forum an Int. Q. J.* **4,** 179–83 (2013).

57. Ackermann, H. W. Bacteriophage observations and evolution. *Research in Microbiology* **154,** 245–251 (2003).

58. Belle, A., Landthaler, M. & Shub, D. A. Intronless homing: Site-specific endonuclease SegF of bacteriophage T4 mediates localized marker exclusion analogous to homing endonucleases of group I introns. *Genes Dev.* **16,** 351–362 (2002).

59. Comeau, A. M., Arbiol, C. & Krisch, H. M. Composite conserved promoter-terminator motifs (PeSLs) that mediate modular shuffling in the diverse T4-like myoviruses. *Genome Biol. Evol.* **6,** 1611–1619 (2014).

60. Jun, J. W. *et al.* Bacteriophage application to control the contaminated water with Shigella. *Sci. Rep.* **6,** 22636 (2016).

61. Hinton, D. M. Transcriptional control in the prereplicative phase of T4 development. *Virol. J.* **7,** 289 (2010).

62. Leiman, P. G. *et al.* Morphogenesis of the T4 tail and tail fibers. *Virol. J.* **7,** 355 (2010).

63. Kramberger, P., Urbas, L. & Štrancar, A. Downstream processing and chromatography based analytical methods for production of

767 vaccines, gene therapy vectors, and bacteriophages. *Human*
768 *Vaccines and Immunotherapeutics* **11,** 1010–1021 (2015).
769 64. Thung, T. Y. *et al.* Use of a lytic bacteriophage to control *Salmonella*
770 *enteritidis* in retail food. *LWT - Food Sci. Technol.* **78,** 222–225
771 (2017).
772 65. Ogola, H., Shitandi, A. & Nanua, J. Effect of mastitis on raw milk
773 compositional quality. *J. Vet. Sci.* **8,** 237–242 (2007).
774 66. Zhanel, G. G., Zhanel, M. A. & Karlowsky, J. A. Oral Fosfomycin for
775 the Treatment of Acute and Chronic Bacterial Prostatitis Caused by
776 Multidrug-Resistant *Escherichia coli*. *Can. J. Infect. Dis. Med.*
777 *Microbiol.* **2018,** 1–9 (2018).
778 67. Domenech, M., Ramos-Sevillano, E., García, E., Moscoso, M. &
779 Yuste, J. Biofilm formation avoids complement immunity and
780 phagocytosis of *Streptococcus pneumoniae*. *Infect. Immun.* **81,**
781 2606–2615 (2013).
782 68. Kao, C. Y. *et al.* The complex interplay among bacterial motility and
783 virulence factors in different *Escherichia coli* infections. *Eur. J. Clin.*
784 *Microbiol. Infect. Dis.* **33,** 2157–2162 (2014).
785 69. Brouillette, E., Grondin, G., Talbot, B. G. & Malouin, F. Inflammatory
786 cell infiltration as an indicator of *Staphylococcus aureus* infection and
787 therapeutic efficacy in experimental mouse mastitis. *Vet. Immunol.*
788 *Immunopathol.* **104,** 163–169 (2005).
789 70. Brouillette, E. & Malouin, F. The pathogenesis and control of
790 *Staphylococcus aureus*-induced mastitis: Study models in the
791 mouse. *Microbes Infect.* **7,** 560–568 (2005).

71. Nazemi, S. *et al.* Expression of acute phase proteins and inflammatory cytokines in mouse mammary gland following *Staphylococcus aureus* challenge and in response to milk accumulation. *J. Dairy Res.* **81,** 445–54 (2014).

72. Trigo, G. *et al.* Leukocyte populations and cytokine expression in the mammary gland in a mouse model of *Streptococcus agalactiae* mastitis. *J. Med. Microbiol.* **58,** 951–958 (2009).

73. Masso-Welch, P. A., Merhige, P. M., Veeranki, O. L. M. & Kuo, S.-M. Loss of IL-10 Decreases Mouse Postpubertal Mammary Gland Development in the Absence of Inflammation. *Immunol. Invest.* **41,** 521–537 (2012).

74. Kaiko, G. E., Horvat, J. C., Beagley, K. W. & Hansbro, P. M. Immunological decision-making: How does the immune system decide to mount a helper T-cell response? *Immunology* **123,** 326–338 (2008).

**Author Contribution Statement**

V.S.D., R.S.D. and S.O.P. conceived and designed the experiments; V.S.D., A.M.K., S.C., L.T., A.X., C.G.F. and P.M.P.V. performed genomic analysis; C.S. contributed to *E. coli*-induced mastitis mouse model; M.S.V., I.S.P., and G.R.S. conducted phage physiological features assays. F.M. took part in the histological analysis; J.S.C. was involved in protein profile experiments; C.C.S. contributed materials. V.S.D. wrote the main manuscript text. All the authors have read and contributed to the final version of the manuscript.

## Additional Information

## Competing Financial Interests

There is no competing interest.

# CONCLUSÕE GERAIS

Neste estudo:

* O vírus vB_EcoM-UFV13, isolado usando-se *E. coli* 30 como hospedeiro, atua prevenindo a formação de biofilme por *T. pyogenes*.

* Usando-se 3 diferentes MOIs, 0.1, 1 e 10, apenas o último foi capaz de inibir o início da formação de biofilme por *T. pyogenes* ($P \leq 0.05$).

* Análises *in silico* das proteínas estruturais do fago UFV13 revelou um amplo espectro de hidrolases associadas à partícula viral (VAPGHs).

* Fagos com amplo número de VAPGHs, como o vírus UVF13, podem possuir atividade não-específica por meio de hidrolases contra hospedeiros não relacionados quando empregados em altos MOIs.

* Análises de bioinformática revelaram que o vírus UFV13 possuí 269 ORFs. Destas, 48 codificam proteínas estruturais. Não foram identificados genes que sejam capazes de conferir resistência à antibióticos ou mesmo módulo de lisogênia.

* Ensaios de estabilidade viral na presença de detergentes, solventes orgânicos e incubação em diferentes pHs e temperaturas revelaram que este fago possui alta sobrevivência em pH básico e é relativamente estável a 62ºC por 40 minutos.

* A aplicação do fago UFV13 usando-se camundongos fêmeas lactentes como modelo foi capaz de reduzir 10X a carga bacteriana total, assim como induzir citocinas pró-inflamatórias (IL-6 e TNF-α).

Desta forma, conclui-se que o fago UFV13 demonstra potencial aplicação para controlar infecções agudas causadas por *E. coli* e prevenir a adesão de *T. pyogenes* em vacas leiteiras.

# ANEXOS

# ANEXO 1

Tabela 3 – Empresas atualmente ativas no mercado que trazem bacteriófagos em seus portfólios. Dados retirados integralmente de http://companies.phage.org/ (acessado: 03/07/2018).

| Empresa | País | Website | Atividades |
|---|---|---|---|
| Adaptative Phage Therapeutics | Estados Unidos | http://www.aphage.com/ | Ensaios pré-clinícos/P&D* |
| AmpliPhi Biosciences | Estados Unidos | http://www.ampliphibio.com/ | Ensaios pré-clinícos /P&D* |
| C3J Therapeutics | Estados Unidos | http://www.c3jtherapeutics.com/ | Ensaios pré-clinícos /P&D* |
| Enbiotix | Estados Unidos | http://www.enbiotix.com/ | Ensaios pré-clinícos /P&D*/Produção de partículas virais não competentes |
| Evolution Biotechnologies | Reino Unido | http://www.evolutionbiotech.com/ | Ensaios pré-clinícos /P&D* |
| InnoPhage | Portugal | http://www.innophage.com/ | Ensaios pré-clinícos /P&D*/ Biocontrole mediado por fagos |
| Technophage | Portugal | http://www.technophage.pt/ | Ensaios pré-clinícos /P&D* |
| Intralytix | Estados Unidos | http://www.intralytix.com/ | Ensaios pré-clinícos /P&D*/ Biocontrole mediado por fagos |
| Locus Biosciences | Estados Unidos | https://www.locus-bio.com/ | Ensaios pré-clinícos /P&D* |
| Phagelux | China | http://www.phagelux.com/ | Ensaios pré-clinícos /P&D* |
| Pherecydes Pharma | França | https://www.pherecydes-pharma.com/ | Ensaios pré-clinícos /P&D* |
| Elio Bioscience | França | http://eligo.bio/ | Produção de partículas virais não competentes |

| | | | |
|---|---|---|---|
| Phico Therapeutics | Reino Unido | http://www.phicotx.co.uk/ | Produção de partículas virais não competentes |
| Pylum Biosciences | Reino Unido | https://pylumbio.com/ | Produção de partículas virais não competentes |
| Biochimpharm | Georgia | http://biochimpharm.ge/ | Distribuição de produtos à base de fagos/P&D* |
| Imbio | Rússia | http://home.mts-nn.ru/~imbio/ | Distribuição de produtos à base de fagos/P&D* |
| Microgen | Rússia | http://www.microgen.ru/ | Distribuição de produtos à base de fagos/P&D* |
| Eliava Phage Therapy Center | Georgia | http://www.mrsaphages.com/ | Elo entre paciente e a fago terapia |
| Phage Therapy Center | Georgia | https://www.phagetherapycenter.com/pii/PatientServlet?command=static_home | Elo entre paciente e a fago terapia |
| Phage Therapy Unit | Polônia | https://www.iitd.pan.wroc.pl/en/OTF/ | Elo entre paciente e a fago terapia |
| Phage International | Estados Unidos | http://www.phageinternational.com/pii/PIIServlet?command=home | Elo entre paciente e a fago terapia |
| APS Biocontrol | Reino Unido | http://apsbiocontrol.com/ | Biocontrole mediado por fagos |
| Epibiome | Estados Unidos | https://www.epibiome.com/ | Biocontrole mediado por fagos |
| Fixed Phage | Reino Unido | https://www.fixed-phage.com/ | Biocontrole mediado por fagos |
| Micreos Food Safety | Netherlands | http://www.micreosfoodsafety.com/ | Biocontrole mediado por fagos/ Produção e uso de enzibióticos |
| Omnilytics | Estados Unidos | http://www.omnilytics.com/ | Biocontrole mediado por fagos |
| Phage Biotech | Israel | http://www.phage-biotech.com/ | Biocontrole mediado por fagos |
| Proteon Pharmaceuticals | Polônia | http://www.proteonpharma.com/ | Biocontrole mediado por fagos |
| Delmont Laboratories | Estados Unidos | https://delmontlabs.com/ | Produção de lisados fágicos |

| | | | |
|---|---|---|---|
| Contrafect | Estados Unidos | https://www.contrafect.com/ | Produção e uso de enzibióticos |
| GangaGen | Estados Unidos/Índia | http://www.gangagen.com/ | Produção e uso de enzibióticos |
| Lysando GmbH | Alemanha | https://www.lysando.com/ | Produção e uso de enzibióticos |
| New Horizons Diagnostics | Estados Unidos | http://www.nhdiag.com/phage.shtml | Produção e uso de enzibióticos |
| GeneWeave | Estados Unidos | http://www.rochemicrobiologytests.com/healthcare-associated-infections/innovative-solutions.html | Detecção bacteriana baseada em fagos |
| Sample6 | Estados Unidos | http://www.sample6.com/ | Detecção bacteriana baseada em fagos |
| Phage Consultants | Polônia | http://www.phageconsultants.com/ | Prevenção de contaminação e controle |
| JAFRAL | Eslovênia | http://www.jafral.com/en/ | Produção fágica para terceiros |
| Clean Cells | França | http://www.clean-cells.com/ | Produção fágica para terceiros |
| Paragon Bioservices | Estados Unidos | http://paragonbioservices.com/ | Produção fágica para terceiros |

## ANEXO 2 – Supplementary Material "A *T4virus* prevents biofilm formation by *Trueperella pyogenes*"

Vinícius da Silva Duarte[a], Roberto Sousa Dias[a], Andrew M. Kropinski[b], André da Silva Xavier[c], Camila Geovana Ferro[d], Pedro M. P. Vidigal[e], Cynthia Canedo da Silva[a], Sérgio Oliveira de Paula[f]

[a] Department of Microbiology, Federal University of Viçosa, Av. Peter Henry Rolfs, s/n, Campus Universitário, 36570-900, Viçosa, Minas Gerais, Brazil

[b] Departments of Food Science, and Pathobiology, University of Guelph, Guelph, Ontario N1G 2W1 Canada

[c] Embrapa Maize and Sorghum, Rodovia MG 424, Sete Lagoas, Minas Gerais, Brazil

[d] Department of Plant Pathology, Federal University of Viçosa, Av. Peter Henry Rolfs, s/n, Campus Universitário, 36570-900, Viçosa, Minas Gerais, Brazil

[e] Núcleo de Análise de Biomoléculas (NuBioMol), Center of Biological Sciences, Federal University of Viçosa, Viçosa, Minas Gerais, Brazil

[f] Department of General Biology, Federal University of Viçosa, Av. Peter Henry Rolfs, s/n, Campus Universitário, 36570-900, Viçosa, Minas Gerais, Brazil

**Supplementary Figure 1.** A – *Escherichia* phage UFV13 plaque formed in double-layer agar displays a 1 mm clear lytic zone with a surrounding halo indicative of phage-derived enzymes able to destroy bacterial cell wall components. B – Transmission electron microscopy of phage UFV13 reveals particles 102 nm in length, an isometric capsid of 32 nm in diameter and contractile tails, which classifies it as belonging to the order *Caudovirales*, family *Myoviridae*. Bar measures 100 nm.

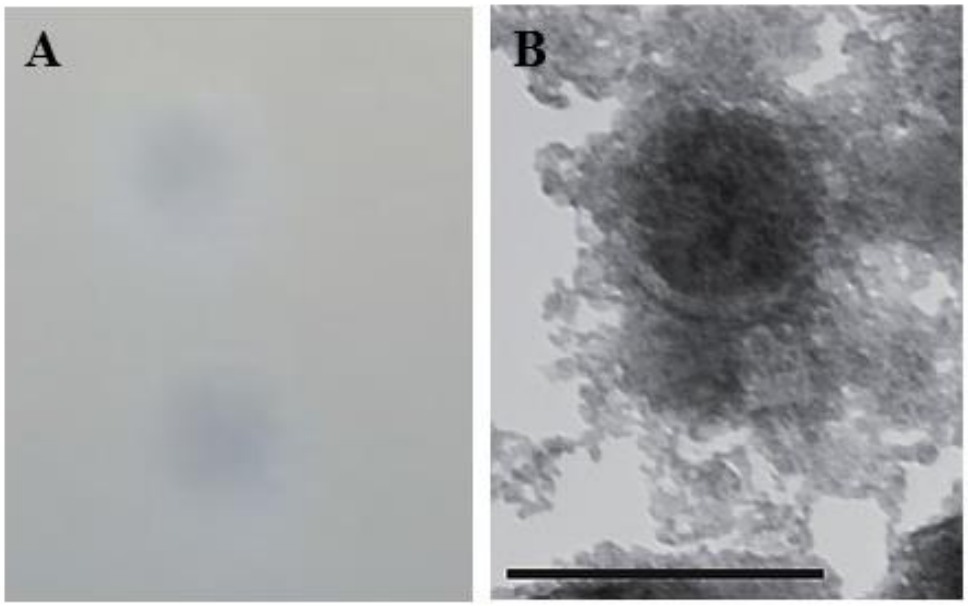

**Supplementary Figure 2.** A reduced final optical density (after 24 hours) of treatment was observed using only MOI 10 (* $P \leq 0.05$).

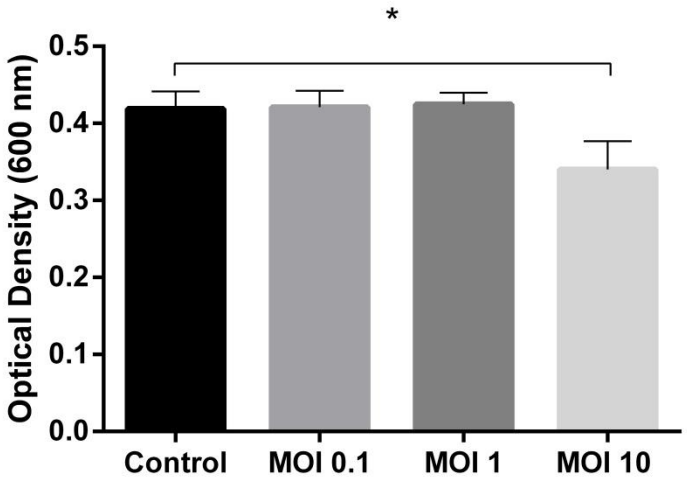


**Supplementary Figure 3.** UFV13 titration after 24 hours show that *T. pyogenes* is not virus-susceptible. Statistically significant differences were not observed between treated and control groups.

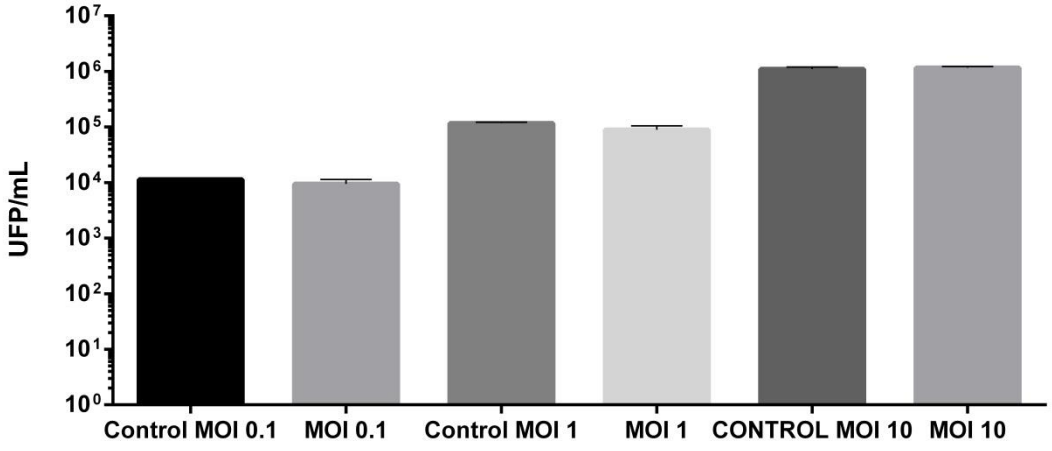

**Supplementary Figure 4.** Pulsed-field gel electrophoresis of phage UFV13 DNA. Electrophoresis was performed on 1% agarose gel in 0,5x TBE buffer. MM – Molecular marker (Pulse Marker™ 0.1-200 kb Sigma-Aldrich); UFV-13 – vB_EcoM-UFV13.

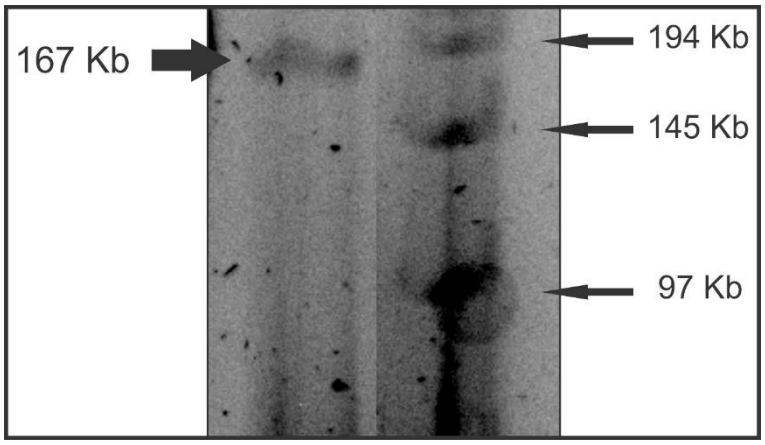


**Supplementary Figure 5.** The canonical Soc of the T4virus is identical to the hypothetical Gram-positive *Clostridioides difficile* protein.

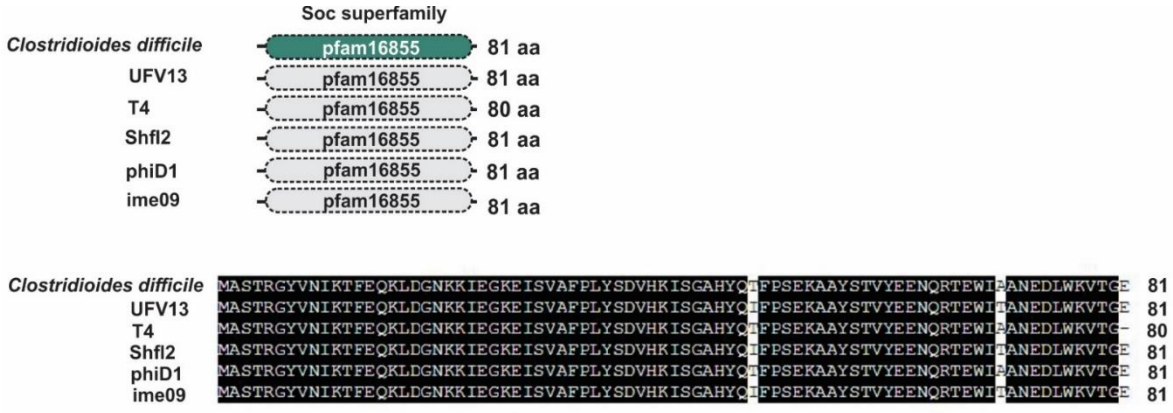

**Supplementary Figure 6.** Scanning Electron Microscopy - Morphological differences are evidenced in this figure. In the control group (A), *T. pyogenes* appear as rod-shaped cells with V-shaped pairs. Phage treatment (B) induces morphological changes, with more coccoid rod cells observed. Bars: 10 µm.

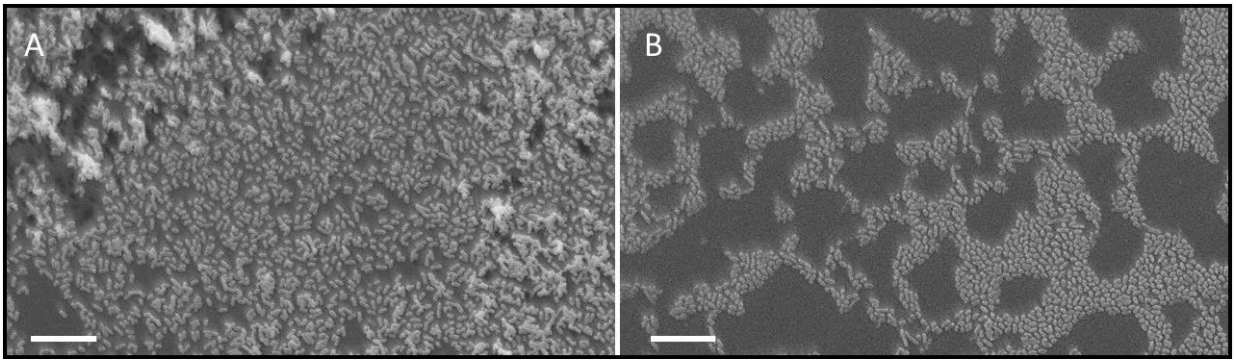

# ANEXO 3 – Supplementary Material "Genomic analysis and immune response in a murine mastitis model of vB_EcoM-UFV13, a potential biocontrol agent for use in dairy cows."

Vinícius da Silva Duarte[a], Roberto Sousa Dias[a], Andrew M. Kropinski[b], Stefano Campanaro[c], Laura Treu[c, d], Carolina Siqueira[e], Marcella Silva Vieira[e], Isabela da Silva Paes[e], Gabriele Rocha Santana[e], Franciele Martins[e], Josicelli Souza Crispim[a], André da Silva Xavier[f], Camila Geovana Ferro[g], Pedro M. P. Vidigal[h], Cynthia Canêdo da Silva[a], Sérgio Oliveira de Paula[e]

**Affiliations:**

[a] Department of Microbiology, Federal University of Viçosa, Av. Peter Henry Rolfs, s/n, Campus Universitário, 36570-900, Viçosa, Minas Gerais, Brazil

[b] Departments of Food Science, and Pathobiology, University of Guelph, Guelph, Ontario N1G 2W1 Canada

[c] Department of Biology, University of Padova, Padova, Italy

[d] Department of Environmental Engineering, Technical University of Denmark, Miljoevej, Building 115, DK-2800 Kgs. Lyngby, Denmark

[e] Department of General Biology, Federal University of Viçosa, Av. Peter Henry Rolfs, s/n, Campus Universitário, 36570-900, Viçosa, Minas Gerais, Brazil

[f] Embrapa Maize and Sorghum, Rodovia MG 424, Sete Lagoas, Minas Gerais, Brazil

[g] Department of Plant Patology, Federal University of Viçosa, Av. Peter Henry Rolfs, s/n, Campus Universitário, 36570-900, Viçosa, Minas Gerais, Brazil

[h] Núcleo de Análise de Biomoléculas (NuBioMol), Center of Biological Sciences, Federal University of Viçosa, Viçosa, Minas Gerais, Brazi

**Supplementary table-1.** vB_EcoM-UFV13 functional genomic annotation. Asterisks mean the best hit for a gene/protein found when no matches were identified on the reference Enterobacteria phage T4 (accession number NC_000866).

| ORF | Predicted Protein & organism* | Genomic Coordinates | Strand | Protein mass (kDa) | Protein pI | Gene & organism* | E-value | Identity (%) |
|---|---|---|---|---|---|---|---|---|
| 1 | RIIA | 0..2177 | Minus | 82.7 | 5.65 | *rIIA* | 0.0 | 98.6 |
| 2 | RIIA.1 | 2188..2391 | Minus | 8.1 | 6.58 | *rIIA.1* | 6.4e-47 | 98.5 |
| 3 | 39 | 2446..4263 | Minus | 68.3 | 7.20 | *39* | 0.0 | 98.5 |
| 4 | 39.1 | 4333..4593 | Minus | 9.2 | 7.71 | *39.1* | 9.4e-55 | 97.7 |
| 5 | Gp20 | 4599..4970 | Minus | 14.1 | 5.50 | *20* (Shigella phage pSs-1) | 5.6e-75 | 95.1 |
| 6 | 39.2 | 4973..5149 | Minus | 6.7 | 8.39 | *39.2* | 3.8e-34 | 81.0 |
| 7 | ComC-α | 5152..5571 | Minus | 16.4 | 4.73 | *goF = comC-α* | 5.3e-79 | 83.7 |
| 8 | Cef | 5571..5786 | Minus | 8.4 | 5.0 | *cef = motC* | 2.4e-51 | 97.2 |
| 9 | Hypothetical Protein (Escherichia coli O157 typing phage 7) | 5800..6069 | Minus | 10.2 | 5.76 | - | 5.6e-57 | 100.0 |
| 10 | MotB | 6167..6655 | Minus | 18.1 | 9.30 | *motB* | 9.1e-111 | 99.4 |
| 11 | MotB.1 | 6732..7265 | Minus | 20.0 | 4.92 | *motB.1* | 4e-22 | 63.3 |
| 12 | MotB.2 | 7268..7768 | Minus | 19.9 | 5.74 | *motB.2* | 2e-109 | 90.9 |
| 13 | DexA | 7832..8515 | Minus | 26.0 | 4.88 | dexA | 2.9e-164 | 98.7 |
| 14 | DexA.1 | 8515..8757 | Minus | 9.4 | 5.10 | *dexA.1* | 5e-55 | 91.3 |
| 15 | DexA.2 | 8750..8995 | Minus | 9.4 | 4.47 | *dexA.2* | 5.8e-57 | 97.5 |

| | | | | | | | | |
|---|---|---|---|---|---|---|---|---|
| 16 | Hypothetical Protein | 8982..9242 | Minus | 9.9 | 8.79 | *30* (Shigella phage pSs-1) | 1.1e-48 | 94.2 |
| 17 | Dda | 9249..10214 | Minus | 37.0 | 6.97 | *dda = sud* | 0.0 | 99.5 |
| 18 | Frameshift | 10298..10567 | | | | Frameshift | | |
| 19 | Dda.1 | 10564..10875 | Minus | 12.0 | 9.47 | *dda.1* | 1e-67 | 98.1 |
| 20 | Srd | 10877..11623 | Minus | 29.0 | 9.99 | *srd = dda.2* | 1.3e-171 | 99.2 |
| 21 | RNA polymerase | 11746..12348 | Minus | 23.4 | 5.86 | *modB* | 6.5e-140 | 98.5 |
| 22 | ADP-ribosylase | 12345..12968 | Minus | 24.2 | 5.43 | *modA* | 5.4e-140 | 95.7 |
| 23 | ModA.2 | 13036..13218 | Minus | 7.0 | 4.27 | *modA.2* | 1.2e-44 | 98.3 |
| 24 | ModA.3 | 13227..13697 | Minus | 18.3 | 6.11 | *modA.3* | 4.3e-101 | 94.9 |
| 25 | ModA.4 | 13690..13842 | Minus | 5.6 | 5.73 | *modA.4* | 8.2e-33 | 98.0 |
| 26 | Srh | 13851..14054 | Minus | 8.0 | 6.27 | *srh* | 1.4e-49 | 98.5 |
| 27 | Mrh | 14029..14514 | Minus | 18.2 | 4.58 | *mrh* | 2.4e-83 | 77.0 |
| 28 | Mrh.1 | 14523..14864 | Minus | 12.6 | 3.85 | *mrh.1* | 9.4e-81 | 99.1 |
| 29 | Mrh.2 | 14864..15070 | Minus | 8.2 | 5.58 | *mrh.2* | 1.6e-49 | 97.1 |
| 30 | Soc | 15166..15411 | Minus | 9.3 | 5.62 | *soc* | 1.3e-60 | 97.5 |
| 31 | Soc.1 | 15428..15637 | Minus | 7.9 | 9.16 | *soc.1* (Shigella phage Shfl2) | 8.8e-54 | 100.0 |
| 32 | Soc.2 | 15634..15834 | Minus | 7.8 | 9.94 | *soc.2* (Shigella phage Shfl2) | 110e-48 | 100.0 |
| 33 | DNA Replication Protein | 15834..16352 | Minus | 20.2 | 5.16 | *56* | 3.4e-76 | 69.2 |
| 34 | Dam.1 | 16424..16624 | Plus | 7.1 | 10.00 | *dam.1* | 5.4e-44 | 98.5 |
| 35 | DNA Primase | 16621..17649 | Minus | 39.7 | 9.31 | *61 = 58* | 0.0 | 100.0 |

| | | | | | | | | |
|---|---|---|---|---|---|---|---|---|
| 36 | Gp61.1 | 17652..17816 | Minus | 5.9 | 5.39 | *61.1* | 1.2e-36 | 96.3 |
| 37 | Gp61.2 | 17818..18174 | Minus | 13.8 | 4.83 | *61.2* | 2.1e-2 | 35.0 |
| 38 | Spackle periplasmic protein | 18187..18480 | Minus | 10.9 | 4.62 | *sp* | 5.4e-62 | 97.9 |
| 39 | Hypothetical Protein (Enterobacteria phage ime09) | 18584..18766 | Minus | 7.1 | 4.84 | - | 510e-45 | 98.3% |
| 40 | Hypothetical Protein (Shigella phage Shfl2) | 18831..19085 | Minus | 9.6 | 5.81 | - | 17e-63 | 100.0 |
| 41 | Gp61.4 | 19149..19391 | Minus | 9.5 | 10.29 | *61.4* | 4.5e-55 | 96.1 |
| 42 | Dmd | 19393..19575 | Minus | 7.0 | 5.24 | *dmd* | 3.8e-43 | 100.0 |
| 43 | DNA Helicase | 19634..21061 | Minus | 53.5 | 5.44 | *41* | 0.0 | 99.8 |
| 44 | Head Formation Protein | 21071..21415 | Minus | 13.2 | 4.99 | *40* | 1.0e-72 | 99.1 |
| 45 | UvsX | 21408..22589 | Minus | 44.0 | 5.35 | *uvsX = fdsA* | 0.0 | 90.3 |
| 46 | Beta-glucosyl-HMC-alpha-glucosyl-transferase | 22667..23509 | Minus | 32.3 | 7.65 | *β-gt* (Enterobacterio phage RB27) | 0.0 | 98.9 |
| 47 | dCMP hydroxymethylase | 23506..24246 | Minus | 28.5 | 5.43 | *42* | 2.1e176 | 97.1 |
| 48 | Inner Membrane Protein | 24400..24651 | Minus | 93.0 | 9.40 | *imm* | 9.9e-87 | 98.8 |
| 49 | Imm Intergenic Region | 24659..25039 | Minus | 14.2 | 7.55 | *imm.1* | 280e-90 | 99.2 |
| 50 | Hypothetical Protein (Enterobacteria phage T2) | 25052..25303 | Minus | 9.3 | 9.60 | - | 10e-60 | 98.8 |

| | | | | | | | | |
|---|---|---|---|---|---|---|---|---|
| 51 | DNA polymerase | 25479..28175 | Minus | 103.5 | 5.96 | *43* | 0.0 | 99.6 |
| 52 | Hypothetical Protein (Enterobacteria phage RB18) | 28254..28475 | Minus | 8.4 | 6.25 | - | 9.7e-53 | 98.6 |
| 53 | RegA | 28477..28845 | Minus | 14.6 | 8.97 | *regA* | 1.2e-83 | 100.0 |
| 54 | Clamp loader small subunit | 28847..29410 | Minus | 21.3 | 7.67 | *62* | 2.1e-129 | 99.5 |
| 55 | Clamp loader small subunit | 29412..30371 | Minus | 35.7 | 6.72 | *44* | 0.0 | 100.0 |
| 56 | DNA polymerase clamp | 30423..31109 | Minus | 24.8 | 4.89 | *45* | 3.6e-156 | 99.1 |
| 57 | RNA polymerase-binding protein | 31165..31554 | Minus | 14.7 | 6.83 | *rpbA* | 16e-87 | 100.0 |
| 58 | Hypothetical Protein | 31564..31752 | Minus | 7.5 | 5.55 | *45.2* | 7.3e-45 | 98.4 |
| 59 | Recombination-related endonuclease | 31808..33448 | Minus | 63.6 | 7.13 | *46* | 0.0 | 95.2 |
| 60 | Hypothetical Protein | 33487..33693 | Minus | 8.1 | 4.24 | *46.1* | 5.1e-50 | 98.5 |
| 61 | Hypothetical Protein | 33674..33937 | Minus | 10.2 | 4.21 | 46.2 | 1.2e-58 | 97.7 |
| 62 | Recombination-related endonuclease | 33934..34953 | Minus | 39.1 | 4.94 | 47 | 0.0 | 96.2 |
| 63 | Alpha glucosyl transferase | 35130..36332 | Minus | 46.8 | 6.05 | *α-gt* | 0.0 | 91.5 |
| 64 | Alpha glucosyl transferase.2 | 36399..36569 | Minus | 6.4 | 9.3 | *α-gt.2* | 1.7e-28 | 88.7 |
| 65 | Alpha glucosyl transferase.3 | 36573..36776 | Minus | 7.9 | 9.42 | *α-gt.3* | 9.7e-50 | 98.5 |
| 66 | Alpha glucosyl transferase.4 | 36745..37062 | Minus | 12.4 | 8.78 | *α-gt.4* | 1.3e-66 | 100.0 |

| | | | | | | | | |
|---|---|---|---|---|---|---|---|---|
| 67 | Alpha glucosyl transferase.5 | 37064..37252 | Minus | 7.4 | 4.10 | *α-gt.5* | 1.8e-44 | 98.5 |
| 68 | RNA polymerase sigma fator for late transcription | 37266..37823 | Minus | 21.5 | 5.44 | *55* | 9.6e-132 | 100.0 |
| 69 | Hypothetical Protein (Shigella phage Shfl2) | 37902..38171 | Minus | 10.7 | 5.64 | - | 8.2e-60 | 100.0 |
| 70 | MobC | 38168..38383 | Minus | 8.0 | 3.69 | *55.1* | 1.6e-49 | 97.1 |
| 71 | Gp55.2 | 38386..38712 | Minus | 12.7 | 9.70 | *55.2* | 3.6e-68 | 99.1 |
| 72 | Gp55.3 | 38765..38965 | Minus | 7.7 | 7.89 | *55.3* | 3.1e-35 | 74.2 |
| 73 | Gp55.4 | 38966..39097 | Minus | 5.1 | 9.60 | *55.4* | 3.8e-34 | 97.7 |
| 74 | Gp55.5 | 39105..39398 | Minus | 11.8 | 9.79 | *55.5* | 2.8e-64 | 100.0 |
| 75 | Gp55.6 | 39391..39573 | Minus | 6.9 | 9.37 | *55.6* | 2.4e-38 | 93.3 |
| 76 | Glutaredoxin | 39732..40040 | Minus | 11.7 | 9.14 | *nrdH* | 2.7e-67 | 100.0 |
| 77 | Gp55.8 | 40043..40255 | Minus | 7.9 | 9.22 | *55.8* | 2.9e-48 | 100.0 |
| 78 | Gp55.9 | 40265..40378 | Minus | 4.4 | 4.54 | *nrdG = 55.9* | 8.8e-30 | 100.0 |
| 79 | Ribonucleotide reductase of class III (anaerobic), activating protein | 40371..40841 | Minus | 18.1 | 5.58 | *nrdG* | 9.6e-93 | 80.1 |
| 80 | Ribonucleotide reductase of class III (anaerobic), large subunit | 40838..42655 | Minus | 67.9 | 6.59 | *nrdD = sunY* | 0.0 | 99.5 |

| | | | | | | | | |
|---|---|---|---|---|---|---|---|---|
| 81 | Gp49 | 42652..43125 | Minus | 18.1 | 8.80 | *49* | 7.7e-112 | 100.0 |
| 82 | Pin | 43167..43652 | Minus | 18.8 | 4.48 | *pin* | 3.4e-110 | 96.3 |
| 83 | Gp49.1 | 43636..43791 | Minus | 6.1 | 3.94 | *49.1* | 4e-40 | 100.0 |
| 84 | Gp49.2 | 43776..44096 | Minus | 12.5 | 4.48 | *49.2* | 2.9e-71 | 97.2 |
| 85 | Hypothetical Protein | 44107..44277 | Minus | 6.5 | 4.07 | *95* (Shigella phage pSs-1) | 130e-36 | 91.1 |
| 86 | Hypothetical Protein | 44280..44495 | Minus | 8.1 | 7.79 | *96* (Shigella phage pSs-1) | 3.1e-51 | 98.6 |
| 87 | Thioredoxin | 44492..44755 | Minus | 10.0 | 6.71 | *nrdC* | 6.6e-58 | 100.0 |
| 88 | NrdC.1 | 44757..44999 | Minus | 9.4 | 7.91 | *nrdc.1* | 1.7e-59 | 100.0 |
| 89 | NrdC.2 | 44986..45303 | Minus | 12.2 | 6.07 | *nrdc.2* | 2.8e-63 | 90.5 |
| 90 | NrdC.3 | 45300..46229 | Minus | 36.0 | 9.10 | *nrdc.3* | 3.6e-124 | 60.6 |
| 91 | NrdC.4 | 46282..47313 | Minus | 40.0 | 6.00 | *nrdC.4* | 0.0 | 96.4 |
| 92 | NrdC.5 | 47341..48366 | Minus | 39.9 | 9.32 | *nrdC.5* | 0.0 | 94.2 |
| 93 | NrdC.6 | 48375..49262 | Minus | 33.7 | 9.15 | *nrdC.6* | 0.0 | 96.6 |
| 94 | NrdC.7 | 49270..49677 | Minus | 15.4 | 5.28 | *nrdC.7* | 7.5e-81 | 88.7 |
| 95 | NrdC.8 | 49733..50260 | Minus | 20.7 | 6.65 | *nrdC.8* | 5.3e-119 | 98.9 |
| 96 | NrdC.9 | 50321..50623 | Minus | 11.9 | 9.68 | *nrdC.9* | 2.3e-67 | 99.0 |
| 97 | NrdC.10 | 50725..51693 | Minus | 36.4 | 5.01 | *nrdC.10* | 0.0 | 99.7 |
| 98 | NrdC.11 | 51809..52819 | Minus | 38.9 | 6.39 | *nrdC.11* | 0.0 | 99.4 |
| 99 | Hypothetical protein (Enterobacteria phage ime09) | 52819..53280 | Minus | 17.9 | 9.33 | - | 420e-111 | 99.3 |
| 100 | MobD.1 | 53283..53804 | Minus | 19.2 | 4.99 | *mobD.1* | 1.1e-1 | 25.6 |
| 101 | MobD.1 | 53811..54368 | Minus | 21.7 | 5.68 | *mobD.1* | 1.2e-109 | 87.5 |

| | | | | | | | | |
|---|---|---|---|---|---|---|---|---|
| 102 | MobD.2a | 54536..54709 | Minus | 6.7 | 5.27 | *mobD.2a* | 5.2e-37 | 96.5 |
| 103 | MobD.3 | 54699..54893 | Minus | 7.6 | 5.04 | *mobD.3* | 4.3e-44 | 95.3 |
| 104 | MobD.4 | 54896..55099 | Minus | 7.4 | 4.29 | *mobD.4* | 6.4e-29 | 77.6 |
| 105 | MobD.5 | 55099..55287 | Minus | 7.1 | 4.19 | *mobD.5* | 9.7e-43 | 100.0 |
| 106 | RI.-1 | 55383..55769 | Minus | 14.6 | 5.53 | *rI.-1* | 1.2e-86 | 100.0 |
| 107 | RI | 55766..56059 | Minus | 11.1 | 4.90 | *rI* | 1.5e-61 | 99.0 |
| 108 | RI.1 | 56072..56284 | Minus | 8.2 | 10.19 | *rI.1* | 4.4e-49 | 100.0 |
| 109 | Thymidine kinase | 56327..56908 | Minus | 21.6 | 6.22 | *tk* | 5.6e-135 | 100.0 |
| 110 | Thymidine kinase.2 | 56918..57103 | Minus | 7.3 | 4.41 | *tk.2* | 5.4e-17 | 54.1 |
| 111 | Hypothetical protein (Enterobacteria phage RB5) | 57100..57273 | Minus | 6.6 | 5.68 | - | 9.3e-38 | 100.0 |
| 112 | Hypothetical protein (Escherichia phage ECML-134) | 57270..57476 | Minus | 7.8 | 6.68 | - | 1.1e-57 | 100.0 |
| 113 | Thymidine kinase.3 | 57473..57685 | Minus | 8.5 | 8.83 | *tk.3* | 2.1e-53 | 92.9 |
| 114 | Thymidine kinase.4 | 57657..58136 | Minus | 17.5 | 5.27 | *tk.4* | 2.6e-60 | 57.4 |
| 115 | Valyl-tRNA synthetase modifier | 58133..58480 | Minus | 13.0 | 8.95 | *vs* | 9.5e-77 | 100.0 |
| 116 | Endoribonuclease RegB | 58473..59018 | Minus | 20.6 | 9.76 | *regB* | 4.5e-128 | 100.0 |
| 117 | Site-specific RNA endonuclease | 59026..59487 | Minus | 17.9 | 8.93 | *regB* | 2.8e-105 | 99.3 |

| | | | | | | | | |
|---|---|---|---|---|---|---|---|---|
| 118 | Vs.3 | 59547..59825 | Minus | 10.9 | 5.45 | *vs.3* | 4.7e-58 | 100.0 |
| 119 | Vs.4 | 59825..60091 | Minus | 10.2 | 4.75 | *vs.4* | 8.2e-57 | 97.7 |
| 120 | Vs.5 | 60084..60305 | Minus | 8.2 | 4.14 | *vs.5* | 2.1e-55 | 97.3 |
| 121 | Vs.6 | 60305..60667 | Minus | 13.8 | 5.80 | *vs.6* | 1.3e-79 | 100.0 |
| 122 | Vs.7 | 60675..61004 | Minus | 12.8 | 8.89 | *vs.7* | 2.7e-73 | 98.2 |
| 123 | Vs.8 | 61001..61570 | Minus | 21.5 | 8.82 | *vs.8* | 2.6e-123 | 95.1 |
| 124 | Internal Head Protein 3 | 61707..62282 | Minus | 21.4 | 9.56 | *ip3* | 9e-124 | 91.7 |
| 125 | Internal Head Protein 10 | 62297..62611 | Minus | 12.0 | 9.49 | *ip10* (Enterobacteria phage Pol) | 1.8e-60 | 97.9 |
| 126 | Hypothetical protein (Escherichia phage Av-05) | 62675..62827 | Minus | 5.3 | 4.60 | - | 6.2e-28 | 93.8 |
| 127 | Hypothetical protein (Shigella phage Shf125875) | 62799..62927 | Minus | 5.0 | 9.22 | - | 6.3e-24 | 94.9 |
| 128 | Endonuclease V | 62940..63353 | Minus | 16.0 | 9.49 | *denV* | 3.1e-84 | 91.2 |
| 129 | Internal Head Protein 5 | 63412..63693 | Minus | 10.4 | 5.54 | *ipV* | 3.4e-17 | 51.2 |
| 130 | Lysozyme | 63690..64178 | Minus | 18.3 | 9.66 | *e* | 7e-106 | 95.0 |
| 131 | Nudix Hydrolase.1 | 64216..64656 | Minus | 17.0 | 5.18 | *nudE = e.1* | 1.7e-101 | 97.9 |
| 132 | Nudix Hydrolase.2 | 64653..65141 | Minus | 19.0 | 8.26 | *e.2* | 2.8e-53 | 84.2 |
| 133 | Nudix Hydrolase.3 | 65138..65500 | Minus | 14.1 | 8.83 | *e.3* | 2.7e-61 | 80.0 |
| 134 | Nudix Hydrolase.4 | 65482..65874 | Minus | 15.2 | 9.67 | *e.4* | 6.5e-80 | 90 |

| | | | | | | | | |
|---|---|---|---|---|---|---|---|---|
| 135 | Nudix Hydrolase.5 | 65843..66445 | Minus | 23.6 | 5.10 | *e.5* | 1.2e-133 | 93.5 |
| 136 | Nudix Hydrolase.6 | 66493..67086 | Minus | 22.0 | 6.06 | *e.6* | 3.5e-126 | 98.5 |
| 137 | Nudix Hydrolase.7 | 67144..67479 | Minus | 12.9 | 4.25 | *e.7* | 14e-69 | 91.0 |
| 138 | Hypothetical protein (Shigella phage SH7) | 67524..67688 | Minus | 6.1 | 3.96 | - | 4.5e-39 | 98.1 |
| 139 | Nudix Hydrolase.8 | 67758..68021 | Minus | 10.1 | 4.46 | *e.8* | 3.3e-58 | 98.9 |
| 140 | Hypothetical protein (Shigella phage Shfl2) | 68260..68826 | Minus | 21.0 | 9.43 | - | 2.3e-126 | 99.5 |
| 141 | Hypothetical protein (Enterobacteria phage RB32) | 68945..69418 | Minus | 17.2 | 9.46 | - | 1.9e-102 | 98.7 |
| 142 | tRNA.2 | 70737..71024 | Minus | 11.2 | 4.93 | *tRNA.2* | 1.9e-61 | 96.8 |
| 143 | tRNA.3 | 71027..71431 | Minus | 15.8 | 4.67 | *tRNA.3* | 2.8e-86 | 85.3 |
| 144 | tRNA.4 | 71432..71617 | Minus | 6.5 | 7.80 | *tRNA.4* | 1.9e-40 | 100.0 |
| 145 | Internal Protein I | 71694..71981 | Minus | 10.1 | 8.93 | *ipI* | 2e-58 | 98.9 |
| 146 | Gp57B | 72054..72509 | Minus | 17.1 | 5.14 | *57B* | 1.7e-105 | 100.0 |
| 147 | Chaperone for tail fiber formation | 72509..72763 | Minus | 9.1 | 4.31 | *57A* | 2e-52 | 94.0 |
| 148 | Deoxynucleotide monophosphate kinase | 72763..73476 | Minus | 26.8 | 5.14 | *1* | 8.8e-165 | 96.7 |
| 149 | Tail completion and sheath stabilizer protein | 73526..74056 | Minus | 19.7 | 4.39 | *3* | 7.8e-124 | 100.0 |

| | | | | | | | | |
|---|---|---|---|---|---|---|---|---|
| 150 | DNA end protector during packaging | 74162..74986 | Minus | 31.6 | 10.12 | *2 = 64* | 0.0 | 100.0 |
| 151 | Head completion protein | 74986..75438 | Minus | 17.6 | 9.78 | *4 = 50 = 65* | 3.5e-109 | 100.0 |
| 152 | Baseplate wedge subunit | 75486..76076 | Plus | 22.9 | 5.92 | *53* | 7.6e-144 | 100.0 |
| 153 | Base plate lysozyme; hub component | 76060..77787 | Plus | 63.1 | 5.35 | *5* | 0.0 | 99.3 |
| 154 | 5.1 | 77780..78316 | Plus | 20.0 | 4.45 | *5.1* | 7.5e-110 | 96.3% |
| 155 | 5.4 | 78317..78610 | Plus | 10.2 | 8.60 | *5.4* | 8.2e-64 | 100.0 |
| 156 | Baseplate wedge component | 78619..80601 | Plus | 74.4 | 4.62 | *6* | 0.0 | 99.5 |
| 157 | Baseplate wedge component | 80658..83696 | Plus | 116.9 | 4.98 | *7* | 0.0 | 98.5 |
| 158 | Baseplate wedge component | 83689..84693 | Plus | 37.9 | 4.58 | *8* | 0.0 | 99.1 |
| 159 | Base plate wedge component, tail fiber socket, trigger for tail sheath contraction | 84757..85623 | Plus | 30.9 | 5.01 | *9* | 0.0 | 99.3 |
| 160 | Baseplate wedge subunit and tail pin (T4-like gp10) | 85623..87431 | Plus | 66.3 | 4.41 | *10* | 0.0 | 99.8 |
| 161 | Baseplate wedge subunit and tail pin (T4-like gp11) | 87431..88090 | Plus | 23.6 | 5.30 | *11* | 3.8e-151 | 98.2 |

| | | | | | | | | |
|---|---|---|---|---|---|---|---|---|
| 162 | Short tail fibers | 88087..89670 | Plus | 55.9 | 7.02 | *12* | 0.0 | 96.6 |
| 163 | Whiskers, facilitate long tail fiber | 89667..91130 | Plus | 51.8 | 4.54 | *wack* | 0.0 | 97.3 |
| 164 | Head completition, neck hetero-dimeric protein (T4-like gp13) | 91163..92092 | Plus | 34.7 | 5.02 | 13 | 0.0 | 99.7 |
| 165 | Head completition, neck hetero-dimeric protein | 92094..92864 | Plus | 29.5 | 4.57 | 14 | 0.0 | 99.6 |
| 166 | Tail sheath stabilization protein | 92906..93724 | Plus | 31.5 | 4.88 | *15* | 0.0 | 100.0 |
| 167 | Terminase, small subunit | 93733..94227 | Plus | 18.3 | 4.55 | *16* | 4.5e-112 | 100.0 |
| 168 | Terminase, large subunit | 94211..96043 | Plus | 69.6 | 5.58 | *17* | 0.0 | 99.7 |
| 169 | Tail sheath stabilization monomer | 96075..98054 | Plus | 71.3 | 4.82 | *18* | 0.0 | 98.8 |
| 170 | Tail fibers | 98171..98662 | Plus | 18.4 | 4.67 | *19* | 1.4e-115 | 100.0 |
| 171 | Portal vertex of the head | 98746..100320 | Plus | 61.0 | 5.36 | *20* | 0.0 | 99.6 |
| 172 | Prohead core protein | 100320..100559 | Plus | 8.9 | 3.96 | *67* | 4.7e-55 | 96.3 |
| 173 | Capsid and scaffold | 100559..100984 | Plus | 15.8 | 10.10 | *68* | 4.9e-90 | 99.3 |
| 174 | Prohead assembly (scaffolding) protein | 100984..101622 | Plus | 23.2 | 4.98 | *21* | 3.9e-152 | 99.5 |
| 175 | Prohead assembly (scaffolding) protein | 101653..102462 | Plus | 29.8 | 4.56 | *22* | 4.2e-176 | 98.1 |

| | | | | | | | | |
|---|---|---|---|---|---|---|---|---|
| 176 | Major capsid protein | 102481..104046 | Plus | 56.0 | 5.34 | *23* | 0.0 | 98.8 |
| 177 | Capsid vertex | 104130..105413 | Plus | 47.0 | 4.70 | *os = 24* | 0.0 | 99.3 |
| 178 | Second RNA ligase | 105443..106447 | Minus | 37.6 | 5.65 | *rnlB = 24.1* | 0.0 | 99.1 |
| 179 | Gp24.2 | 106457..106735 | Minus | 10.9 | 4.87 | *24.2* | 5.8e-59 | 96.7 |
| 180 | Gp24.3 | 106722..106925 | Minus | 7.8 | 10.34 | *24.3* | 1.9e-33 | 83.6 |
| 181 | Capsid and scaffold | 107027..108157 | Minus | 40.7 | 4.51 | *hoc = eph* | 0.0 | 88.0 |
| 182 | Inh inhibitor of gp21 prohead protease | 108167..108847 | Minus | 25.5 | 4.43 | *inh = lip* | 9.3e-158 | 99.1 |
| 183 | DNA helicase | 108898..110409 | Plus | 57.9 | 9.29 | *uvsW = dar* | 0.0 | 98.8 |
| 184 | DNA helicase | 110435..110665 | Plus | 8.8 | 4.24 | *uvsW = dar* | 9.5e-50 | 100.0 |
| 185 | UvsY intergenic region | 110721..110888 | Minus | 6.0 | 4.44 | *uvsY.-2* | 2.9e-39 | 100.0 |
| 186 | UvsY.-1 | 110917..111141 | Minus | 8.9 | 5.02 | *uvsY.-1* | 2.4e-56 | 98.6 |
| 187 | Single Stranded DNA-binding protein | 111141..111554 | Minus | 15.7 | 7.75 | *uvsY* | 1.8e-90 | 98.5 |
| 188 | Baseplate wedge subunit | 111621..112019 | Minus | 15.1 | 4.57 | *25* | 7.9e-87 | 98.5 |
| 189 | Baseplate hub assembly chaperone | 112019..112645 | Minus | 23.8 | 5.56 | *26* | 1.1e-149 | 99.5 |
| 190 | Baseplate | 112696..113445 | Plus | 29.2 | 6.02 | *51* | 7.2e-174 | 96.0 |
| 191 | Baseplate hub subunit | 113445..114620 | Plus | 44.3 | 5.20 | *27* | 0.0 | 99.2 |
| 192 | Baseplate hub | 114640..115098 | Plus | 17.3 | 5.01 | *28* | 9e-107 | 99.3 |
| 193 | Baseplate hub | 115095..116867 | Plus | 64.2 | 5.05 | *29* | 0.0 | 95.8 |

| | | | | | | | | |
|---|---|---|---|---|---|---|---|---|
| 194 | Baseplate tube cap (T4-like gp48) | 116876..117970 | Plus | 39.6 | 8.71 | *48* | 0.0 | 97.8 |
| 195 | Tail assembly | 117970..118935 | Plus | 34.8 | 5.08 | *54* | 0.0 | 97.8 |
| 196 | Alt.-3 | 118964..119254 | Minus | 10.7 | 4.67 | *alt.-3* | 1.9e-59 | 100.0 |
| 197 | Alt.-2 | 119315..121372 | Minus | 76.0 | 6.01 | *alt.-2* | 2e-147 | 41.5 |
| 198 | Alt | 121376..123469 | Minus | 77.8 | 5.97 | *alt* | 0.0 | 70 |
| 199 | Alt.1 | 123522..123710 | Minus | 7.1 | 4.50 | *alt.1* | 4.7e-41 | 90.3 |
| 200 | DNA ligase | 123707..125170 | Minus | 55.2 | 6.14 | *30 = lig* | 0.0 | 99.6 |
| 201 | Gp30.1 | 125167..125436 | Minus | 10.8 | 7.82 | 30.1 | 7.1e-61 | 98.9 |
| 202 | Gp30.2 | 125436..126275 | Minus | 32.4 | 5.93 | 30.2 | 0.0 | 96.8 |
| 203 | Gp30.3 | 126272..126652 | Minus | 14.0 | 9.33 | 30.3 | 2e-80 | 96.8 |
| 204 | Gp30.4 | 126723..126938 | Minus | 8.2 | 4.94 | 30.4 | 1.7e-16 | 50.7 |
| 205 | Gp30.6 | 126943..127230 | Minus | 10.8 | 6.26 | *30.6* | 1.2e-59 | 96.8 |
| 206 | Gp30.7 | 127272..127637 | Minus | 14.1 | 6.05 | *30.7* | 1.9e-84 | 98.3 |
| 207 | Gp30.8 | 127705..128037 | Minus | 12.8 | 6.11 | *30.8* | 2.9e-73 | 97.3 |
| 208 | Gp30.9 | 128148..128366 | Minus | 8.1 | 11.33 | *30.9* | 2.1e-50 | 98.6 |
| 209 | RIII | 128445..128693 | Minus | 9.3 | 8.06 | *rIII* | 3.2e-61 | 100.0 |
| 210 | Gp31 | 128841..129176 | Minus | 12.0 | 5.30 | *31* | 1.3e-74 | 100.0 |
| 211 | Gp31.1 | 129233..129541 | Minus | 11.4 | 9.35 | *31.1* | 2.9e-64 | 100.0 |
| 212 | Gp31.2 | 129542..129778 | Minus | 9.3 | 9.78 | *31.2* | 1.3e-56 | 96.2 |

| | | | | | | | | |
|---|---|---|---|---|---|---|---|---|
| 213 | tRNA-specific adenosine deaminase | 129778..130359 | Minus | 21.2 | 8.04 | *cd* | 2.3e-141 | 99.5 |
| 214 | Cd.1 | 130356..130694 | Minus | 12.8 | 7.87 | *cd.1* | 1.1e-71 | 99.1 |
| 215 | Cd.2 | 130691..130930 | Minus | 8.9 | 5.31 | *cd.2* | 1.1e-47 | 98.6 |
| 216 | Cd.3 | 130992..131267 | Minus | 10.1 | 4.90 | *cd.3* | 3.3e-55 | 98.9 |
| 217 | Cd.4 | 131270..131470 | Minus | 7.9 | 4.35 | *cd.4* | 1.2e-47 | 97 |
| 218 | Cd.5 | 131463..131660 | Minus | 7.5 | 6.71 | *cd.5* | 1.8e-47 | 97 |
| 219 | 3’-phosphatase, 5’-polynucleotide kinase | 131660..132568 | Minus | 34.8 | 8.62 | *pseT* | 0.0 | 95.0 |
| 220 | Hypothetical protein (Escherichia phage slur14) | 132565..132885 | Minus | 12.1 | 8.55 | | 1.8e-68 | 100.0 |
| 221 | PseT.1 | 132882..133112 | Minus | 8.9 | 8.02 | *pseT.1* | 1.4e-55 | 98.1 |
| 222 | PseT.2 | 133109..133408 | Minus | 11.6 | 8.76 | *pseT.2* | 6.2e-67 | 99.0 |
| 223 | PseT.3 | 133405..133758 | Minus | 13.0 | 8.89 | *pseT.3* | 9.7e-68 | 92.3 |
| 224 | Alc | 133749..134252 | Minus | 19.0 | 6.42 | *alc* | 9.9e-113 | 97.6 |
| 225 | RNA ligase I | 134317..135441 | Minus | 43.4 | 5.02 | *rnlA = 63* | 0.0 | 98.4 |
| 226 | Endonuclease II | 135494..135904 | Minus | 15.7 | 9.21 | *denA* | 2.9e-91 | 99.3 |
| 227 | NrdB (beta subunit) | 135932..137101 | Minus | 45.2 | 5.13 | *nrdB* | 0.0 | 91.3 |
| 228 | NrdB (alfa subunit) | 137153..139417 | Minus | 86.0 | 5.87 | *nrdB* | 0.0 | 98.4 |
| 229 | NrdA.1 | 139408..139734 | Minus | 12.4 | 9.22 | *nrdA.1* | 7.2e-73 | 96.3 |

| | | | | | | | | |
|---|---|---|---|---|---|---|---|---|
| 230 | NrdA.2 | 139688..139951 | Minus | 9.9 | 5.28 | *nrdA.2* | 1e-54 | 96.6 |
| 231 | Thymidylate synthase | 139975..140835 | Minus | 32.9 | 8.57 | *td* | 0.0 | 94.1 |
| 232 | Thymidylate synthse.1 | 140881..141228 | Minus | 13.7 | 7.69 | *td.1* (Enterobacteria phage T6) | 42e-81 | 98.3 |
| 233 | frd | 141248..141829 | Minus | 21.7 | 5.58 | *frd* | 6.1e-132 | 97.4 |
| 234 | Hypothetical protein (Enterobacteria phage RB9) | 141829..142074 | Minus | 9.6 | 4.05 | - | 870e-66 | 98.8% |
| 235 | Frd.1 | 142085..142327 | Minus | 9.4 | 4.91 | *frd.1* | 3.7e-62 | 97.5 |
| 236 | Frd.2 | 142382..142747 | Minus | 14.4 | 5.41 | *frd.2* | 3.6e-48 | 65.1 |
| 237 | Frd.3 | 142792..143019 | Minus | 8.6 | 3.86 | *frd.3* | 4.2e-37 | 70.7 |
| 238 | Single-stranded DNA-binding protein | 143164..144072 | Minus | 33.5 | 4.87 | *32* | 0.0 | 97.7 |
| 239 | DNA Helicase loader | 144172..144825 | Minus | 26.0 | 9.33 | *59* | 2.8e-152 | 99.5 |
| 240 | Gp33 | 144822..145160 | Minus | 12.8 | 4.47 | *33* | 1e-69 | 98.2 |
| 241 | Double-stranded DNA-binding protein | 145138..145407 | Minus | 10.3 | 5.04 | *dsbA* | 1.4e-55 | 100.0 |
| 242 | Ribonuclease H | 145416..146333 | Minus | 35.5 | 8.61 | *rnh = das* | 0.0 | 99.7 |
| 243 | Long Tail fiber proximal subunit | 146438..150307 | Plus | 140.0 | 5.49 | *34* | 0.0 | 95.6 |
| 244 | Hinge connector of long tail fiber proximal connector | 150316..151431 | Plus | 40.2 | 5.27 | *35* | 0.0 | 97.6 |

| | | | | | | | | |
|---|---|---|---|---|---|---|---|---|
| 245 | Hinge connector of long tail fiber distal connector | 151494..152156 | Plus | 23.2 | 6.82 | *36* | 5.9e-132 | 85.5 |
| 246 | Tail fibers | 152165..156025 | Plus | 137.8 | 8.30 | *37* | 0.0 | 55.2 |
| 247 | Assembly catalyst of distal tail fiber | 156056..156847 | Plus | 25.5 | 9.79 | *38* (Shigella phage Shfl2) | 0.0 | 99.2 |
| 248 | Holin | 156879..157535 | Plus | 25.1 | 7.70 | *t = rV = stII* | 9.2e-154 | 99.1 |
| 249 | Anti-sigma 70 protein | 157536..157808 | Minus | 10.6 | 5.42 | *asiA* | 1.1e-55 | 98.9 |
| 250 | asiA.1 | 157821..157973 | Minus | 5.8 | 4.92 | *asiA.1* | 2e-30 | 94.0 |
| 251 | Inhibitor of MrcBC | 157970..158248 | Minus | 10.8 | 4.48 | *arn* | 3.3e-58 | 97.8 |
| 252 | Hypothetical protein (Shigella phage SHBML-50-1) | 158238..158357 | Minus | 4.6 | 10.20 | - | 8.3e-28 | 100 |
| 253 | Arn.1 | 158332..158463 | Minus | 5.2 | 8.57 | *arn.1* | 3.8e-34 | 97.7 |
| 254 | Arn.2 | 158534..158830 | Minus | 11.3 | 8.93 | *arn.2* | 2.4e-63 | 96.9 |
| 255 | Arn.3 | 158830..159291 | Minus | 17.9 | 5.31 | *arn.3* | 1.5e-104 | 98.0 |
| 256 | Arn.4 | 159288..159617 | Minus | 12.7 | 9.24 | *arn.4* | 4.7e-74 | 99.1 |
| 257 | MotA | 159628..160263 | Minus | 23.5 | 7.78 | *motA = sip* | 1.2e-138 | 97.6 |
| 258 | Uncharacterized 4.8 kDa protein in motA-Gp52 intergenic region | 160390..160539 | ααMinus | 4.8 | 9.50 | *motA.1* | 9.5e-37 | 100.0 |
| 259 | DNA Topoisomerase | 160536..161864 | Minus | 50.4 | 8.45 | *52* | 0.0 | 99.3 |
| 260 | Ac | 162002..162160 | Minus | 5.5 | 4.21 | *ac* | 3.7e-32 | 96.1 |

| | | | | | | | | |
|---|---|---|---|---|---|---|---|---|
| 261 | Nucleoid disruption protein | 162248..162706 | Minus | 17.1 | 10.05 | *ndd* = D2b | 5.1e-100 | 96.7 |
| 262 | Ndd.1 | 162767..162982 | Minus | 8.1 | 4.22 | *ndd.1* | 3.4e-49 | 95.8 |
| 263 | Ndd.2 | 162991..163116 | Minus | 5.0 | 5.75 | *ndd.2* | 1.3e-30 | 97.2 |
| 264 | Ndd.3 | 163098..163295 | Minus | 7.4 | 9.40 | *ndd.3* | 3.6e-21 | 95.0 |
| 265 | Ndd.5 | 163481..163612 | Minus | 5.0 | 4.65 | *ndd.5* | 1.6e-22 | 96.9 |
| 266 | Hypothetical protein (Enterobacteria phage RB9) | 163691..163996 | Minus | 11.6 | 8.69 | - | 84e-39 | 100.0 |
| 267 | Endonuclease IV | 163978..164535 | Minus | 21.1 | 6.89 | *denB* | 2e-133 | 98.4 |
| 268 | denB.1 | 164598..164792 | Minus | 7.5 | 6.21 | *denB.1* | 8.6e-40 | 93.8 |
| 269 | RIIB | 164821..165759 | Minus | 35.6 | 6.26 | rIIB | 0.0 | 98.7 |

**Supplementary table-2.** Functional categorization of vB_EcoM-UFV13 genes based on the reference Enterobacteria phage T4.

| Functional category | ORFs |
|---|---|
| **Transcription** | 7, 10, 11, 12, 19, 20, 22, 23, 24, 25, 26, 27, 28,29, 57, 58, 68, 70, 71, 72, 73, 74, 75, 87, 88, 89, 90, 91, 92, 93, 94, 95, 96, 97, 98, 240, 241, 249, 250, 257 |
| **Translation** | 8, 21, 42, 53, 115, 116, 117, 118, 119, 120, 121, 122, 123, 178 |
| **Nucleotide metabolism** | 33, 47, 76, 78, 79, 80, 87, 110, 113, 114, 131, 132, 133, 134, 135, 136, 137, 139, 148, 213, 214, 215, 216, 217, 218, 219, 221, 226, 227, 228, 229, 230, 231, 232, 233, 235, 236, 237, 267, 268 |
| **DNA replication, recombination, repair, packaging, and processing** | 3, 4, 6, 13, 14, 15, 17, 35, 36, 37, 43, 45,51,54, 55, 56, 59, 60, 61, 62, 81, 83, 84, 128, 167, 168, 183, 184, 185, 186, 187, 200, 201, 202, 203, 204, 205, 206, 207, 208, 238, 239, 242, 259 |
| **Virion proteins** | 30, 31, 32, 124, 125, 129, 145, 149, 150, 151, 152, 153, 156, 157, 158, 159, 160, 161, 162, 163, 164, 165, 166, 169, 170, 171, 172, 173, 174, 175, 176, 177, 179, 180, 181, 182, 188, 189, 191, 192, 193, 194, 195, 225, 243, 244, 245, 246 |
| **Chaperonins/assembly catalysts** | 44, 147, 174, 175, 190, 209, 210, 211, 212, 225, 247 |
| **Host or phage interactions** | 1, 2, 34, 46, 48, 49, 63, 64, 65, 66, 67, 82, 219, 225, 251, 253, 254, 255, 256, 260, 269 |
| **Host or phage interactions** | 1, 2, 34, 46, 48, 49, 63, 64, 65, 66, 67, 82, 219, 225, 251, 253, 254, 255, 256, 260, 269 |
| **Host alteration/shutoff** | 127, 196, 197, 198, 199, 224, 261, 262, 263, 264, 265 |
| **Homing endonucleases and homologs** | 100, 101, 102, 103, 104, 105 |

| | |
|---|---|
| **Predicted integral membrane or periplasmic proteins** | 77, 144, 222, 223, 252 |
| **Unknown function** | 5, 9, 16, 39, 40, 41, 50, 52, 69, 85, 86, 99, 111, 112, 126, 138, 140, 141, 220, 234, 258, 266 |

**Supplementary figure-1.** vB_EcoM-UFV13, *Yersinia* phage PST and *Shigella* phage Shfl2 genomes alignment with progressive Mauve showing collinear blocks between the genomes. In each alignment is possible observe base pairs scale and histogram with degree of similarity. BLASTn analyze revealed an identity of 97% between vB_EcoM-UFV13 and *Yersinia* virus PST and *Shigella virus* Shfl2, but greater coverage (96%) with the latter.

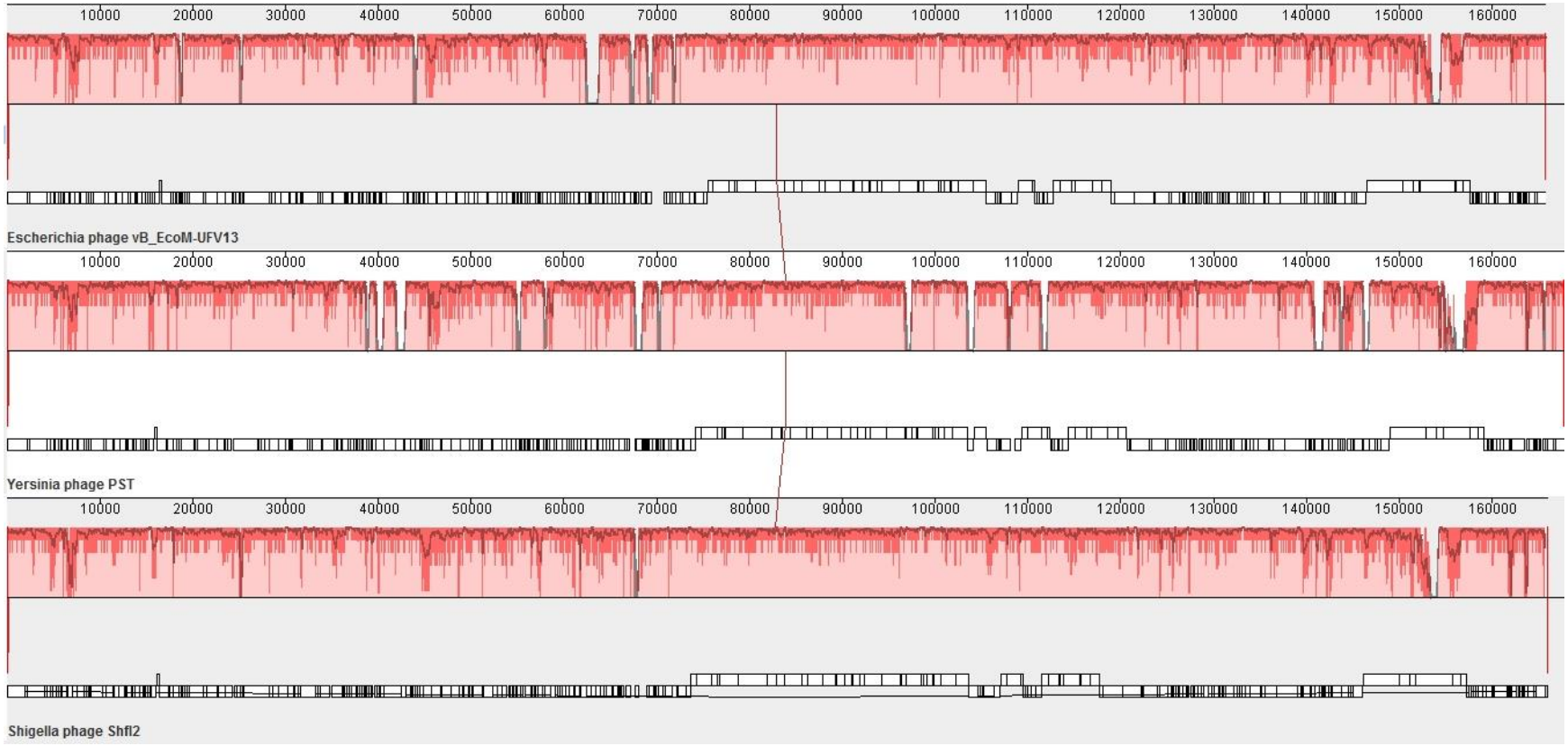

**Supplementary table-3.** Early, middle and late promoters prediction.

| Pe (Early promoter) | vB_EcoM-UFV13 (Genome position) | T4 (Genome position) | Pm (Middle promoter) | vB_EcoM-UFV13 (Genome position) | T4 (Genome Position) | Pl (Late promoter) | vB_EcoM-UFV13 (Genome position) | T4 (Genome position) |
|---|---|---|---|---|---|---|---|---|
| **1.4..3.9** | 2418..2447 | 2429..2458 | **Pm** | * | * | **soc** | 15434..15451 | 15593..15643 |
| **(3.6)** | Without *mobA* | 2422 | **Pm** | * | * | **Pl** | | |
| **(5.9..7.3) = (motB)** | 6684..6738 | 7169..7225 | **Pm(rIIA)** | 2241..2296 | 2252..2307 | **56/69** | Without gp69 | 16803..16856 |
| **(8.1)** | 7797..7826 | 8189..8218 | **Pm(39)** | 4275..4328 | 5339..5392 | **I..TevII** | Without *tevII* | 45621..45671 |
| **(11.5)** | 11661..11690 | 11822..11851 | **Pm(56/69)** | 139406..139429 | 16803..16856 | **49** | 43147..43197 | 46875..46925 |
| **12.8 = mod** | 12982..13036 | 13140..13196 | **Pm(61)** | 17800..17853 | 19112..19165 | **rI.1** | 59740 | * |
| **15.0 = soc** | 15434..15451 | 15593..15643 | **Pm(uvsX)** | * | 23742..23796 | **Pe(2)** | 64184..64234 | 67001..67051 |
| **19.8** | 18501..18539 | 20070..20119 | **Pm(segA)** | Without *segA* | 24446..24500 | **Pe(1)** | 64197..64247 | 67014..67064 |
| **20.3 = dmd** | 19590.. 19646 | 20566..20622 | **Pm(42)** | 24339..24392 | 26310..26363 | **Pe(w)** | 64413..64463 | 67230..67280 |
| **26.4 = imm.1** | 25319..25373 | 27034..27090 | **Pm(43)** | 28205..28259 | 29921..29977 | **Pl** | * | 72863 |
| **35.3** | 34167..34216 | 35659..35708 | **Pm(45)** | 31124..31177 | 32616..32669 | **Pl** | * | 74999 |
| **40.4** | 39151..39200 | 41222..41271 | **Pm(45.2)** | 31755..31807 | 33247..33299 | **4** | 75457..75507 | 77354..77404 |
| **41.0** | 39596..39645 | 41667..41716 | **Pm(46)** | 33512..33566 | 35004..35058 | **Pl** | * | 77362 |
| **46.7** | 43685..43734 | 47413..47462 | **Pm(47)** | 35070..35127 | 36562..36619 | **Pl** | * | 77381 |
| **50.0 = nrdC.4** | 47297..47353 | 50927..50983 | **Pm(mobB..gt)** | * | * | **53.0** | 75419..75469 | 77316..77366 |
| **54.0** | 50281..50330 | 53904..53953 | **Pm(55)** | 37838..37891 | 40170..40223 | **5.1** | 77856..77906 | 79753..79803 |
| **54.4** | 51720.. 51769 | 55345..55394 | **Pm(55.8)** | 40739..40774 | 42795..42849 | **7** | * | * |
| **Pe** | Without mobD.2 | 57954 | **Pm(nrdG)** | * | * | **8** | 83306..83356 | 85766..85816 |

| | | | | | | | | |
|---|---|---|---|---|---|---|---|---|
| **Pe(57.9)** | 55308.. 55357 | 58741..58790 | **Pm(nrdD+)** | * | * | **9(b)** | 84694..84744 | 87154..87204 |
| **Pe (62.2)** | 59507..59556 | 62758..62807 | **tRNA** | 70970..71020 | 72859..72909 | **9(a)** | 84254..84304 | 86714..86764 |
| **64.6 = denV** | 67498..67541 | 65375..65423 | **57A** | 72983..73035 | 74867..74919 | **10** | 85379..85429 | 87839..87889 |
| **Pe (65.0)** | Without *lpll* | 65760..65809 | **1** | 73486..73539 | 75382..75435 | **15** | 92832..92882 | 95291..95341 |
| **Pe** | | 66462 | **uvsY** | 111580..111634 | 115361..115415 | **17** | 93648..93698 | 96107..96157 |
| **69.9** | 67116.. 67155 | 69928..69977 | **Pm(30)** | * | * | **18(w)** | 96008..96058 | 98467..98517 |
| **69.4** | 71640..71677 | 70320..70369 | **Pm(30.2)** | * | * | **PI** | * | * |
| **69.8** | 68057..68106 | 70657..70706 | **Pm(31)** | * | * | **P19(a)** | 98059..98109 | 100518..100568 |
| **tRNA.4 = 72.6** | 71633..71687 | 73526..73582 | **Pm(I..tevIII)** | * | * | **P19(b)** | 98118..98168 | 100577..100627 |
| **73.0** | 72004..72053 | 73900..73949 | **Pm(nrdB)** | * | 139868..139921 | **20** | 98679..98729 | 101138..101188 |
| **Pe** | * | 79405 | **Pm(nrdA)** | 139453..139508 | 142714..142769 | **67** | 100034..100084 | 102493..102543 |
| **alt.3** | F:119252..119300 | 123057 | **Pm(td+)** | 141272..141326 | 145131..145185 | **21** | 100638..100688 | 103100..103150 |
| **128.2** | 127666..127714 | 129880..129928 | **Pm(32)** | 143143..143192 | 148054..148101 | **22** | 101587..101637 | 104049..104099 |
| **128.6** | 128057..128106 | 130271..130320 | **Pm(dsbA)** | 145492..145547 | 149861..149916 | **PI** | * | * |
| **131.7** | 130952..131001 | 133292..133341 | **Pm(34)** | 146365..146415 | 150734..150784 | **23** | 102309..102358 | 104770..104820 |
| **134.4** | 134276..134325 | 136297..136346 | | | | **23(w)** | 102279..102329 | 104741..104791 |
| **144.6** | 143055..143104 | 146836..146885 | | | | **hoc.1** | 108867..108886 | 112025..112075 |
| **148.6** | 146355..146404 | 150724..150773 | | | | **hoc.2** | )8830..108880 | 111988..112038 |
| **158.7** | 157832.. 157881 | 161172..161221 | | | | **PI** | * | * |
| **161.1 = motA** | 160290.. 160346 | 163627..163683 | | | | **PI(segE)** | * | * |
| **164.2** | 163437..163484 | 166768..166817 | | | | **PluvsY..2** | * | * |
| **164.5** | 163924..163973 | 167047..167096 | | | | **PI** | * | * |
| | | | | | | **P26(a)** | 112659..112709 | 116440..116490 |
| | | | | | | **P26(w)** | 112650..112700 | 116431..116481 |
| | | | | | | **PI** | | |

| | | | |
|---|---|---|---|
| | **PI(alt)** | 123490..123534 | 125521..125571 |
| | **PI(rIII)** | * | * |
| | **PI(alc)** | * | |
| | **PI(I..TevIII)** | * | * |
| | **PI(I..TevI)** | * | 144445..144495 |
| | **PI(32)** | * | 147994..148044 |
| | **PI(rnh)** | * | |
| | **PI35** | * | |
| | **PI36** | 151432..151482 | 155804..155854 |
| | **PI37** | 151948..151998 | 156323..156373 |
| | **PI38** | * | |

**Supplementary figure-2.** SNP-based phylogentic tree supports the phylogenetic relationship between UFV13 and *Shigella* phage Shfl2.

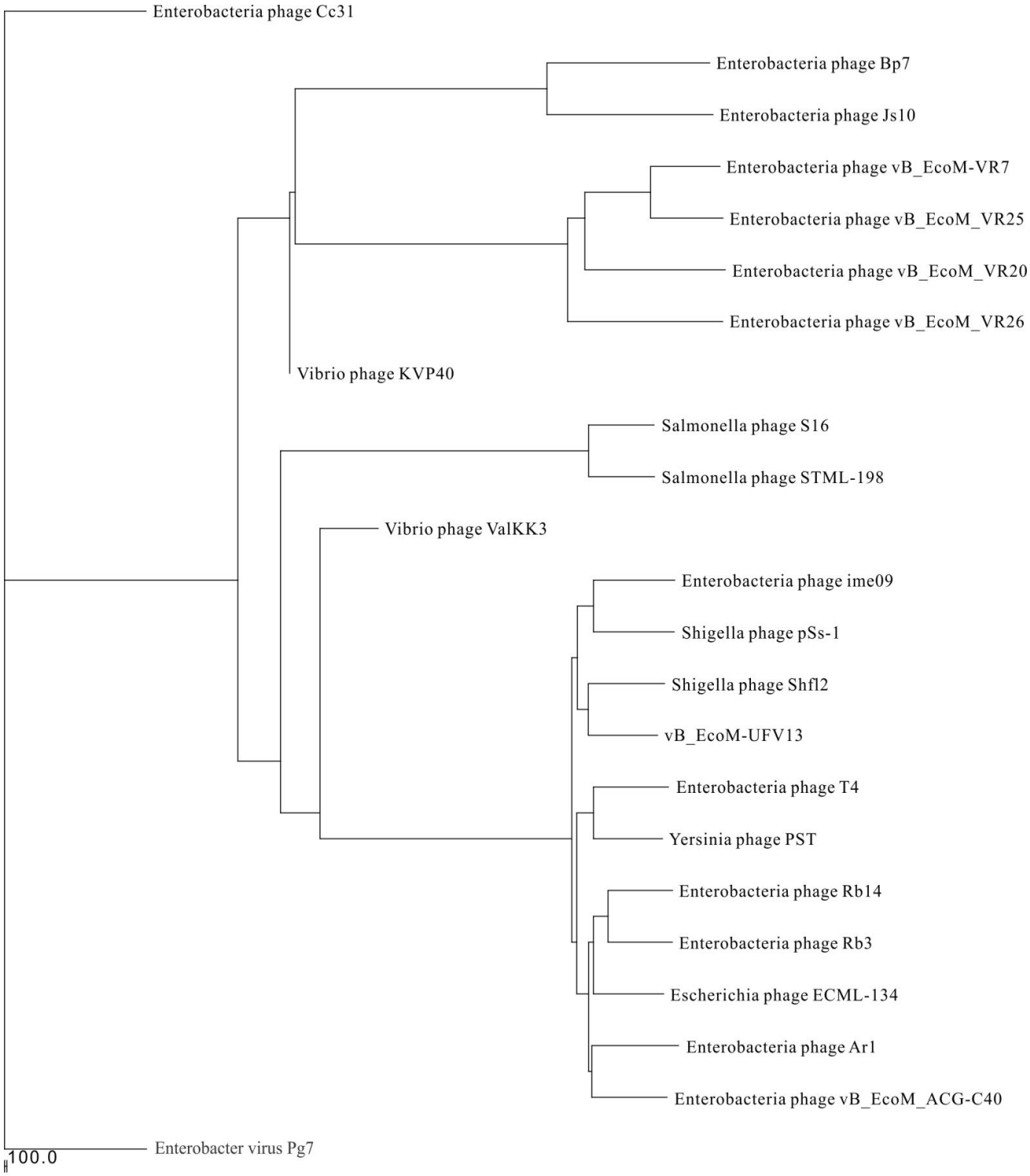

**Supplementary figure-3.** *Escherichia phage* UFV13 protein profile by SDS-PAGE. MALDI/TOF-TOF analyze revealed the presence of host receptor protein after virus purification. Sample 1 – vB_EcoM-UFV13 long tail fiber proximal subunit); Sample 2 – *E. coli* chaperonin GroL; Sample 3 – *Escherichia* phage major capsid protein; Sample 4 – *E. coli* outer membrane protein C (OmpC). Three lanes were loaded with the aim to increase protein yield for MALDI/TOF-TOF analyze.

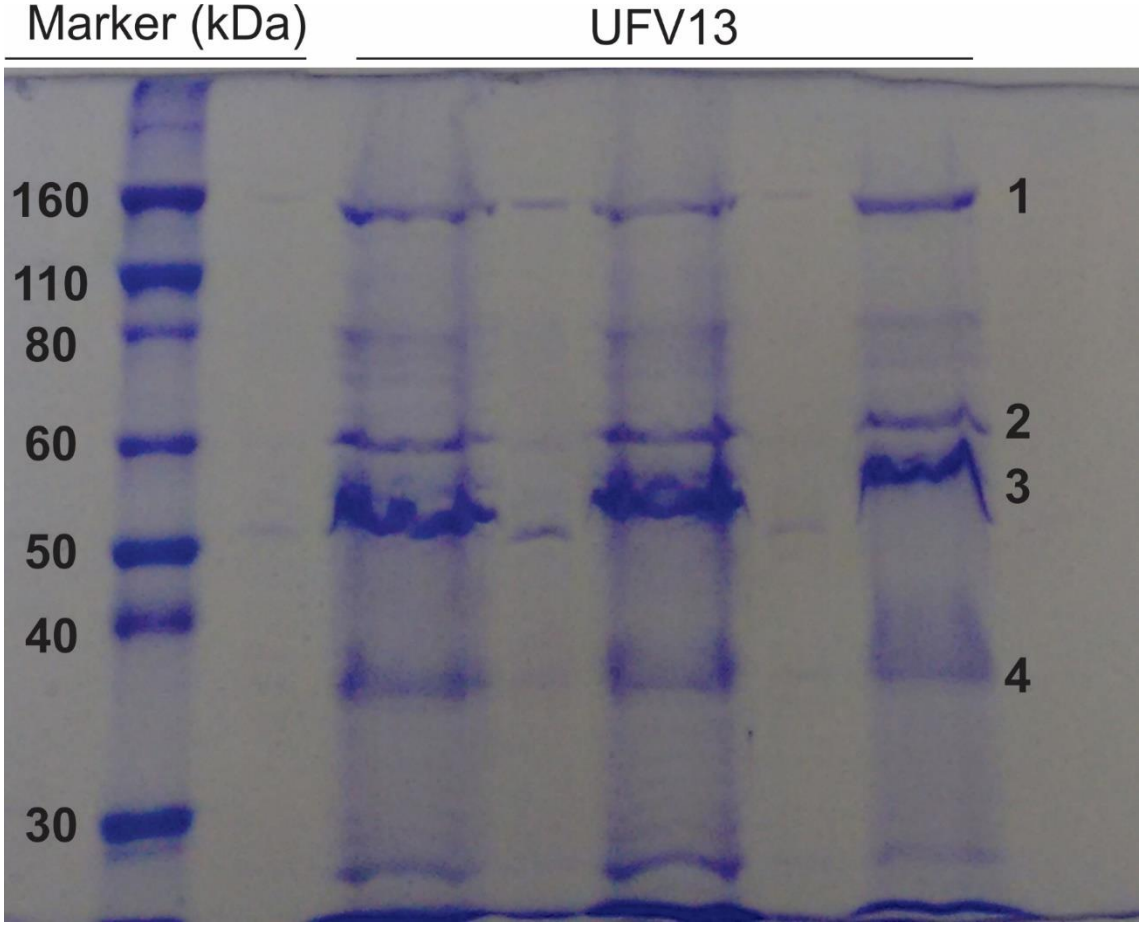

**Supplementary table-4.** NCBI accession number list of all viral genomes used in this study.

| Virus | Accession number |
|---|---|
| *Escherichia virus RB3* | KM606994 |
| *Escherichia virus RB14* | NC_012638 |
| *Escherichia virus ECML134* | JX128259 |
| *Escherichia virus C40* | JN986846 |
| *Escherichia virus AR1* | AP011113 |
| *Escherichia virus T4* | AF158101.6 |
| *Yersinia virus PST* | KF208315 |
| *Escherichia virus UFV13* | NC_031103 |
| *Shigella virus Shfl2* | HM035025 |
| *Escherichia virus ime09* | JN202312 |
| *Shigella virus Pss1* | KM501444 |
| *Enterobacter virus CC31* | NC_014662 |
| *Enterobacter virus PG7* | NC_023561 |
| *Salmonella virus S16* | NC_020416 |
| *Salmonella virus STML198* | JX181825 |
| *Enterobacter virus JS10* | NC_012741 |
| *Enterobacter virus VR26* | NC_028957 |
| *Enterobacter virus VR20* | NC_028894 |
| *Enterobacter virus VR7* | NC_014792 |
| *Enterobacter virus VR25* | NC_028925 |
| *Bacillus virus BMBtp1* | KT852578 |

**Supplementary figure-4.** Experimental design of *E. coli*-induced mastitis in mouse. A – The last two abdominal ceilings (R5 and L5) of each animal were used. B – After that the lactating mouse was intraperitoneally anesthetized, R5 and L5 were assessed by cutting the teat canal.

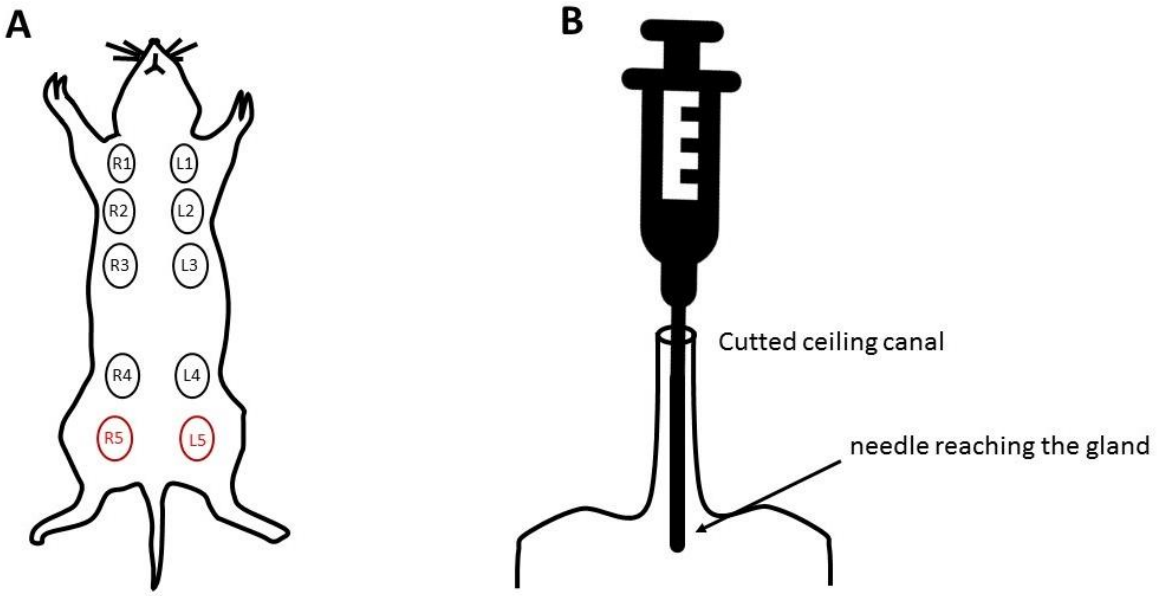

**Supplementary Figure-5.** A 10-fold reduction of *E. coli 30* load was observed after viral inoculation using MOI 10.

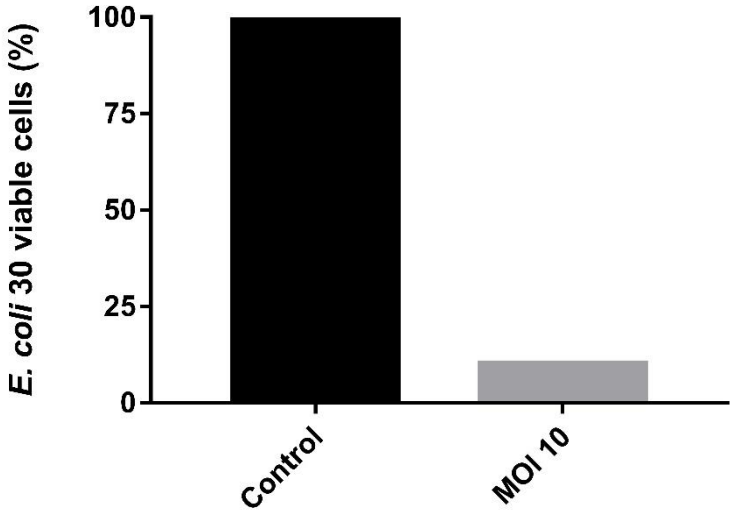

**Supplementary Table-5.** Antimicrobial susceptibility test was performed by disc diffusion assay using 25 different antibiotics. *E. coli* 30 was resistant to 56% of antibiotics tested.

| Antibiotics | Code | Resistant | Intermediate | Susceptible | Diameter (cm) | Result |
|---|---|---|---|---|---|---|
| Ceftriaxone | CRO 30 | ≤19 | 20-22 | ≥23 | 19 | Resistant |
| Bacitracin | BAC 10 | - | - | - | 0.6 | Resistant |
| Amoxicillin | AMO 10 | - | - | - | 0.6 | Resistant |
| Cefalotin | CFL 30 | ≤14 | 15-17 | ≥18 | 13 | Resistant |
| Linezolid | LNZ 30 | ≤20 | 21-22 | ≥23 | 0.6 | Resistant |
| Sulfamethoxazole/Trimethoprim | SUT 25 | ≤10 | 11-15 | ≥16 | 0.6 | Resistant |
| Tetracyclin | TET 30 | ≤11 | 12-14 | ≥15 | 0.6 | Resistant |
| Penicillin G | PEN 10 | ≤28 | - | ≥15 | 0.6 | Resistant |
| Erythromycin | ERI 15 | ≤15 | 16-20 | ≥21 | 0.6 | Resistant |
| Oxacillin | OXA 01 | - | - | - | 0.6 | Resistant |
| Ampicillin | AMP 10 | ≤13 | 14-16 | ≥17 | 0.6 | Resistant |
| Clindamycin | CLI 02 | ≤15 | 16-18 | ≥21 | 0.6 | Resistant |
| Vancomycin | VAN 30 | ≤14 | 15-16 | ≥17 | 0.6 | Resistant |
| Rifampicin | RIF 05 | ≤16 | 17-18 | ≥19 | 0.6 | Resistant |
| Chloramphenicol | CLO 30 | ≤12 | 13-17 | ≥18 | 25 | Susceptible |
| Ceftazidime | CAZ 30 | ≤17 | 18-20 | ≥21 | 28 | Susceptible |
| Aztreonam | ATM 30 | ≤17 | 18-20 | ≥21 | 32 | Susceptible |
| Amikacin | AMI 30 | ≤14 | 15-16 | ≥17 | 28 | Susceptible |
| Amoxicillin/Clavulanate | AMC 30 | ≤13 | 14-17 | ≥18 | 20 | Susceptible |
| Cefepime | CPM 30 | ≤18 | - | ≥21 | 35 | Susceptible |
| Ciprofloxacin | CIP 05 | ≤15 | 16-20 | ≥21 | 29 | Susceptible |

| | | | | | | |
|---|---|---|---|---|---|---|
| Azithromycin | AZI 15 | ≤13 | 14-17 | ≥18 | 27 | Susceptible |
| Cefoxitin | CFO 30 | ≤14 | 15-17 | ≥18 | 32 | Susceptible |
| Gentamicin | GEN 10 | ≤12 | 13-14 | ≥15 | 22 | Susceptible |
| Piperacillin/Tazobactam | PIT 110 | ≤17 | 18-20 | ≥21 | 23 | Susceptible |

**Supplementary Table-6.** Biofilm formation and motility assays. *E. coli* 30 displays the capability to form biofilm and possesses swarming and swimming abilities.

| **Virulence factors** | **Result** |
|---|---|
| Swarming | + |
| Swimming | + |
| Twitching | - |
| Biofilm | + |